5-2016

Design and Initial Verification of a Novel Total Knee Replacement that Incorporates Synthetic Ligaments to Influence Knee Stability

Michael David Stokes

Clemson University, mdstoke@g.clemson.edu

Follow this and additional works at: https://tigerprints.clemson.edu/all_theses

DESIGN AND INITIAL VERIFICATION OF A NOVEL TOTAL KNEE
REPLACEMENT THAT INCORPORATES SYNTHETIC
LIGAMENTS TO INFLUENCE KNEE STABILITY

A Thesis
Presented to
the Graduate School of
Clemson University

In Partial Fulfillment
of the Requirements for the Degree
Master of Science
Bioengineering

by
Michael David Stokes
May 2016

Accepted by:
Dr. John DesJardins, PhD, Committee Chair
Dr. Jeremy Mercuri, PhD
Dr. Brian Burnikel, M.D.

ABSTRACT

In the United States, the number of patients under the age of 65 who are receiving total knee replacements (TKRs) is rising due to increasing demand for and access to this life-changing orthopaedic procedure. Although this younger population tends to have a higher life expectancy, they have also been shown to have a lower implant survival rate than patients over the age of 65 (Julin, Jämsen, Puolakka, Konttinen, & Moilanen, 2010), possibly due to their more active lifestyles. Thus, there will be a rising demand for implants that have both a higher functionality and survivorship to meet performance demands of younger patient's lifestyles.

The purpose of this study was to design and initially verify a novel TKR design that incorporates artificial ligaments into a knee replacement whose stability and eventual kinematic performance will be driven by both geometry and ligamentous structure. A computational model was first developed that incorporated synthetic ligaments into an existing knee replacement within an anatomical knee model using the AnyBody modeling software system. Simulated A/P drawer tests at different flexion angles were analyzed for over 2,916 possible anterior and posterior cruciate ligament location and length combinations to determine the effects of ligament length and location on the A/P stability of the TKR. A complete physical model was then designed and constructed, and the computational model was verified by performing mechanical testing on an Instron system. A/P drawer tests were performed under 710 N of simulated body weight. Tibial A/P displacement was tracked for the TKR system with and without cruciate ligaments to determine the effect of ligament placement on resulting TKR stability.

Ligament length and location were found to significantly influence knee laxity and knee flexion. Knee flexion was determined to be more sensitive to the ACL attachment location on the femur than on the tibia. As ACL insertion location moved posteriorly on the femur, it was found to decrease ACL ligament strain enabling a higher range of flexion. In general, as ACL and PCL length increased, the A/P laxity of the TKR system increased linearly. Interestingly, range of motion was found to be more dependent on ligament attachment location than ligament lengths.

Knee replacement stability is clearly affected by synthetic ligament length and location within a TKR system. A knee replacement that incorporates synthetic ligaments with calibrated location and lengths should be able to significantly influence kinematic performance of the TKR system, possibly influencing long-term functional outcomes.

DEDICATION

To my grandpa, Dr. David Kershaw Stokes Jr., in memory.

You were the smartest, most hardworking, and caring person I have ever known.

I hope I make you proud in everything I do.

I love you and miss you, grandpa.

ACKNOWLEDGMENTS

TABLE OF CONTENTS

Table of Contents (Continued)

Table of Contents (Continued)

LIST OF TABLES

LIST OF FIGURES

Figures (Continued)

Figures (Continued)

CHAPTER ONE

GENERAL INTRODUCTION

The knee is characterized as a complex hinge joint that encompasses bones and surrounding soft tissues that control its function. The knee provides movement that is required for everyday activities like rising from a chair or walking. A knee can become damaged or diseased, resulting in pain and loss of function. At the end of the orthopaedic treatment spectrum, a total knee replacement (TKR) can be performed, and is now a common procedure to relieve pain, correct, deformity, and regain function. There are many types of TKR designs that can vary in kinematic stability and range of motion. During the procedure, both the load-bearing articular geometry and stabilizing cruciate ligaments are removed. The removed articular cartilage is often replaced with metal and plastic that mimics the load bearing capacity and geometric form of the knee. However, the removed cruciate ligaments are not replaced, and additional geometric constraints are often used within the knee design to compensate for the increased knee instability that results from the loss of cruciate function. So, unfortunately, no TKR design can fully restore native knee function, because once native anatomy is removed, it cannot be replaced.

In sports medicine, if a cruciate ligament is damaged it can be reconstructed using a graft substitute to regain function. But, during a knee replacement the cruciate ligaments are not replaced by a graft substitute. They are either substituted by the geometry of the implant or by a mechanical system. This thesis will discuss the design and initial testing of a TKR that incorporates artificial cruciate ligaments into its design

and the effect that these ligaments and their locations have on TKR kinematics. It will focus specifically on strain of the ligaments and anterior/posterior (A/P) translation. This work includes a literature review on the anatomy, pathology, and treatment methods of the knee and its soft tissues.

1.1 AIMS OF THE STUDY

The purpose of this study is to determine if synthetic ligaments can be incorporated into an existing TKR design and then to determine the effect of these ligaments' locations and lengths on initial stability. There are previous studies on TKR function and ligament location with ACL repair, but there is no previous research that combines the effects of ligament location with TKR performance. The first aim will be to design a TKR that incorporates synthetic ligaments. Next, this study will use computational modeling to determine the optimal ligament location and length for the knee replacement design by tracking strain of the ligaments and A/P translation. Then, this study will verify the computational model by constructing a physical prototype, and evaluating the performance of the device using mechanical testing to recreate the anterior drawer test and knee flexion. Using analyses from the computational model and mechanical testing, we hope to identify the optimal ligament location and length for this knee replacement design.

1.2 CLINICAL SIGNIFICANCE

There are over half a million total knee replacement (TKR) procedures performed each year in the United States and is projected to increase to over 3.48 million by 2030 (Kurtz, Ong, Lau, Mowat, & Halpern, 2007). Concurrent with the increase in number of TKRs is a trend of patients receiving knee implants under the age of 65 (Losina, Thornhill, Rome, Wright, & Katz, 2012). This is leading to a problem because patients under the age of 65 have a lower implant survival rate then patients over the age of 65 (Julin et al., 2010). There is therefore a need for an implant that has the stability and motion to withstand the active lifestyles of patients under the age of 65.

The development of a more functional TKR design can have a substantial clinical impact by providing a knee replacement option that allows patients of all ages to regain more normal function and perform more everyday activities.

CHAPTER TWO

KNEE ANATOMY AND PATHOLOGY

The knee is characterized as a complex hinge joint that allows the body to perform everyday movements. It is a complex system that is made up of different bones and soft tissues. Overtime the bones and soft tissues can wear down and become damaged or diseased, reducing knee function. This chapter focuses on the background of the knee, ligaments, kinematics and associated pathologies.

2.1 KNEE ANATOMY

The anatomy of the knee is reflective of its function as a complex hinge joint. The knee is composed of three bones that provide function: the femur, tibia, and patella as depicted in Figure 2.1. The distal end of the femur consists of medial and lateral condyles that articulate with the tibia and patella. The tibia articulates with the distal medial and lateral femoral condyles to form the tibiofemoral joint (Blackburn & Craig, 1980). The shape of the femoral condyles and the tibial plateau is important in guiding the movement of the tibia in relation to the femur. The patella articulates anteriorly to the femoral condyles in the region of the trochlear groove to form the patellofemoral joint (Blackburn & Craig, 1980). The patellofemoral joint allows the knee to flex more efficiently and protect the tibiofemoral joint (Waryasz & Mcdermott, 2008). These bones provide the structure of the knee, but there are additional soft tissues that assist with the articulation and stability of the knee joint.

Soft tissues that provide stability and create smooth surfaces for articulation include: menisci, articular cartilage, synovial membrane, and ligaments as depicted in Figure 2.1. The knee contains a pair of menisci, medial and lateral, that are fibrocartilaginous pads shaped like wedges that attach to the intercondylar area and periphery of the tibial plateau joint (Brindle, Nyland, & Johnson, 2001). The menisci widen and deepen the articulating surface between the femur and tibia in order to improve the congruency between the two articulating surfaces to help provide stability. The menisci also act as a shock absorber to resist compression in the knee joint (Brindle et al., 2001). Articular cartilage covers the surface of the bones in the knee joint, providing smooth articulation and cushioning during movement (Kuettner, 1992). When articular cartilage is damaged it can significantly impact the function of the knee by disturbing the smooth gliding surface needed for articulation. The synovial membrane surrounds the knee joint and secretes synovial fluid which transports nutrients to the joint, but more importantly lubricates the joint (Owellen M, 1997). There are additional soft tissue components of the knee that provide stability and guidance called ligaments.
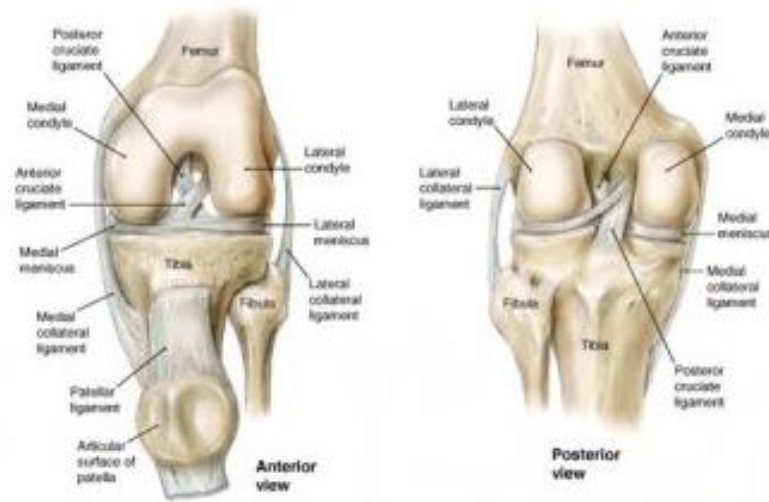
Figure 2.1 Structure of the knee joint (ChiroMatrix, 2016)

2.2 KNEE LIGAMENTS

The functions of the knee ligaments are to provide stability and guidance for the knee during flexion and extension by attaching the femur to the tibia. Ligaments of the knee are divided into two groups: the collateral and cruciate ligaments as depicted in Figure 2.1. Each group has its own role in order to allow the knee to function properly. To understand the function of the cruciate ligaments and collateral ligaments it is important to understand their anatomy and material properties.

Cruciate ligaments are located in the interior of the knee joint between the medial and lateral condyles and serve as the primary stabilizers to anterior and posterior movement of the tibia with respect to the femur. There are two cruciate ligaments: the anterior cruciate ligament (ACL) and the posterior cruciate ligament (PCL). The ACL and PCL are generically composed of two bundles each: the anteriomedial (AM) and posteriolateral (PL) bundles and anterolateral (AL) and posteromedial (PM) bundles

6

respectively. The AM and AL bundle are tight in flexion while the PL and PM bundles are tight in extension (Kweon & Lederman, 2013). The ACL insertion is located posteriorly on the medial aspect of the lateral femoral condyle and its origin is located on the anterior aspect of the tibial spine (Nissman D, 2008). The PCL insertion is located anteriorly on the lateral aspect of the medial femoral condyle and its origin is on the posterior eminence of the tibia (Nissman D, 2008). The insertion and origin of the ACL and PCL are opposite of each other allowing them to work together to create a four bar linkage in seen in Figure 2.2 (Kweon & Lederman, 2013). The ACL prevents anterior translation of the tibia with respect to the femur while the PCL prevents posterior translation. The ACL ranges from 31 to 38 mm in length and 10 to 12 mm in width. The average PCL length and width are 32 to 38 mm and 13 mm respectively (Kweon & Lederman, 2013). The ligaments can experience strain up to 8-10% before rupturing (Withrow, Huston, Wojtys, & Ashton-Miller, 2006). The insertion and origin of the cruciate ligaments, as well as their lengths, play a major role in their function to maintain the anteroposterior relationship between the femur and tibia (Nissman D, 2008).

(a) Straight leg (b) 45 degrees bent (c) 90 degrees bent
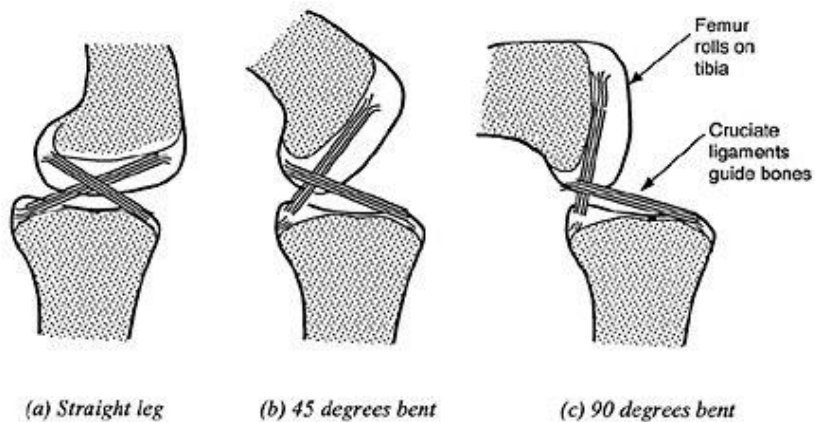
Figure 2.2 Cruciate ligaments functions as 4 bar linkage (Burgess, 1999)

Collateral ligaments are located exteriorly on the sides of the knee joint in order to provide primary stability in varus and valgus angulation of the tibia with respect to the femur. There are two collateral ligaments: the lateral collateral ligament (LCL) and the medical collateral ligament (MCL). The LCL insertion location is on the outside of the lateral femoral condyle and its origin is on the proximal head of the fibula. The MCL insertion is outside and slightly posterior to the center of the medial femoral condyle and its origin is on the medial side of the tibia approximately 6 cm distal to the join line (LaPrade et al., 2007). The average length for an LCL and MCL is 54 mm and 87 mm respectively (Park et al., 2005). The LCL resists varus forces and the MCL resists valgus forces in order to provide stability in the frontal plane of the knee. The combination of the cruciate and collateral ligaments provides the primary source of stability within the knee.

Ligaments are constituted by a water rich ground substance reinforced with collagen fibers, which creates a gel of high water content when stretched, providing a high resistance to tension (Galbusera et al., 2014). Knee ligaments are non-linear viscoelastic bands of soft tissue (Galbusera et al., 2014). When measuring load-elongation behavior, ligaments have an initial toe region with low stiffness and non-linear response due to collagen fibers extending easily. Following the trend, ligaments with stretched collagen fibrils have a higher stiffness (Galbusera et al., 2014). A ligament's toe region of low stiffness is from 0-2% strain and the linear region of high stiffness is from 2-6% as depicted in Figure 2.3 (Woo et al., 1991). A ligament's ultimate strain varies from patient to patient and is around 8-10% (Withrow et al., 2006). During normal knee flexion, a

ligament strains between 2-5% (Withrow et al., 2006). Stiffness of the ligaments in the linear region are found to be 242 (± 28) N/mm. The ultimate load of ligaments is found to be 2,160 (±157) N (Woo et al., 1991). The average modulus and ultimate tensile strength are measured to be 278 and 35 MPa respectively (Woo et al., 1991). As patients get older their ligament material properties decrease resulting in decrease stability and function of the knee.
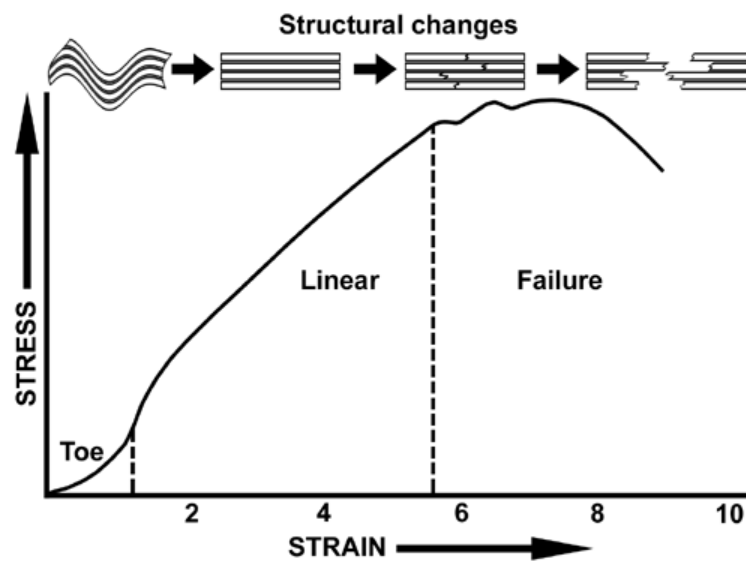
Figure 2.3 Biomechanical properties of ligaments for stress vs strain (Lenard, 2014)

The ACL is the primary restraint to anterior tibial displacement and a secondary stabilizer of tibial rotation. ACL experiences its maximum force and length at 15 degrees and continually decreases until 90 degrees of flexion. From 30-90 degrees the ACL provides 80% of the anterior restraining force (Dargel et al., 2007). The PCL is the primary restraint to posterior tibial displacement and provides proprioceptive function to the knee (Eguchi et al., 2014). PCL tension and length increase as the knee flexion

increases. The PCL experiences its peak elongation between 90-120 degrees. The PCL begins to shorten when the knee is flexed greater than 120 degrees (Papannagari et al., 2007). The MCL is the primary resistant to valgus motion as well as a secondary stabilizer for anterior displacement. The MCL elongates and provides stability from 0-90 degrees but, at greater than 90 degrees, the MCL decreases its length sharply (Hosseini et al., 2014). The LCL is the primary restraint to varus motion. The LCL does not change its length significantly from 0-90 degrees of flexion, but begins to elongate when knee flexion exceeds 90 degrees (Hosseini et al., 2014). The individual properties of each ligament combine to provide stability for the normal knee.

2.3 KNEE JOINT KINEMATICS

The knee has six degrees of freedom (DOF) characterized as 3 rotations (flexion and extension, external and internal rotation, varus and valgus angulation) and 3 translations (anterior posterior glide, medial and lateral shift, compression and distraction) as depicted in Figure 2.4 (Komdeur, Pollo, & Jackson, 2002). The 6 DOF allows for up to 140 degrees of flexion and -5 degrees of extension in a normal knee, which is enough to perform daily movements. The 6 DOF also allow the knee to have 8-13 degrees of varus-valgus movement, 25-30 degrees of internal-external rotation, and 3-5 mm of anterior-posterior translation during normal activities (Levangie & Norkin, 2005).
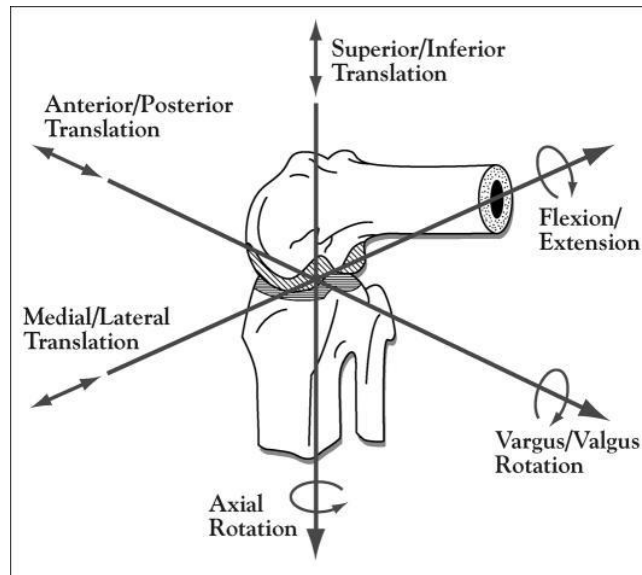
Figure 2.4 Six degrees of freedom of the knee joint (Komdeur et al., 2002)

During flexion-extension, the femur moves about the center of rotation, a horizontal line passing through the femoral epicondyles (Levangie & Norkin, 2005). Although the axis of the center of rotation represents an accurate estimate of the axis for flexion-extension, the axis is not fixed and shifts throughout motion due to the incongruence of joint surfaces. The initiation of knee flexion (0- 25 degrees) occurs primarily as posterior rolling of the femoral condyles on the tibia shifting the contact point posteriorly on the tibia. As flexion continues past 25 degrees, the femoral condyles continue to roll and begin to glide anteriorly which creates a pure spin of the femur (Levangie & Norkin, 2005).

In order for a knee to follow this path during flexion-extension, two actions must occur: femoral rollback and screw-home mechanism. Femoral rollback is when the femur rolls posteriorly on the tibia in the first 25 degrees of flexion in order to increase the

potential for further flexion by preventing posterior structures from impingement as depicted in Figure 2.5. Screw-home mechanism is the prolonged anterior glide of the medial condyle that produces an external tibial rotation during the last 30 degrees of knee extension (Levangie & Norkin, 2005). This mechanism locks the knee in place to provide it with stability in full extension. These two motions allow the knee to perform greater degrees of flexion-extension without running into interference.

2.4 LIGAMENT KINEMATICS

A central component of this thesis is how ligaments might be able to influence the stability of a TKR system. Anteroposterior displacements, medial-lateral displacements, axial rotations, and valgus-varus displacements occur in the normal knee as a result of variations in ligamentous elasticity. These translations are necessary for normal joint motions to occur; however, excessive translational motions are considered abnormal and indicate damage to a ligament (Levangie & Norkin, 2005). Without ligaments, the knee can have excessive translation, which can result in damaging kinematics to the knee. TKR systems often show excessive laxity and it is a primary cause for TKR revision. Laxity is considered the amount of movement that the knee has between the femur and tibia. Excessive laxity is when the knee does not provide enough constraint where the femur and tibia move a significant amount about one another that the knee becomes damaged. Ligaments are the primary source of constraint in the knee. Constraint is considered the stability needed to counteract forces about the knee. It is imperative that a

TKR system have a combination of both laxity and constraint, whether this comes from ligaments or additional material.

Femoral roll back and screw home mechanism of the normal knee require ligaments to obtain natural kinematics. During flexion, the femur rolls posteriorly on the tibia as far as anatomically possible. The ACL elongates until it becomes taut around 20 degrees of flexion, preventing further femoral roll back, to keep the femur from rolling off the posterior aspect of the tibia (Levangie & Norkin, 2005). ACL holds it length constant between 20 and 30 degrees of flexion as it has reached it maximum elongation. ACL decreases in length, becomes lax, as the knee continues to flex past 30 degrees of flexion (Hosseini, Gill, & Li, 2009). PCL increases in length constantly from 0 to 90 degrees of flexion and then slowly decreases its length as the knee flexes beyond 90 degrees as seen in Figure 2.5 (Nakagawa et al., 2004). During extension, the PCL becomes taut, preventing further anterior progression of the femur to keep the knee from hyperextending (Levangie & Norkin, 2005). As the ACL and PCL control the anterior and posterior progression of the tibia and femur, they limit the AP translation to 3-5 mm during normal activities (Galbusera et al., 2014). However, if an external force is applied to the knee, the ligaments can allow up to a total of 13 mm of AP translation (Un et al., 2001). In the last 30 degrees of extension, the knee joint rotates, a result of the screw-home mechanism, allowing the knee to become locked. Muscles drive this motion, but increasing tension in the cruciate ligaments also contributes to the rotational motion. Medial/lateral displacement and varus/valgus rotation are not common but can occur if ligaments become lax. The MCL and LCL, as well as surrounding muscles, help restrict

13

these motions (Levangie & Norkin, 2005). The interaction between the ligaments, contributing to overall knee stability, is crucial, and damage to one or multiple ligaments can affect knee stability and kinematics significantly.
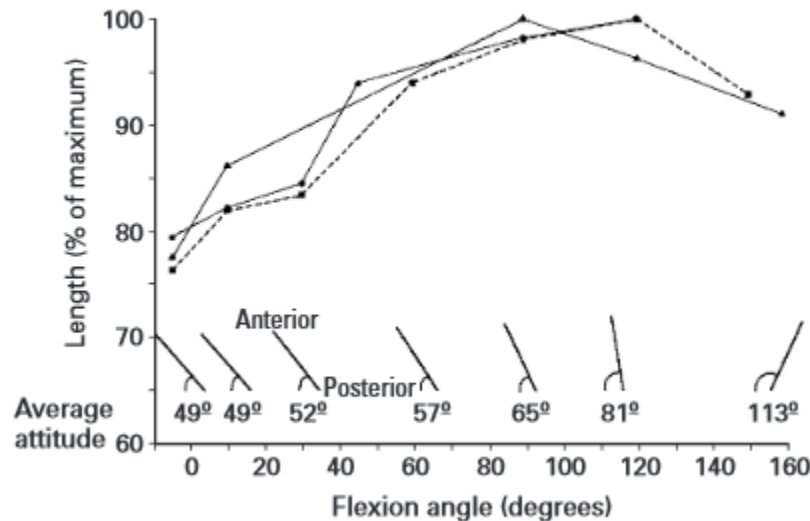
Figure 2.5: PCL length percentage during flexion (Nakagawa et al., 2004)

2.5 KNEE PATHOLOGIES

The knee joint is one of the most used joints in the body making it a high risk for injury. Knee pathologies can occur acutely, such as injuries when playing sports, or they can occur chronically, such as degradation of the knee joint. There are a wide range of knee pathologies, but this section focuses on the common injuries where chronic pain is experienced. In a later section, knee ligament injuries will be discussed.

Knee pathologies are common in soft tissues within the knee: ligaments, menisci, and patella. Ligament injuries include ACL, PCL, MCL, and LCL tears and will be

14

discussed in more detail later in the paper. Meniscal tears are normally non-contact and occur while cutting, decelerating, or landing from a jump (Rath & Richmond, 2000). Meniscal tears are due to a combination of compressive and rotational tibiofemoral joint forces (Brindle et al., 2001). If the meniscus is not repaired within eight weeks of the injury, it can lead to degeneration of the knee (Rath & Richmond, 2000). Patellar injures consist of both dislocations and tears that are diagnosed as Patellofemoral Pain Syndrome (PFPS). PFPS is a variety of patellar pathologies that can cause anterior knee pain. PFPS commonly is due to degradation or disease of the cartilage of the patella which can cause chronic pain of the knee (Waryasz & Mcdermott, 2008).

Osteoarthritis (OA) is the most common knee pathology that affects more than 20 million individuals in the United States. It is a degenerative disorder due to the biochemical breakdown of articular cartilage and subchondral bone. Many consider OA a degenerative disease; however, recently OA has been determined to be caused by abnormal mechanics and inflammation of the cartilage which is not considered degenerative (Dieppe, 2011). OA causes a loss of joint space which leads chronic pain. Over 50% of adults older than 65 years are affected by OA, making it a major focus for the medical field.

2.6 KNEE TREATMENTS

Treatment options for knee injuries depend on the type of injury, but most injuries require surgery and then rehabilitation to regain function. The nature of a meniscal tear will determine if the meniscus should be repaired or resected. If the meniscus can be

repaired, a vertical suture is considered the gold standard because they provide strength and stiffness (Stärke, Kopf, Petersen, & Becker, 2009). If the meniscus cannot be repaired, then a meniscectomy is performed to remove the meniscus. Surgeons avoid performing meniscectomies because there is an increased risk of developing OA (Stärke et al., 2009). Patellar injuries are commonly diagnosed as Patellofemoral pain syndrome (PFPS); unfortunately, there is not surgical treatment for PFPS (Petersen et al., 2014). Surgeons have tried performing arthroscopy in the past, but there was no positive effect compared to physiotherapy. Currently treatments for PFPS include physiotherapy and orthotics (Petersen et al., 2014).

Osteoarthritis is the most common knee pathology that encompasses a range of possible treatments depending on the severity of the disease. The goals of osteoarthritis treatments are to alieve pain and improve function. Treatment options can be preventive, pharmacologic, or operative which include weight loss, Acetaminophen, and arthroplasty, respectively. There are plenty of treatment options for osteoarthritis, but the most effective treatment is a total knee arthroplasty.

2.7 LIGAMENT PATHOLOGIES

Injuries to ligaments in the knee are common and can often lead to loss of function of the knee. The ACL is the most commonly injured ligament in the knee. ACL injuries occur when the tibia travels anteriorly on the femur until the ACL ruptures (Gianotti, Marshall, Hume, & Bunt, 2009). This injury can lead to a loss of stability both anteriorly and rotationally. In order to assess the injury an anterior drawer test and a pivot

shift test are performed (Ferretti, Monaco, & Vadalà, 2014). Most of the time when an ACL is injured, other ligaments are affected as well, leading to a loss in function of the knee. The other ligaments that can be damaged as well are the PCL, MCL, and LCL. Injuries to the PCL occur when the tibia travels posteriorly on the femur until the ligament ruptures. This injury can lead to a loss of posterior stability. In order to assess the injury a posterior drawer test is performed (Fanelli & Edson, 1995). MCL injury is one of the most common knee injuries in young patients. This injury occurs when the knee experiences a high valgus stress, external force to outside of knee, or external rotation (Phisitkul, James, Wolf, & Amendola, 2006). Injury to the LCL can occur due to high varus stresses, external force to inside of knee, or rotational force. Injury to the LCL leads to rotational instability.

2.8 LIGAMENT TREATMENTS

Treatments for ligament injuries depend on the extent of the injury and the patient. In all cases, the focus of the treatment is to provide stability for the knee through surgery or rehab in order to prevent further damage due to the lack of stability. The most common ligaments that require surgical repair are the ACL and PCL. When one of the cruciate ligaments is torn they are replaced arthroscopically with a graft. These grafts include: bone-patellar tendon-bone, hamstring autograft, allograft, and synthetic grafts. It is projected that the future graft for the cruciate ligaments is a synthetic graft the can mimic the properties of a normal ligament more accurately (Bach, 2009). Most collateral ligaments can be treated non-operatively by rehabilitative devices and bracing the knee

(Chen, Kim, Ahmad, & Levine, 2008). The important thing to note is when a cruciate ligament is torn it has to be replaced in order to return function to the knee and prevent future damage.

2.9 LIGAMENT BIOMECHANICS BEFORE AND AFTER REPAIR

In the 2013 study by Angoules et al., they examined anterior-posterior knee laxity of 40 patients who had torn their ACL (Angoules, Balakatounis, Boutsikari, Mastrokalos, & Papagelopoulos, 2013). 20 of the patients underwent reconstruction using four-strand hamstrings, and 20 underwent reconstruction using bone-patellar tendon-bone autografts. Using a KT-1000 arthrometer, knee instability was calculated in both knees of patients preoperatively and 3, 6, and 12 months after ACL reconstruction. They measured stability at 30 degrees of flexion with external forces of 89 N. They measured 6.7 ± 1.95 mm of displacement in ACL-deficient knees and 2.0 ± 1.21 mm in the patient's healthy knee. They also measured 3.1 ± 1.29 mm of displacement 3 months after surgery using hamstrings and 1.95 ± 1.39 mm of displacement using bone-patellar tendon bone (Angoules et al., 2013). This information is influential for this study because it characterizes the laxity of an ACL deficient knee and provides a range of laxity for acceptable repair.

CHAPTER THREE

TOTAL KNEE REPLACEMENTS

The most common treatment option for osteoarthritis is total knee replacements (TKR), which can relieve pain and regain function in a knee for 10-20 years. Total knee replacements are primarily performed in patients over the age of 65. Recently, there has been a trend of younger patients between the ages of 50 and 65 receiving TKRs (Julin et al., 2010). There are many different TKR designs that allow patients to obtain stability or motion. However, there is not a TKR design that allows patients to regain stability and motion that younger patients need to maintain their active life styles.

3.1 TOTAL KNEE REPLACEMENTS SURGICAL PROCEDURE

Total knee replacements consist of three main parts: femoral component, tibial plate, and polyethylene insert. The femoral component is typically a cobalt chromium material, the tibial base plate is titanium or cobalt chromium, and the polyethylene insert is UHMWPE (Castiello & Affatato, 2015). There are a variety of designs that have additional parts, but the most common TKR have these three parts. These parts are large and require an invasive procedure that removes bone and soft tissue in order to allow the implant to fit.
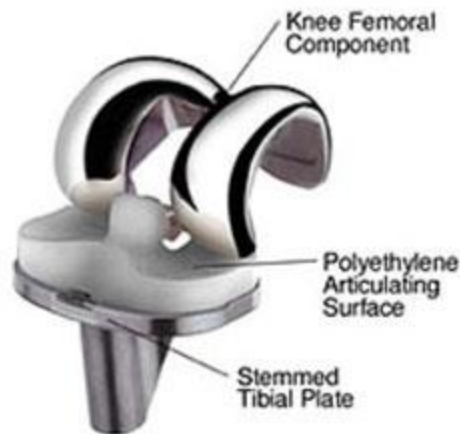
Figure 3.1 Three main parts of a TKR: femoral component, tibial plate, and polyethylene articulating surface (Windsor & Padgett, 2013)

Total knee replacement surgery is an open operation that begins with the surgeon making a large incision over the front of the knee joint approximately 4-6 inches long. The surgeon then moves the patella to expose the knee joint. The damaged cartilage and bone on the femur is removed by cutting the knee to fit the femoral component (Castiello & Affatato, 2015). The femoral component is then placed in the knee where the bone was cut away and often secured by bone cement. The tibia is then resurfaced, beginning with the removal of damaged cartilage and bone from the proximal end. When the tibia is resurfaced, the ACL footprint is usually removed and depending on the case the PCL footprint is removed. This causes the ACL to be removed in almost all procedures and the PCL to be removed for cruciate sacrificing implants (Houston Methodist, 2014). The tibial baseplate is then placed on the tibia and usually secured by bone cement. Once the tibial baseplate is held in place, the polyethylene insert is snapped into the tibial

baseplate. In some cases, before the patella is moved back, it is resurfaced with a UHMWPE button to create a second articulation with the rest of the femoral component. Before the knee is closed, it is flexed and rotated to insure the knee has an appropriate range of motion and stability. The process of ligament balancing refers to the idea that during these range of motion and stability tests, residual ligaments such as the LCL, MCL, and sometimes the PCL need to function in harmony with the new implant surfaces. Usually this means that the ligaments should not become too taut during these motions and restrict knee motion, and to a lesser extent, they need to guide knee motion and restrict the extremes of knee motion. Regardless, if the ACL and PCL are removed and not replaced, it can affect the overall function of the knee (Houston Methodist, 2014).

3.2 TOTAL KNEE REPLACEMENT DESIGNS AND FUNCTIONS

There is a wide range of patients with different life styles that require a total knee replacement. In order to satisfy the different needs for each patient, there is a variety of TKR designs that have different functions to help the patient get back to their lifestyle. TKR designs can vary in mobility, stability, and ligament sacrificing. Depending on the patient's lifestyle, the surgeon will choose a TKR to best allow the patient to return to their activities of daily living.

Current total knee replacements can be subdivided into two groups based on different fundamental design principals: fixed-bearing knees and mobile-bearing knees. Fixed-bearing knee replacements have the polyethylene insert locked with the tibial baseplate. Mobile-bearing knee replacements allow movement of the polyethylene insert

relative to the baseplate (Huang, Liau, & Cheng, 2007). Implant loosening and polyethylene wear in fixed-bearing knees are recognized as a major cause of failure. These problems in the fixed-bearing knee are due to the kinematic conflict between low-stress articulation and free rotation (Huang et al., 2007). As discussed, the femoral condyles rotate and translate about the tibia, so with the polyethylene fixed, it is not able to withstand these forces and it fails. Mobile-bearing knees were designed to reduce polyethylene wear and implant loosening by adding mobility in the tibiofemoral surface. This design allows low contact stress and constraint force by solving the kinematic conflict of high conformity with free rotation (Huang et al., 2007). The main risks with mobile-bearing knees are the increased occurrence of dislocations. Hypothetically, the mobile bearing knee looks to have a higher success rate then the fixed-bearing knee; however, the clinical success rates between the two are similar. It has been suggested that a fixed-bearing knee should be implanted for an older inactive person, and a younger more active person should receive a mobile-bearing knee (Huang et al., 2007).

Total knee replacements can be further subdivided into three groups: PCL retaining, PCL sacrificing, or PCL substituting as depicted in Figure 3.2 (Huang et al., 2007). PCL retaining knees keep the anatomical PCL intact but remove the ACL. PCL sacrificing knees remove both the ACL and PCL, but do not substitute either ligament. Instead, it uses a doubled dished articular geometry to control kinematics (Harwin & Kester, 2010). PCL substituting knees remove both the PCL and ACL, but replace them with a mechanical mechanism like a CAM system. Potential advantages of PCL retaining knees include preservation of bone, more normal knee kinematics, increased

proprioception, femoral rollback, and greater stabilization (Kolisek et al., 2009). Potential advantages of PCL sacrificing knee include easier correction of deformity, a better range of motion, predictable kinematics, and early return of range of motion (Harwin & Kester, 2010). PCL substituting knee designs include a less technically demanding procedure, a more stable component interface, and increased range of motion (Kolisek et al., 2009). Clinical studies have shown that PCL substituting knees do have an increased range of motion over PCL retaining knees (131 degrees to 122 degrees) while maintaining more stability. PCL substituting knees did not allow for any anterior translation while the PCL retaining knees did translate anteriorly between 30-60 degrees. For this thesis it is important to note several things (Kolisek et al., 2009). First, the stability of the implants was obtained in one of two ways: geometry with the polyethylene or with ligaments (intact and CAM system). Secondly, stability of the knee was never recreated with the PCL substituting, for it was too stable, and the PCL retaining did not have enough stability. Thirdly, the full range of motion of 140 degrees of flexion was not fully returned in any of the designs, but the PCL substituting was the closest with 131 degrees of flexion. Finally, anatomical kinematics, like femoral rollback and anterior translation, is not fully returned in any of the designs. All of these designs have good results, but there is room for improvement to design knee implants that have greater stability and range of motion.
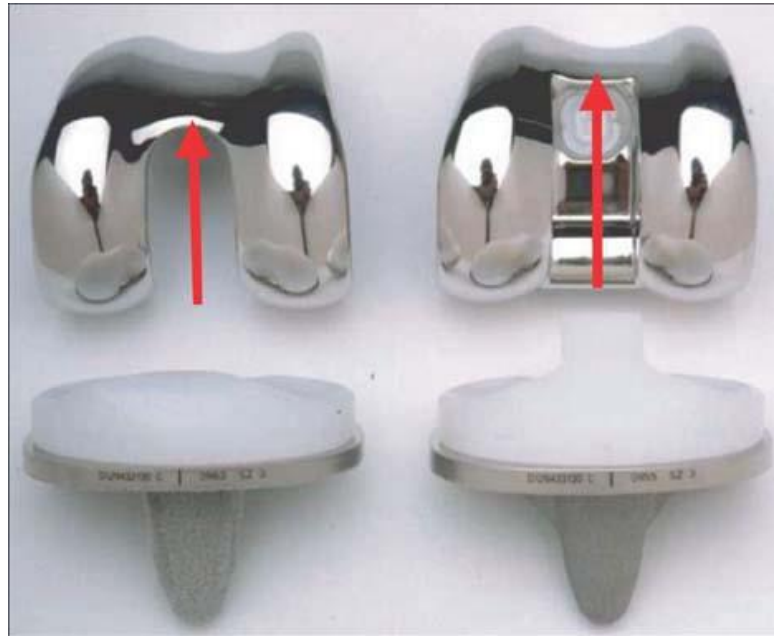
Figure 3.2 Cruciate retaining implant (left) vs posterior stabilized implant (right)

(Conrad & Dennis, 2014)

Bi-cruciate retaining knee replacements maintain both the ACL and PCL. The implant is designed by splitting the tibial baseplate into two parts, a medial and a lateral side. Potential advantages of a bi-cruciate retaining knee include preserving ligaments, minimizing bone resection, and limiting constraint to allow for more natural movement of the knee compared to other implants (Pritchett, 2015). By maintaining more of its natural anatomy, the knee can maintain more natural kinematics such as physiologic femoral rollback and external rotation with knee flexion (Banks et al., 2003). In younger patients with intact cruciate ligaments, bi-cruciate knee replacements appear to be a viable option due to maintaining more natural kinematics, preserving more of the natural anatomy, and allowing higher functionality (Banks et al., 2003). A few drawbacks of the

bi-cruciate TKR systems are that they are difficult to implant and align when there is anatomical deformity, depend on the integrity of the native ligaments and their boney attachments, and that they have more dimensionally complex tibial tray and UHMWPE inserts which could lead to early failure from loading and fatigue.

3.3 JOURNEY II KNEE

The Smith and Nephew Journey II Knee is used for experiments throughout this thesis. The Journey II TKR is a common choice clinically and can be bi-cruciate sacrificing (BCS) or PCL retaining (CR). The Journey II BCS has an asymmetrical tibial plateau and anterior and posterior cams designed to control tibiofemoral kinematics to duplicate the movements of the natural knee more closely than other TKR's and the Journey II CR knee (Halewood, Risebury, Thomas, & Amis, 2014). The Journey II BCS is indicated for more active patients due to its increased tibial anterior laxity (ability to move) and internal rotation during knee flexion, as well as reach knee flexion angles of up to 155 degrees. However, there has been a high incidence of patients reporting knee pain and adverse events with the Journey knee (Halewood et al., 2014). The problems have been attributed to excessive femoral rollback and internal rotation of the tibia during flexion due to the excessive laxity (Halewood et al., 2014). It could be hypothesized that even though the Journey II knee has a similar knee flexion and greater AP translation than a normal knee, it lacks the stability to withstand activity without causing damage.

3.4 KNEE REPLACEMENT COMPLICATIONS

Total knee replacements are one of the most successful orthopaedic procedures that have high patient satisfaction. However, failure remains a complication that can require a revision surgery. The three most common long-term complications with total knee replacements are wear, aseptic loosening, and instability. Two primary factors that affect wear are conformity and material. Highly conformed polyethylene inserts have a wear rate three times higher than that of low conformity polyethylene inserts. Wear rates for moderately cross-linked UHMWPE have less than half of that of conventional UHMWPE (Abdelgaied et al., 2014). Wear can lead to significant implant and systemic problems but these issues do not occur until several years after implantation. Aseptic loosening has become more of a complication recently as high flexion TKR designs have been developed. High flexion designs increase the stress imposed on the femoral component during deep flexion. This leads to the loosening complications that require revision procedures (Bollars et al., 2011). One of the most common knee complications is instability.

At this point, it is important to note the differences between kinematic instability and implant-bone interface instability. This thesis focuses on kinematic instability, which is a result of the articulation between the implant surfaces, and is affected by implant alignment, loading, geometry and ligamentous constraint. Implant-bone instability describes loosening of the implant-bone interface, and is often the result of wear-induced bone resorption, called osteolysis. Osteolytic instability is a long-term complication, and not the focus of this work.

Instability complications are a key idea throughout this thesis. 22% of TKR revisions are due to instability problems. Knee instability is the abnormal and excessive displacement of the femoral component (Rodriguez-Merchan, 2011). Instability can be caused by malalignment of the components, improper balancing of the ligaments, or rupture of a ligament or tendon. Anteroposterior instability is seen most often in cruciate retaining ligament designs, so cruciate substituting designs are used for patients at risk of instability. Instability of the knee can be prevented in most cases with an adequate selection of implants and good ligament balancing (Rodriguez-Merchan, 2011). Even though knee replacements do a successful job of relieving pain and regaining function, they create additional complications. This leaves room for improvement in the TKR design field.

3.5 TOTAL KNEE REPLACEMENT STANDARDS

Total knee replacements have been used since the early 1970's. With their development, have been a number of tests and standards developed to assist in the characterization of TKR stability, kinematics and performance. These standards are developed by the American Society for Testing and Materials (ASTM Standard F1223, 2014). The standard that this thesis is focusing on is ASTM F1223-14, "Standard Test Method for Determination of Total Knee Replacement Constraint." This test method covers the establishment of a database of TKR motion characteristics with the intent of developing guidelines for the assignment of constraint criteria to TKR design (ASTM Standard F1223, 2014). The tests deemed applicable to the constraint determination of

anteroposterior drawer, mediolateral shear, rotary laxity, varus-valgus rotation, and distraction. Laxity is considered the amount of movement that the knee has between the femur and tibia. Excessive laxity is when the knee does not provide enough constraint where the femur and tibia move a significant amount about one another that the knee becomes damaged. Constraint is considered the stability needed to counteract forces about the knee.

An anteroposterior drawer test is performed to determine AP laxity. This begins by setting the movable component in a fixture free to move in linear directions parallel to the x-axis only (ASTM Standard F1223, 2014). Before starting the tests, lubricant needs to be applied to the surfaces to reduce frictional effects. Applying a compressive force of 100 N and marking where the implant settles determines the neutral position. Then, a 710 N joint reaction force is applied. When the test is performed, AP motion of 10 mm/second and 10 degrees/second for rotation is not exceeded (ASTM Standard F1223, 2014). For the AP laxity test, the external force is applied slowly and the AP displacement (mm) and force (N) is recorded (ASTM Standard F1223, 2014). ASTM F1223 is used to determine TKR constraint during in-vivo test, but the test setup can also be used for in-vitro and computational studies.

CHAPTER FOUR

ARTIFICIAL LIGAMENTS

Synthetic ligaments became popular in the 1980s as an alternative to allografts for ACL reconstruction. The draw to the synthetic ligaments was the lack of harvest site pathology, abundant supply, and significant strength. Synthetic ligaments are made of different materials such as carbon fiber, polypropylene, Dacron, and polyester (Legnani, Ventura, Terzaghi, Borgo, & Albisetti, 2010). Different procedures and various materials have been used over the years contributing the use of artificial ligaments as a therapeutic option in knee surgery.

4.1 MATERIAL HISTORY

Artificial ligament materials began with carbon fiber in the 1970s as a substitute for human tissue. The first two synthetic ligaments were Proplast ligaments made of Teflon and carbon and Polyflex made of polypropylene. Both products were withdrawn from the market due to their high rupture rate and inflammatory reaction. The significant side effects of carbon fiber resulted in it being abandoned as a material option (Legnani et al., 2010).

In the mid-1980s, Gore-Tex, expanded polytetrafluorethylene (PTFE), was approved by the FDA to use as an artificial ligament. Gore-Tex has an ultimate tensile strength of 5300 N, stiffness of 322 N/mm, and ultimate strain of 9 % providing excellent stability in the knee immediately. However, long-term results of Gore-Tex were poor due to mechanical fatigue from the lack of tissue ingrowth. In 1993, Gore-Tex was removed

from the market and abandoned as a material due to its long term instability (Legnani et al., 2010).

In 1989, Dacron, composed of polyester, was used as a synthetic ligament graft. It has an ultimate tensile strength of 3,631 N, stiffness of 420 N/mm, and an ultimate elongation of 18.7%. Initial results were good short term; however, long term the ligament experienced over a 35% fail rate. In 1994, Striker removed Dacron from the market (Legnani et al., 2010).

The only materials implanted recently were polyester composites like the Trevira-hochfest. Trevira-hochfest has been used the most by orthopaedic surgeons. The Trevira ligament has been implanted since 1980. It has an ultimate tensile strength of 1,866 N and a stiffness of 68.3 N/mm. The Trevira has shown good long-term results with only 16% of patients having anterior instability greater than 5 mm after 8 years of implantation. There have been reports of failures with this graft due to bone impingement leading to fiber damage. Polyester ligaments are still used today, but with limited use due to the lack of trust in synthetic ligaments by the orthopaedic community (Legnani et al., 2010).

Recently there has been a resurgence of interest in the use of artificial ligaments due to the new artificial ligament, Ligament Advanced Reinforcement System (LARS). LARS is made of polyethylene terephthalate that allows for tissue ingrowth. Early results of LARS compare favorably to autologous grafts. Studies advocate that LARS ligament could lead to high activity levels but the long term results are still needed (Legnani et al.,

2010). Thanks to this new improvement, the orthopaedic community is attempting to regain their trust in artificial ligaments.

4.2 TELOS KOSA-HOCHFEST LIGAMENT

The KoSa-hochfest ligament by Telos is one of the few artificial ligaments in current use by the orthopaedic community. KoSa-hochfest is the former Trevira ligament made out of polyethylene terephthalate (PET) mentioned above that is still used. This thesis focuses on the KoSa ligament because it was used in the studies talked about later. The tensile strength of the KoSa ligament is significantly greater than a natural cruciate ligament, so as to compensate for the expected fatigue of the material. The ligament is twisted at a defined pretension to give it a modulus of elasticity equivalent to that of a natural cruciate ligament. KoSa Ligament has a flat structure that allows the surgeon to twist the ligament in the joint space while laying it flat at the exit tunnels. The ligament comes in different sizes, but the size used for cruciate reconstruction is 8 mm wide x 300 mm long. Other polyethylene terephthalates have been used in the past and failed, but the KoSa Synthetic Ligament has been successfully used since 1980 (Telos, n.d.).

CHAPTER FIVE

PRIOR COMPUTATIONAL AND MECHANICAL STUDIES

Computational modeling and mechanical testing have become common practices for evaluating knee replacement and ligament function. Computational models help to better understand clinical problems like ligament balancing with TKR surgery and ligament function with ACL repair. Mechanical studies are often used to verify these computational studies, as it is difficult to fully model the real-life conditions of the anatomy and environment of use. It is important to review previous computational studies in the area of TKR mechanics and ligaments to better understand the current model and testing setup of this study.

5.1 COMPUTATIONAL STUDIES

One of the main challenges in bi-cruciate retaining arthroplasty is proper ligament balancing. In a 2012 study by Amiri et. al, they focused on evaluating the biomechanics of ligament balancing using a computational model of the knee joint that simulated intraoperative balancing of ligaments. Knee laxity was evaluated based off of anterior-posterior, internal-external, and varus-valgus loads. The results were compiled into a map of sensitivity for all ligament bundles to determine the components of laxity most suitable for examination during intraoperative balancing (Amiri & Wilson, 2012). The computational model was built by first laser scanning a cadaveric specimen and generating a stereolithography (STL) mesh file of the articular surfaces of the tibia and femur. The STL files were then inserted into MSC.ADAMS/View 2003 computer

software to construct the model. Six ligament groups were considered including ACL, PCL, LCL, sMCL (superficial medial collateral ligament), dMCL (deep medial collateral ligament), and PMC (posterior medial capsule). The attachment locations for each ligament were chosen based on literature and the footprints from the STL scan. A non-linear force-displacement relationship was used to define the deformation of the spring elements in the ligaments. A 100 N external force was applied to determine the anterior-posterior laxity. Laxity was tested at 0, 30, 60, 90, 120 degrees of flexion. Variables that were evaluated at each angle were the stiffness, attachment, location, and reference strain (Amiri & Wilson, 2012). The study by Amiri and Wilson concluded that it is important to consider multiple degrees of freedom in balancing soft tissues during knee arthroplasty. They concluded that AP laxity is sensitive to ACL tensioning, which is correlated to reference strain. It was determined that AP laxity is affected by variations in strains of all the ligament bundles, and based on this work, the authors created an intra-operative plan for soft tissue balancing (Amiri & Wilson, 2012). The Amiri & Wilson study was informative for the work in this thesis because it provided values for modeling the ACL, PCL, LCL, and MCL. If the study would have published their finding for anterior-posterior laxity at all angles, it would have made their work easier to relate to this thesis. Their work also came to a conclusion that AP laxity is affected by ACL tensioning which is hypothesized in this thesis.

In a 1991 study by Blankevoort et al., they analyzed the effect of articular contact on the passive motion characteristics in relation to experimentally obtained joint kinematics. Two different mathematical contact descriptions were compared: rigid

contact and deformable contact. A model was created by positioning the femur relative to the tibia after solving an equilibrium equation for force and moments. The locations of the ligament insertions were determined from a joint specimen. The ligaments were modeled as non-linear elastic line elements. Mechanical properties of ligaments were modeled using a non-linear equation that comprised of variables such as stiffness and reference strain. Once the model was created, the rigid contact and deformable contact were analyzed. A parametric model showed that deformable contact did not alter the motion compared to the rigid contact. The data show as the surface stiffness decreased the ligaments became lax (Blankevoort & Huiskes, 1991). The Blankevoort & Husikes study was influential to the work in this thesis by providing additional information to the equations used to model ligaments and surface contacts to better understand how to incorporate them into AnyBody.

In order to understand the kinematics of the knee, it is important to understand the properties and functions of ligaments. To better understand ligaments and their function, research has become focused on computational modeling. Ligaments are among the most complicated structures to simulate, and at the same time, the most critical in determining the biomechanics of the knee (Galbusera et al., 2014). An integral part of the computational model for this project was creating ligaments with normal biomechanical properties. In order to create the most accurate ligament properties a review of previous models was put together below. The most common method to model ligaments is to use 1D elements while other methods use 2D or 3D elements. 1D models consist of line elements such as springs, trusses, and beams to resemble the mechanical role of the

ligaments. Springs are most commonly used for 1D models. The ligaments are modeled as non-linear springs consisting of a toe region initially and a linear spring afterward. This behavior is formulated as follows in equation 1:

$$
\begin{aligned}
f &= \tfrac{1}{4} k \tfrac{\varepsilon^2}{\varepsilon_l}, & 0 \le \varepsilon \le 2\varepsilon_l \\
f &= k(\varepsilon - \varepsilon_l), & \varepsilon > 2\varepsilon_l \\
f &= 0, & \varepsilon < 0
\end{aligned}
\tag{1}
$$

Where f is the axial force sustained by the ligament, k is a stiffness parameter, ε is strain, and $2\varepsilon_l$ is the threshold strain, which indicates the change from the toe to the linear regions (Galbusera et al., 2014). Another important variable that is not shown in this equation is the reference strain or initial strain, ε_0. This strain value indicates what the ligament properties are when at full extension. Common values used for modeling the ACL are: k=5000N, ε_l=0.03, and ε_0=0.10. The elements represent the ligament's ability to sustain tensile load while offering no resistance to compression or shear. Common values used for modeling the PCL are: k=9000N, ε_l=0.03, and ε_0= -0.068. Common values used for modeling the MCL are: k=2750N, ε_l=0.03, and ε_0=0.04. Common values used for modeling the LCL are: k=2000N, ε_l=0.03, and ε_0= 0.05 (Amiri & Wilson, 2012). There is a large amount of variability in literature for the reference strain values. However, these are the most commonly used values. Two other variables that are used to model ligaments are the reference length, L_r, which is the length of the ligament at full extension, and the slack length, L_0, which is the length of the ligament when it first becomes taut. The reference length is determined by measuring the length of the ligament

at full extension, and the slack length is determined by equation 2 (Blankevoort & Huiskes, 1991):

$$L_0 = \frac{L_r}{(\varepsilon_0 + 1)} \qquad (2)$$

Using the slack length, the stiffness of the ligament can be calculated using equation 3 below:

$$Stiffness = \frac{k}{L_0} \qquad (3)$$

A biomechanically functioning ligament can be modeled by defining all of the material properties. Even though there is a large variability between sources for these values, an accurate ligament model can be designed to advance the knowledge of both ligament and knee joint kinematics. These equations were combined from multiple computational studies which were used to develop the code to model the ligaments in the AnyBody model used for this thesis.

5.2 IN VIVO COMPUTATIONAL STUDIES

In vivo function of the cruciate ligaments of the knee is not well understood. It is important to have knowledge of in vivo ACL and PCL function to provide a guideline for surgical treatment of ligament injuries. In a 2004 study by Li, DeFrate, Sun, and Gill, they investigated in vivo elongation of the ACL and PCL during weight bearing flexion using 3-dimensional computer modeling techniques in order to provide surgeons with more information (Li, DeFrate, Sun, & Gill, 2004). Five 3D knee models were created in solid modeling software based off of five magnetic resonance (MR) scanned knees. From the MR scans, the insertion areas for the ACL and PCL were determined. Next, each

subject performed a quasi-static lunge at 0, 30, 60, 90 degrees of flexion as a 3D fluoroscope was used to capture images of the knee. The images were used to recreate the in vivo knee positions at each flexion angle in the solid modeling software. These models represented the position of the knee during weight bearing flexion, and from this, the positions of the ACL and PCL insertion areas were determined. The lengths of the ACL and PCL were measured from the knee models at each flexion angle (Li et al., 2004). The study by Li et al, concluded there is reciprocal function between the ACL and PCL along the flexion path, with the ACL playing an important role in low-flexion angles and the PCL playing an important role at high-flexion angles. Understanding the biomechanical role of the knee ligaments in vivo is essential to reproduce the structural behavior of the ligament after injury and thus improve surgical outcomes (Li et al., 2004). The study by Li informs the current work of what to expect from the cruciate ligaments as the knee is flexed from 0 to 90 degrees of flexion. The study also provides information on reasonable strain percent's of ligaments during flexion.

In a 2012 study by Bloemker et al., they presented a subject specific method of determining zero-load lengths of cruciate and collateral ligaments using computational modeling. Previous studies used a force-displacement curve to find the zero-load length by using the reference length and previously published reference strain values, but the method used in this paper uses generalized reference strain values which do not take subject specific ligament information into account. The objective of this study was to determine the sensitivity of the kinematics of the knee joint to the zero-load length percentage (Bloemker, Guess, Maletsky, & Dodd, 2012). Three cadaveric knees were

imaged using magnetic resonance imaging to create the bone, cartilage, and ligament geometries. The cadaveric specimens were then placed into a knee simulator and the kinematics of the femur, tibia, and patella were obtained. A computer model was developed to validate the cadaveric data. The images taken of the cadavers were placed into a validated multibody model. A compliant contact force between the articulating surfaces was created. The ACL and PCL were modeled as two bundles each while the LCL and MCL were modeled as three bundles each. The ligaments were modeled as one-dimensional, non-linear spring damper elements using values from literature. Insertion and origins for the ligaments were determined by dissecting the cadaver knees. The zero-load length of each ligament was determined by calculating the maximum straight-line distance between insertion and origin sites throughout the motion for each ligament and then applying a correction percentage. The model then simulated a walking cycle as the kinematics were measured (Bloemker et al., 2012). The study by Bloemker et al., concluded that knee kinematics during simulated walking were extremely sensitive to zero-load length parameters of both the cruciates and the collaterals. It was also determined that knee laxity is extremely sensitive to variation in the reference length parameters (Bloemker et al., 2012). The study by Bloemker was informative to this thesis because it compared a new method of modeling ligaments to the reference strain method which was used for this thesis. It provided good insight of where to be careful when modeling ligaments in order to eliminate some errors in the force-displacement behavior.

5.3 MECHANICAL STUDIES OF KNEE LAXITY AND KNEE REPLACEMENTS

In a 2001 study by Un et al., they presented the Vermont knee laxity device (VKLD) that evaluates AP displacement during weightbearing and non-weightbearing conditions. This study compared the VKLD to the KT-1000 arthrometer and planar stress radiography that are used clinically to assess AP displacement. The purpose of the study was to determine the repeatability and reliability of the VKLD measurements of AP laxity (Un et al., 2001). For the VKLD testing, six subjects sat in a reclined seat in which the subjects lay supine. Each foot was supported in a cradle which was locked at a 20 degree angle and a force equal to 40% of the subjects body weight was applied depending if the test was weightbearing or not. External loads of 200 N were applied to the midpoint of both the femur and tibia five times. Electromagnetic position sensors are strapped to the mid-portion of the patella and medial flare of the tibia and the difference in distance between the two was used to measure AP displacement (Un et al., 2001). KT-1000 knee arthrometer was used according to its instructions with posterior loads of 68 N and 90 N and anterior loads of 68, 90, and 133 N. The anterior and posterior displacements were summed to produce total AP displacement values. An examiner performed planar stress radiography to the test subjects using a Telos loading fixture. Four AP load cycles were applied to the femur 3 cm above the patella at a magnitude of 130 N anteriorly and 90 N posteriorly. An X-ray was aligned in the horizontal plane parallel to the contours and a roentgen exposure was obtained. AP displacements were measured with reference to a line parallel to the shift of the tibial cortex. The KT-1000 and the planar stress radiograph test was examined at non-weightbearing while the VKLD was tested with both

weightbearing and non-weightbearing setups (Un et al., 2001). The study by Un et al., determined that there was a significant difference between AP knee laxity between examiners for both KT-1000 and VKLD. At 90 N of applied load, the KT-1000, VKLD, and planar stress radiography measured an average AP translation in patients of 11.9, 13.3, and 9.2 mm respectively during non-weightbearing. At 130 N of applied load the KT-1000 and VKLD measured an average AP translation of 13.2 and 14.3 mm respectively during non-weightbearing. During the weightbearing experiments the VKLD measured an AP translation of 4.4 and 4.9 mm for 90 and 130 N of applied load respectively as depicted in Figure 5.1. They concluded that there is a 65-70% reduction in AP knee laxity between non-weightbearing and weightbearing conditions. They also concluded that the small amount of movement during weightbearing is due to the anterior neutral position shift. A crucial conclusion of this study was a common measurement reference point has to be used so a direct comparison can be made between setups and patients (Un et al., 2001). The study by Un was important for the work done in this thesis because it compared methods of measuring AP laxity clinically. It also provided information on external forces used to measure AP laxity as well as values to expect during weight bearing and non-weight bearing.
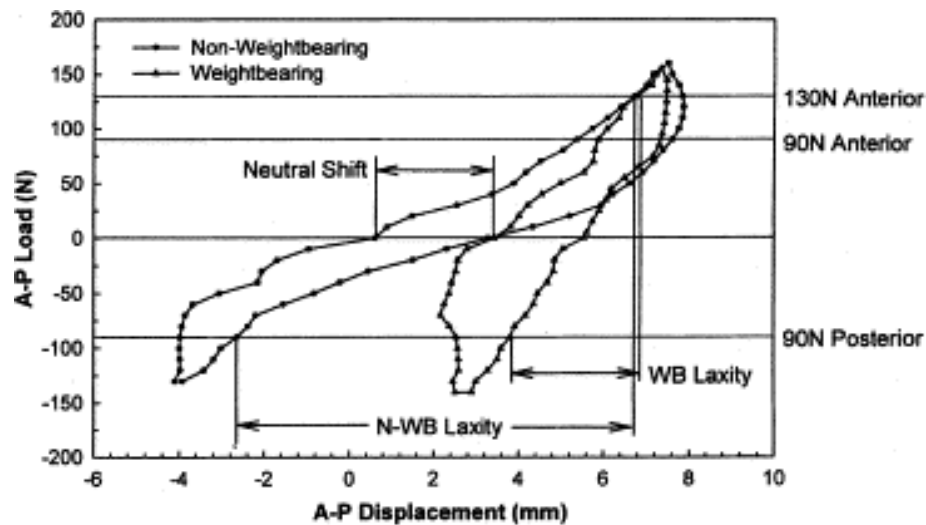
Figure 5.1 Output from VKLD used to measure AP laxity during weightbearing

and non-weightbearing (Un et al., 2001)

In a 1998 study by Webright et al., they examined the influence of the trunk-thigh

position of the patient on laxity measurements. The reasoning behind the study was

clinicians may obtain false-negative Lachman tests for tibial displacement when the trunk

position of the athlete varies as the anterior cruciate ligament injury is assessed on the

field or clinic. The study used fifteen subjects without prior knee injury. Each subject was

tested at 15, 45, and 90 degrees of hip flexion while the knee was maintained at 29 ± 3.1

degrees of flexion. A 133 N (30lb) anterior force was applied to each knee and a KT-

1000 knee arthrometer was used to measure the displacement of the tibia. Three tibial

displacement trials were performed for each trunk position resulting in an average tibial

displacement of 7.9 ± 2.3 mm (supine), 8.1 ± 2.5 mm (semireclined), and 8.3 ± 2.6 mm

(sitting). These results revealed no significant difference in anterior tibial displacement

among the three trunk-thigh positions suggesting alterations in trunk position are not a

41

problem in assessment of anterior tibial displacement (Webright, Perrin, & Gansneder, 1998). The study by Webright was influential to this thesis because their conclusion that the angle of the hip does not cause a significant difference in AP translation helped to know not to focus on the hip angle when creating the model.

The 2014 work by Halewood et al., hypothesized that abnormal knee kinematics that included excessive tibial internal rotation and femoral rollback during flexion caused dissatisfaction after total knee arthroplasty (TKA). Eighteen specimens were used to compare three TKAs (Journey, Journey II, and Genesis II PS TKA) and an intact knee in two different studies. The first study placed the specimens in a knee extension rig with transducers to measure ligament length during flexion from 0 to 120 degrees. The second study used a knee flexion rig and optical trackers to measure tibiofemoral kinematics (Halewood et al., 2014). Anterior and posterior loads of 135 N were applied to measure the AP motion allowed by the implants during flexion as depicted in Figure 5.2. The results showed that TKA did not cause significant elongation of any of the ligaments examined. TKA caused the MCL to become slack and caused the superficial iliotibial band to become tight but neither change was significant. All three TKAs caused an increase in anterior laxity up to 90 degrees of flexion. 135 N anterior drawer force produced significantly greater tibial translation for all three TKAs compared to intact knee. There were no significant differences of tibial posterior laxity between intact knee and three TKAs. In conclusion, the over-internal rotation and rollback in the TKA caused excessive tightening in the soft tissues surrounding the knee which led to anterolateral knee pain (Halewood et al., 2014). The study by Halewood was informative to this thesis

42

because it provided information on the AP translation of the Journey II knee which this thesis evaluated.
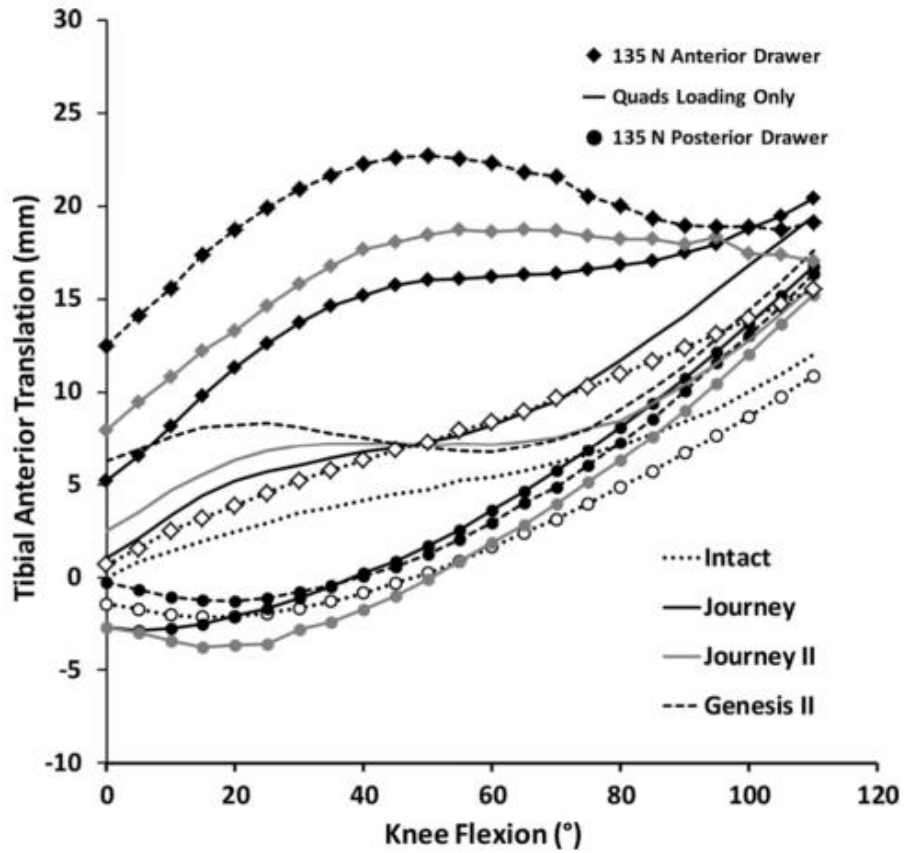
Figure 5.2 Limits of AP translation laxity for four knee states under three loading conditions: 400 N quadriceps tension, 135 N anterior drawer, and 135 N posterior drawer (Halewood et al., 2014)

CHAPTER SIX

PRIOR ART FOR TKR WITH LIGAMENT SUBSTITUTES

Total knee replacements and artificial ligaments have been discussed separately, but what about incorporating the two designs together? As mentioned previously, when a TKR is implanted, ligaments are removed possibly leading to instability issues associated with increased motion. Artificial ligaments are used to replace ruptured ligaments to regain stability in the knee. By incorporating artificial ligaments with the TKR, the loss of natural ligaments, and the resulting instability, can be overcome to produce a knee with more normal motion and stability. There have already been several patents submitted considering this idea of combining artificial ligaments with a TKR.

Three patents will be focused on: W0 2012100962, US 8,343,227, and US 8,888,856 as depicted in Figure 6.1. W0 2012100962 – is a knee prosthesis that uses artificial ligaments to replace the functionality of the missing ligaments (Donno & Munchinger, 2012). This patent claims that the ligaments can be manipulated with minimal surgical intervention even after final assembly. This device can also adjust the tension of the ligaments. It claims to produce stabilization by connecting the artificial ligament from the medial femoral condyle to the tibial component and a second ligament is connected from the lateral femoral condyle to the tibial component. US 8,343,227 – is a knee prosthesis assembly with ligament link (Metzger, Uthgenannt, & Stone, 2013). This patent claims a prosthesis assembly that can include a ligament link that is an autograft, an allograft, a xenograft, an artificial graft, or any combination. The ligament link connecting the prosthesis to the ligament can pierce and extend through the ligament

or be coupled to the ligament via fasteners and sutures. The ligament is attached to both the femur and tibial baseplate. US 8,888,856 – is a total knee implant that has a prosthetic ligament wrapped around a crossbar on the femur and secured to attachment points on the tibial component (Byrd et al., 2014). This patent claims that a plurality of ligaments can be attached to a plurality of locations on the femoral component and tibia baseplate in order to create natural articulation of the knee joint.

These three patents provide an example of what the prior art consists of for knee replacements that incorporate ligament substitutes into their design. Most of the claims are similar by listing some sort of ligament substitute to recreate the stability of the ligaments. Some of the interesting claims included being able to adjust the tensioning, attaching the ligament to the implants via sutures, and claiming the ligaments can be placed in a plurality of locations. Being able to adjust the tension is an interesting idea that correlates to ligament balancing. However, what stands out is the claim that the ligaments can be placed in a plurality of locations. Further into the thesis optimal ligament location will be evaluated and discussed, so this is an interesting claim that should be investigated. Overall, the patent landscape is crowded and very broad, but there are still claims that are missing that should be considered.
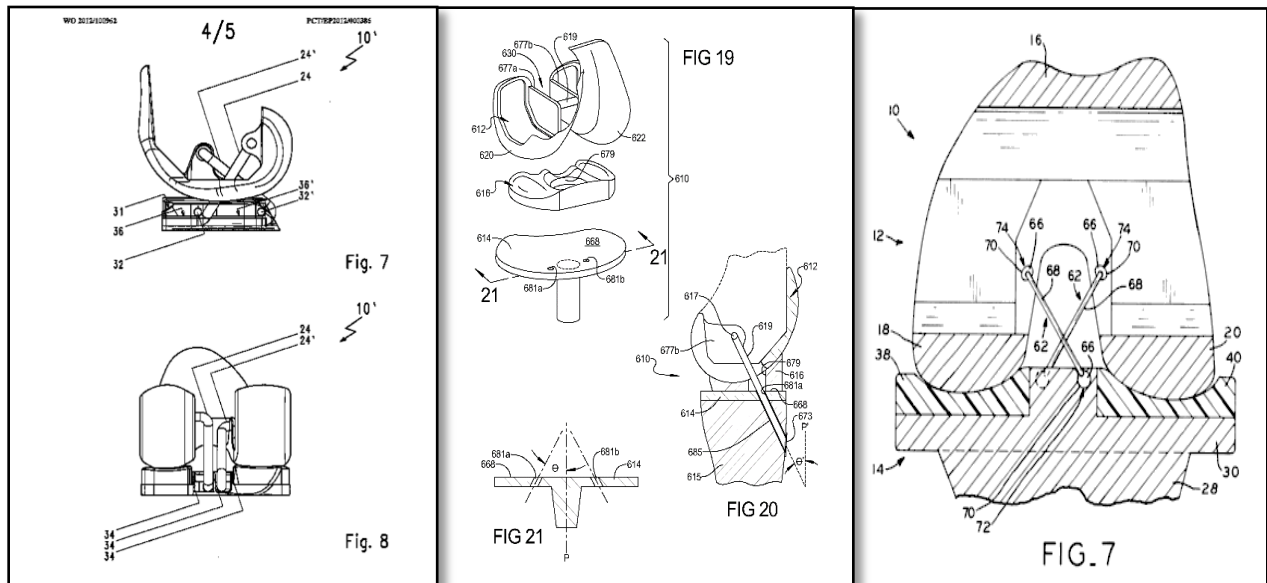
Figure 6.1 Patents W0 2012100962 (left), US 8,343,227 (middle), and US 8,888,856 (right)

CHAPTER SEVEN

SUMMARY OF AIMS AND INTRODUCTION

The intact knee joint provides six degrees of freedom that are dictated by the anatomy of the bones and soft tissues of the joint such as cartilage, menisci, ligaments and the joint capsule. With the implantation of a TKR system however, the kinematics of the knee change, and are dictated by implant geometry and any remaining soft tissues of the knee. Many different TKR designs exist, but on primary distinction in design function is whether or not they retain a posterior cruciate ligament or not. It can be hypothesized that in order to obtain more normal knee kinematics, the TKR implant should mimic the anatomy of the knee as closely as possible, which is difficult to do if ligaments are removed during surgery.

The aim of this study was to determine the effect of artificial ligaments and their location and length on a total knee replacement's stability. A computational model was designed to incorporate ligaments with a TKR where the ligament locations and lengths could be changed. 2,916 different location and length combinations were evaluated by tracking ligament movement and loading during flexion and tibial translation during an anterior and posterior drawer test. The computational data was validated by designing and constructing a TKR system that incorporates ligaments into its design, and using an Instron mechanical testing machine to evaluate stability.

CHAPTER EIGHT

MATERIALS

This chapter will detail the relevant materials used to complete this study. The materials and equipment discussed in this section include implants, mechanical testing machines, and computer software.

8.1 SOLIDWORKS 2014

In order to design a total knee replacement and an attachment mechanism that incorporated ligaments, a 3D modeling software was needed. Solidworks 2014 is a 3D CAD software that provides powerful 3D design solutions for rapidly creating parts, assemblies, and 2D drawings (Solidworks 3D CAD, n.d.). For the purposes of this study, Solidworks was used to design and assemble knee replacements and attachment mechanisms. With its capabilities to create 2D drawings, prototypes were able to be designed. Solidworks also has finite element analysis (FEA) capabilities which were used for preliminary analysis on the deformation of the attachment mechanism.

8.2 TELOS KOSA-HOCHFEST LIGAMENT

Telos KoSa-hochfest ligament is a polyethylene terephthalate synthetic ligament as depicted in Figure 8.1. The KoSa-hochfest is more commonly known as the Trivera-hochfest ligament. Its tensile strength is greater than that of a natural cruciate ligament in order to compensate for expected fatigue under prolonged stress (Telos, n.d.). Because of these properties, it has been successfully used for reconstruction surgery since 1980, and

is one of the few synthetic ligaments still used by orthopaedic surgeons. KoSa-hochfest ligament was used for the testing in this study to replicate the cruciate ligaments, connecting the femoral component to the tibial component.
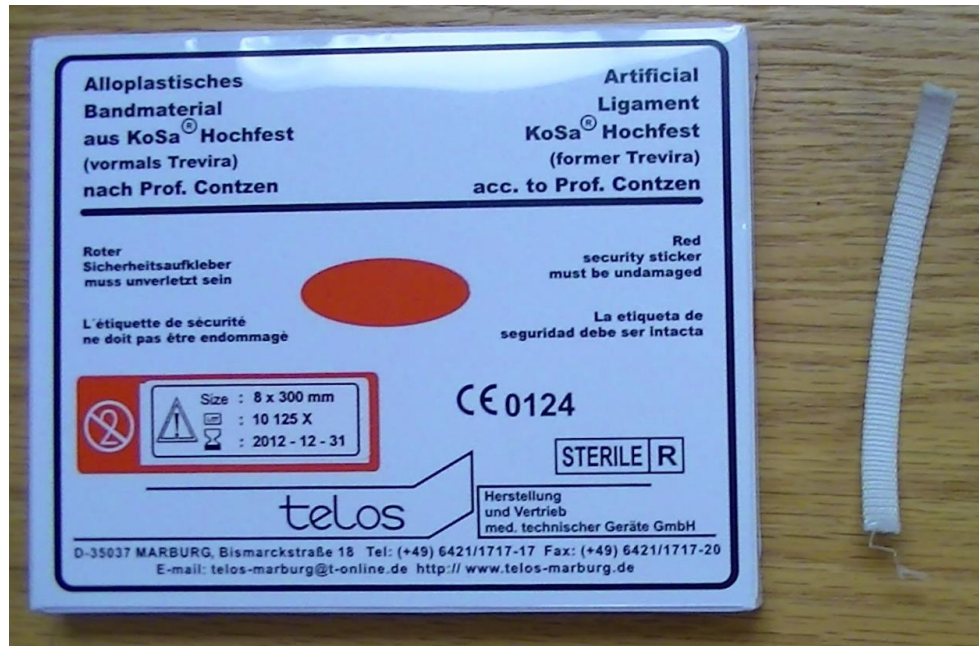
Figure 8.1 KoSa-hochfest ligament from Telos

8.3 JOURNEY II KNEE

For this study, the Smith and Nephew, Journey II CR (PCL retaining) knee implant was used. It was obtained by Dr. Brian Burnikel for this study, and it is one of the most commonly used implants by our clinical collaborator. Three parts of the implant were used for the study: the femoral component, tibial baseplate, and polyethylene insert as depicted in Figure 8.2. The patella button was not modeled or tested in this thesis. The femoral component is multi-axial with a larger medial and lateral condyle. The tibial baseplate and polyethylene insert were fixed instead of mobile bearing.

Figure 8.2 Journey II CR knee implant (Smith & Nephew, 2015)

8.4 NEXTENGINE 3D LASER SCANNER

In order to create 3D models of the Journey II knee that could be used in a computational model, a 3D scanner was needed. The complexity of a knee replacement design required a 3D scanner with accuracy. The NextEngine 3D scanner provides 0.005 inch accuracy, which is ideal to create a scan of a knee implant (NextEngine 3D Laser Scanner, n.d.).

8.5 3MATIC STL

To prepare the 3D scanned model generated by the NextEngine 3D Laser Scanner for computational simulation, the STL files needed to be remeshed. 3Matic STL allows design modifications directly on STL, scanned, and CAD data. 3Matic offers the ability to make additional design modifications, design simplifications, 3D texturing, remeshing, and forward engineering, all on an STL level (Taylor, n.d.). For the purposes of this

study, the focus was on the remeshing capabilities of 3Matic to adjust the mesh size of STLs in order for their incorporation into the computational model.

8.6 ANYBODY MODELING SYSTEM

Computational simulation was carried out in AnyBody Modeling System (AnyBody 6.0, AMMR 1.6.2, AnyBody Technology, Aalborg, Denmark). AnyBody is the leading musculoskeletal modeling and ergonomics software capable of analyzing musculoskeletal systems of humans as rigid body systems. AnyBody Managed Model Repository (AMMR) is a collection of unique models of different bodies and kinematic movements that are ready to use in the AnyBody Modeling System ("The AnyBody Modeling System," n.d.). The simulations done for this research were all done using AMMR 1.6.2 Free Posture model. This model provided the femur, tibia, and patella with the ability to simulate motion. This model also contained the ability to simulate ligaments and their properties. AnyBody models can be either forward or inverse dynamic models. All simulations for this project were run using inverse dynamics. Inverse dynamics computes muscle activation or ligament activation based on a specific task like known motion (Damsgaard, Rasmussen, Christensen, Surma, & de Zee, 2006). AnyBody Modeling System's ability to analyze the musculoskeletal system and its kinematics using inverse dynamics was the reason it was utilized in this study.

8.7 MATLAB

MATLAB (R2015a, MathWorks, Natick, Massachusetts) is a high-level computer language and interactive environment that allows for algorithm development, data analysis, and more (MATLAB, n.d.). It allows for the creation of mathematical algorithms to run large scale iterative simulations and design mathematical functions to process large data sets. For this study, an algorithm in MATLAB was used to run scripts that enabled us to run over 2,916 iterations in the AnyBody model.

8.8 INSTRON 8874

The Instron 8874 (Instron, Norwood, Massachusetts) is a bi-axial tabletop servo-hydraulic testing system as depicted in Figure 8.3. It uses a combined axial and torsion dynamic actuator to allow for both axial and torsional fatigue testing. For this study, a 25 kilo-newton load cell (Model: M211-113 S/N 97506) was used. The system has a twin column frame and a lower t-slot table allowing for a range of both static and dynamic testing. The Instron console software (version 8.4) includes waveform generation (version 1.6), calibration, and status monitoring to record forces and movements during testing (Instron, n.d.). For the purposes of this study, Instron was used to apply a body weight to knee laxity and flexion testing.

Figure 8.3 Instron 8874 axial-torsion fatigue testing system (Instron, n.d.)

8.9 Linear Variable Displacement Transducer

MACRO SENSORS GHSE 750-1000 Linear Variable Displacement Transducer (LVDT) is a spring loaded single ended DC operated LVDT position sensor as depicted in Figure 8.4. It is designed for a wide range of position measurement applications. It allows for measurement repeatability of 0.000025 inches or 0.6 microns. The GHSE 750-1000 allows for a nominal range of 25.4 mm (MACRO SENSORS, n.d.). The LVDT was used to measure the translation of the tibia.

Figure 8.4 Linear variable displacement transducer (American Sensor Technologies, 2015)

CHAPTER NINE

METHODS

The materials previously described were used to create each method of testing. This chapter will describe the steps performed to design and test the attachment system, create a kinematic computational model, and mechanically test a knee implant.

9.1 IMPLANT AND ATTACHMENT DESIGN

A knee replacement that incorporates ligaments was designed using Solidworks 2014. To start the design process, measurements were taken of current knee replacement designs in the lab using a caliper. The measurements were used to model a basic TKR.

Once a model was designed in Solidworks, an attachment mechanism was to be designed in order to attach the ligaments to the implant. A three part, pin attachment system was designed as depicted in Figure 9.1. Part A was a block built up from the interior side of both femoral condyles. The block contained two holes: one for the ligament insertion and one for the pin securing the ligament. Part B was a small dumbbell shaped piece that the ligament was wrapped around. Part B was inserted into the hole on the extruded block on the femur and the block on the tibia. Part C was a pin that goes into the extruded block and through the dumbbell to hold everything in place. The key feature of this design was that the ligaments were able to be replaced arthroscopically, which required the parts to be small enough to fit through an arthroscopic portal limiting the design complexity.
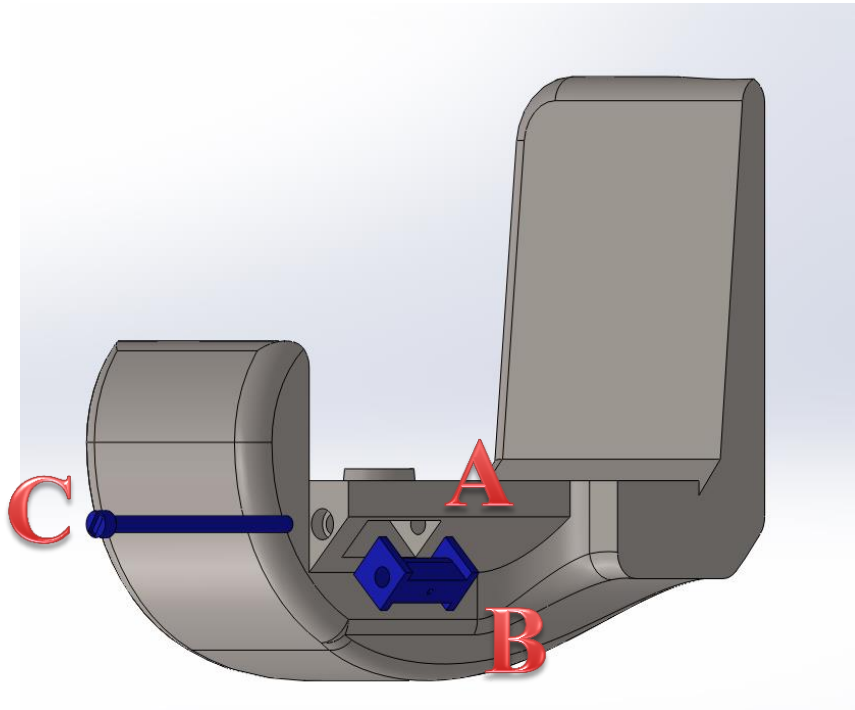
Figure 9.1 Solidworks drawing of the attachment mechanism: implant block (A),

dumbbell attachment (B), and pin (C)

9.2 ATTACHMENT VERIFICATION

Mechanical testing was performed to determine if the attachment design could withstand the forces in a knee and ensure that the ligament failed before the implant. First, the attachment mechanism was machined by the Clemson University Machine Shop using medical grade titanium, Ti-6Al-4V, as depicted in Figure 9.2.
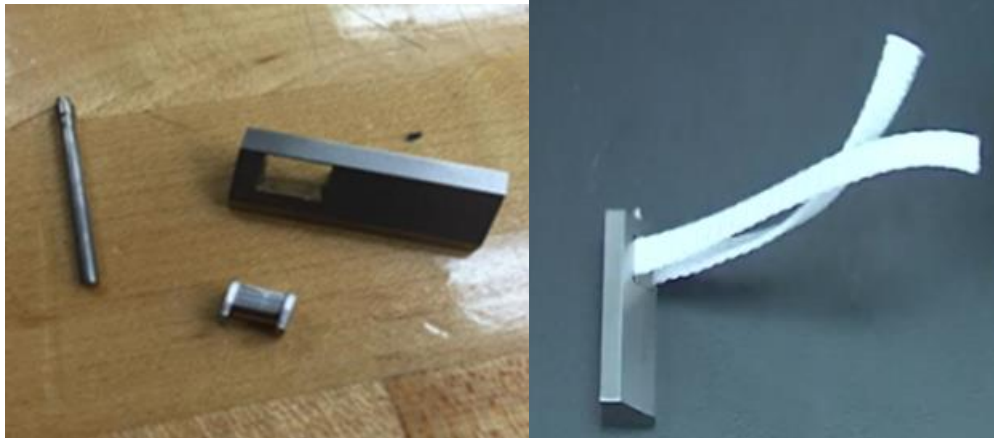
Figure 9.2 Attachment mechanism (left) and assembly with ligament (right)

Next, KoSa-hochfest synthetic ligament was tested to failure, by performing a tensile test with the Instron system, as depicted in Figure 9.3. One end of the ligament was sutured around a bolt fixed in place using toe clamps, and the other end was sutured around a carabineer held in place by the Instron upper grip. The ligaments were tensile tested in position control where the grip was raised at 3 mm per minute as the load was recorded.

Then, the attachment mechanism was tested to failure as depicted in Figure 9.3. The attachment mechanism was tested using shim stock steel to replicate a stronger ligament. It was wrapped around the dumbbell part of the attachment and both parts were inserted into the block as the pin was inserted. The attachment mechanism was fixed using toe grips. The shim stock steel was then placed in the Instron upper grip. This tensile test was performed using load control because the shim stock steel would slip out of the grips with position control. The tensile force was increased by 200 N, and the attachment mechanism was taken apart each time to determine if it failed. Failure of the

attachment mechanism was determined if the pin became deformed where it could not be pulled out with needle nose pliers. This was repeated every 200 N until the attachment mechanism failed.
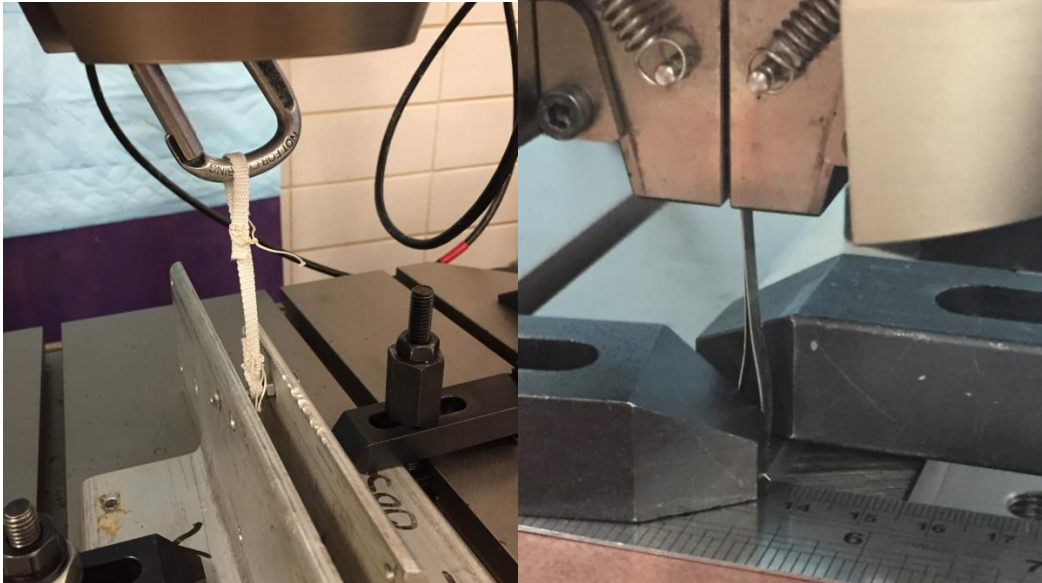
Figure 9.3 Ligament (left) and attachment mechanism (right) tensile test setup

9.3 NEXTENGINE 3D LASER SCANNER

The Journey II knee was positioned in front of the NextEngine 3D laser scanner, located at Clemson's Advanced Materials Research Laboratory, on a turntable that is positioned 17" from the front of the scanner. The NextEngine software was started by clicking the triangular scan button to enter the scan window. A preliminary scan was done by selecting 'single scan'. If the preliminary scan was satisfactory, the scan was started by clicking 'scan' in the top toolbar. After a few minutes, the scan finished. Finally the file was saved in an STL format that was used for the next step (Shearer, n.d.).

9.4 3MATIC STL

The STL file produced from the laser scanner did not have the appropriate mesh size or surface finish for AnyBody to run efficiently, so 3Matic STL was used to remesh the STL file. The STL file was imported into 3Matic. Once the file was opened, 'Auto Fix Wizard' was selected at the top left of the tool bar under the 'Fix' tab. The 'Auto Fix Wizard' improved the surface roughness by creating a smooth surface.

The STL file was then remeshed by clicking 'Auto Remesh' at the top of the tool bar under the 'Remesh' tab. The implant was selected and apply was clicked while leaving the remesh numbers as recommended. The mesh was still too coarse for AnyBody, so the Auto Remesh was be run again but this time the length of the triangles was changed to adjust the mesh size. Once the mesh was finished the model was exported to AnyBody.

9.5 ANYBODY MODELING SYSTEM

AnyBody Modeling System is software for computer analysis that simulates the mechanics of the body working with its environment. AnyBody contains the abilities used to create an anatomical kinematic model that incorporates bones and soft tissues. This section covers the method used to create a knee joint model and simulation to evaluate knee kinematics.

First, the 'FreePosture' model that was located under AMMR 1.6.2, Applications, Examples, FreePosture was opened. This provided an outline of code to start creating the

59

model. The FreePosture model provided all the bones needed for the model in this study. Next, the STLs were imported by inserting the command 'AnySurfSTL' with the filename of the STL for both the femoral and tibial components. Then, the following components were referenced, the femoral STL to the thigh segment and the tibial STL to the shank segment. This allowed the STL's to follow the path of the segments they were implanted into. The position of the STL was adjusted using the 'sRel' and 'aRel' commands. 'sRel' was used for translation and 'aRel' was used for rotation. Both STL's were placed in their correct locations based off of anatomical landmarks in the model. A contact force was created to prevent the implants from penetrating one another. Using the 'AnyForceSurfaceContact' command, a 'PressureModule' = 5e9*2 was created to provide enough force to keep the implants from penetrating one another.

After the implants were in place, the ligaments were modeled. Four different 'AnyRefNode' commands were created on both the thigh and shank segment for the ACL, PCL, MCL, and LCL. These nodes were the insertion and origin locations of the ligaments for their respected segments. For each ligament, a separate 'AnyKinPLine' was inserted. This was the command that created the ligament as a spring. Under the 'AnyKinPLine,' the reference nodes created for the ligaments were then referred to in the 'AnyRefFrame'. Using the 'AnyDrawPLine' command, the thickness and color of the ligaments were controlled, in order to see where the ligaments were located. The ligaments were modeled with a round cross section with a thickness of 0.003 m or 3 mm. 'AnySurface' command was used to wrap the ligament around the implant and bones instead of going through them as depicted in Figure 9.4.
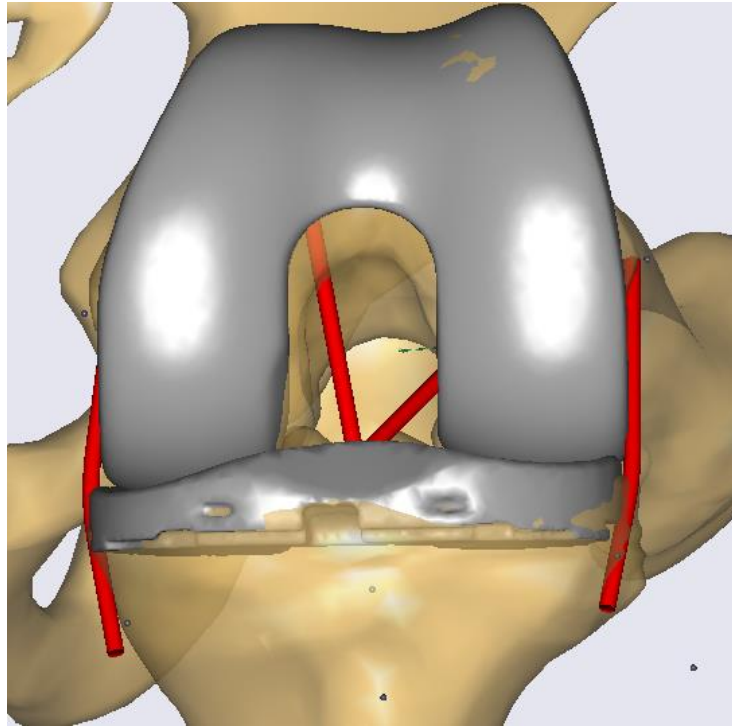
Figure 9.4 AnyBody model consisting of the implant

and ligaments flexed to 90 degrees

Once the ligaments were modeled, they needed to be given mechanical properties in order to function like ligaments. The 'AnyForce' command was used to give the ligaments mechanical properties. Under 'AnyForce' a list of variables and equations were inserted using 'AnyVar' and 'AnyFloat' commands. The variables inserted were stiffness "k", reference length "lr", reference strain "er", slack length "lo", constant "esp0", and current strain "esp". All of these ligaments were combined into a non-linear equation called 'Val' using the 'AnyFloat' command. The equation used for 'Val' was:

```
Val = {iffun(gteqfun(esp,0.0),iffun(gtfun(esp,2*esp0),-
       k*(esp-esp0),-k*1/4*(esp^2/esp0)),0.0)}
```

To provide a force to the ligament, one last variable had to be set, F= Val. In order to measure the length of the ligament, the command 'AnyKinMeasure' was used. These values were determined from literature, calibration or equations. Table 9.1 shows the values and equations used for each variable used to define the ligaments.

Table 9.1: Values and equations used to determine variables for each ligament

	ACL	PCL	LCL	MCL
K	5000	9000	2000	2750
Lr	Calibrated	Calibrated	Calibrated	Calibrated
Er	0.1	-0.068	0.05	0.04
Lo	Lr/(Er+1)	Lr/(Er+1)	Lr/(Er+1)	Lr/(Er+1)
Esp0	0.03	0.03	0.03	0.03

Now that the ligaments are modeled, a calibration study called 'KinStudy' was created to determine the reference length of the ligaments. Reference length was defined as the length of the ligaments at full extension. Three separate 'AnyKinEqSimpleDriver' commands consisting of a linear driver, a rotational driver, and a measurement command were created. The driver's position and velocities were set to 0 in order to measure the knee at full extension. The calibration study was run and the lengths of the ligaments were found in the 'PLine' output. These values were used as the reference length values.

In order to create the knee joint used in this study, the original knee joint was removed. Using the 'AnyObjectPtrArray,' the previous knee joint was selected and

excluded using the 'MechObjectExclude' command. 'AnyKinPLine' was used to model the patella tendon and 'AnyKinEqSimpleDriver' was used to give the patella a driver position, velocity, and rotation. Another 'AnyKinEqSimpleDriver' was created to provide the knee joint with a position, velocity, and rotation. All the 'CType' and 'Reaction.Type' for the 'AnyKinEqSimpleDriver' commands were turned to 'ForceDep' and 'off' respectively for both the knee joint and the patella. This allowed the entire joint to be force dependent.

Finally, the study was created by setting 'tEnd=1.0' and 'Gravity = {0.0, -9.81, 0.0}'. The number of time sets were set to 100 by setting 'nStep= 100'. The final step was to turn inverse dynamics on in order to make the study force dependent. The command 'InverseDynamics.ForceDepKinOnOff' was entered and set equal to 'On'. The basic model was now finished and additions were made to this model in order to create specific kinematic studies.

Once the basic model was created, it was used to test ligament strain during knee flexion. The knee replacement model that was created previously was opened and saved as 'KneeFlex'. Insertion and origin locations were chosen for evaluation by commenting out all other possible location options. The 'HipFlexion' and 'KneeFlexion' variables in the 'BM_MANNEQUIN_FILE' path, located at the being of the model, were changed to the flexion angle being evaluated. This value was set to 120 for both variables in order to have the knee flex from 0 to 120 degrees. The calibration study, 'KinStudy', was run to determine the reference length of the ligaments by clicking on the study in the operations tab and clicking run. When the calibration finished, a 'Chart 2D/3D' was created by

going to the 'Window' tab. The 'PLine' for each ligament was graphed by selecting the ligaments output file in the chart. The value recorded was entered as the reference length, Lr, for each ligament under their 'AnyForce'. 'F7' was pressed to update the model after every change. The model was updated and ready to run the 'InverseDynamics' study under the 'Study' tab in 'Operations'. Another chart and graph of the ACL and PCL 'PLine' were created. These graphs showed the change in length of the ligaments during flexion. Ligament strain was determined by subtracting the slack length, determined by equation, from the maximum length found during flexion and dividing by the slack length. These steps were repeated for all 81 location combinations. Strain values for all location combinations were then compared to literature to determine the viable locations. Location combinations with a strain percent greater than forty were not considered viable. Only viable locations were used in the next study, knee laxity.

After testing all location combinations, four additional locations were added to each location group to make a total of seven locations expanding over 15 mm for each group. This allowed the study to better understand the trends observed between location and strain. One location was held constant for three insertion groups as the forth insertion group changed to all seven locations covering a 15 mm distance. This was done for all four location groups. Each location was evaluated as the knee flexion study.

After testing all location combination, one location combination was chosen to evaluate length change. Using the same study, ACL and PCL lengths were increased from 0-5 mm in 1 mm intervals. The length was changed by increasing the value for the

reference length. The study was run and evaluated the same way as the knee flexion study.

The second study replicated an anterior and posterior drawer test. First, an external force was created using the 'AnyForce3D' command. The external force was placed on the anterior surface of the shank (tibia) using 'AnyRefFrame'. The magnitude of the force was controlled using 'Flocal'. 130 N force was applied in the x direction for anterior drawer and -90 N was applied for posterior drawer. Once the force was set, the location of the ligaments were chosen, their reference lengths were calibrated, and the flexion angle was set as mentioned in the other study. Using 'AnyFunInterpol' the knee was flexed to the desired flexion angle and then the external force was applied as depicted in Figure 9.5. Once the study was prepared, it was run by clicking 'inversedynamics' and 'run'. When the model finished, a new chart was created and the output file that displayed the movement of the tibia was selected. Translation of the tibia was found by taking the displacement of the location of the tibia between the final location and initial application of the force. The final and initial locations were determined by taking the location of the reference node of the tibia in the knee joint compared to the global reference frame of the entire model. Translation values were evaluated for over 2,916 different combinations of viable locations at ACL and PCL length combinations from 0-5 mm in 1 mm intervals.
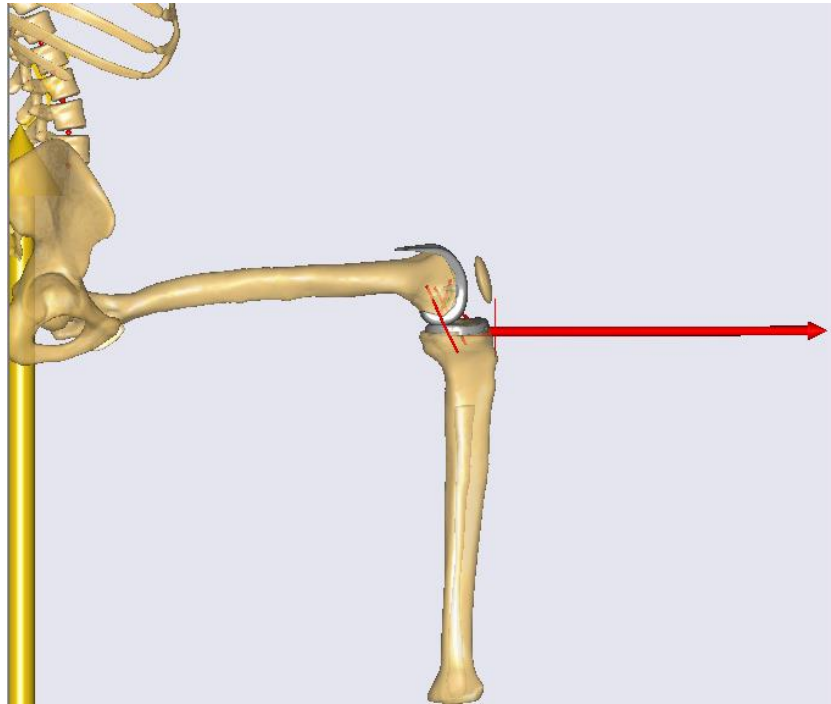
Figure 9.5 130 N anterior force applied to

tibia at 90 degrees of flexion

9.6 MATLAB ITERATIONS

It was necessary to develop a program in MatLab to run numerous iterations of the AnyBody model code efficiently. The key to allowing MatLab to send information to AnyBody was the combination of MS-DOS (Microsoft Disk Operating System) commands and the AnyBody console application. The console application was simply the AnyBody application without the graphical user interface, and it was run using the command line. MatLab sends information and commands to the MS-DOS command line that initiate and orchestrate the AnyBody console application.

The next challenge was allowing the MatLab code to define parameters in the AnyBody code for every iteration of the model. AnyBody had macro functionality that allowed simple functions like Load, Run, and Exit to be performed automatically. The macro files were saved with the extension '.anymcr', however they can be read by a plain text editor if the extension is changed to '.txt'. Again, MS-DOS commands made the final link between MatLab and AnyBody. MatLab was used to write a new macro for every iteration that made the necessary changes to certain parameters such as the ligament origin and insertion locations, ligament reference lengths, external force values, and the angle of flexion. The macro was then saved to a '.txt' file on the hard drive. Then, MatLab used MS-DOS to rename the '.txt' file to an '.anymcr' file so that AnyBody could read it. Finally, MatLab told DOS to load the '.anymcr' file in the console application.

In order for the macro to have made the appropriate changes to the AnyBody model, the parameters were made into variables. Variables were created in AnyBody by creating pseudo code statements in the AnyBody model before the Main{} statement as shown below.

```
#ifndef NewParameter
#define NewParameter  value
#endif
```

This pseudo code initiated a variable 'NewParameter' with the value 'value'. The variable could have been a string, a number, a vector among other data types. The variables created for this study were locations and lengths for the ACL and PCL, external force value, and flexion angle. A corresponding change was made to the Load statement

of the macro. The 'sprint()' function in MatLab was utilized to change the '–def' statements for every iteration of the loop so that the AnyBody code changed appropriately.

While AnyBody worked on the iterations, all control left MatLab and it waited for AnyBody to exit before returning power back to the MatLab program. Once the iteration was complete, AnyBody saved an output text file containing all pertinent values. The last thing that MatLab did before beginning the next iteration was to manipulate the data in the output text file.

MatLab imported the output text file from AnyBody and then saved it to the Excel file. Finally, Excel was used to complete the rest of the data analysis and graphing. MatLab enabled the scanning of over five thousand iterations of the AnyBody model and manage the output data from each iteration.

9.7 INSTRON TESTING

Instron testing began by designing a fixture that could mount the femoral component to the load cell while being able to change the angle of the implant and the location of the ligaments easily, as depicted by E in Figure 9.6. The femoral fixture was designed by machining two interchangeable side blocks where one block contains angles of 0, 60, and 120, and the second block contains angles of 30, 90, and 150, as depicted by A in Figure 9.6. These blocks were screwed into the part that attaches to the load cell to create the femoral attachment. The femoral implant then attached to these blocks via a femoral block as depicted by C in Figure 9.6. A femoral block was designed by taking the

inner dimensions of the implant. Two additional slots were made in the femoral block that allowed the ligaments to be attached depicted by F and G in Figure 9.6. The femoral implant was attached to the femoral block using a two-step fiberglass epoxy. This allowed the femoral implant to attach to the load cell by screwing the femoral block to the femoral attachment. Ligaments were attached to the femoral implant by creating slider pieces that inserted into the slots in the femoral block as depicted by D in Figure 9.6. Ligaments were looped through a hole in the sliders that was located at a specific location for each combination. Each part was screwed together to hold the entire fixture in compression to limit any unwanted movement.

Figure 9.6 Femoral attachment fixture and assembly: side blocks (A), femoral attachment (B), femoral block (C), sliders (D), full assembly (E), and ligaments inserted (F and G)

Another fixture had to be designed that could fix the tibial component to a xy-table, while still allowing the xy-table freedom to move and the ability to change ligament location as depicted by D in Figure 9.7. The tibial fixture was designed by first

machining a tibial attachment part that would allow ligament location to be changed. This part had multiple slots throughout its body to allow for the ligament to attach, and it had holes at the end in order for a bolt to go through it as depicted by A in Figure 9.7. The tibial attachment sat on top of a tibial baseplate containing a hole through its stem which allowed for a bolt to go through the tibial attachment and the baseplate to secure them together using a nut. The polyethylene insert was then cut into two pieces to fit around the tibial attachment. The tibial baseplate was then fixed in PVC pipe using a two-step resin epoxy. The PVC pipe and tibial baseplate were then mounted inside a four sided metal box that was fixed to the xy-table. The xy-table had a pulley system attached to it. The PVC pipe was mounted into the box by having four bolts pin it in place as depicted by D in Figure 9.7. This setup was put in compression during testing so the combination of the points of contact and the compressive load, the unwanted movement, was minimized.

Figure 9.7 Tibia attachment fixture and assembly: tibial attachment (A), tibial baseplate (B), ligament attachment (C), and xy-table setup (D)

71

After all the parts were machined and assembled, the testing was begun. The artificial ACL and PCL were looped through the femoral sliders and around the tibial attachment slots to where the ends were brought together. A caliper was used to measure the length of the ligament from the top of the slot on the tibia to the bottom of the hole on the slider. Ligament length was adjusted until it matched the value obtained in the computational model. The ligament was held at that length with a metal crimp. The femoral sliders were placed in the slots in the femoral block and screwed into place using the three set screws inside of the femoral block. The tibial attachment was then placed onto the tibial baseplate and held in place by passing a bolt through. The tibial baseplate fixed in the PVC was mounted onto the xy-table and fixed in place. XY-table was moved to the Instron table where it was centered between the two pistons. XY table was then secured into place using the toe clamps. Femoral attachment was screwed into the load cell that was attached to the actuator. At this point all the parts were in place.

Now that the parts were secured in place, the Instron was used to apply body weight axial compressive force. The computer was logged into and the Instron Console was opened. The Instron was turned on by flipping the switch on the back of the Instron computer. The control pad on the floor was watched until it said to press any button to continue. Once it said to continue, Instron was turned to low on the front of the Instron computer. Instron was switched to high after a minute. Actuator was adjusted to a position of -30 mm. Once in position, the crossbar and yellow safety bar were lowered using the knobs on the left side of the Instron. The crossbar was adjusted until the femoral block could slide between the femoral attachment. The crossbar and safety bar

72

were tightened back into place. The load was zeroed by clicking 'balance' in the console menu, this could only be done before the limits were set. The primary limits were set to -45 mm and 0 mm position, 100 N and -2000 N load, and then all of the physical limits were enabled. The actuator was rotated and lowered to a position where the femoral block was aligned with the holes in the femoral attachment. The femoral block was screwed into place using four bolts. Actuator was lowered down until a -50 N load appeared on the console menu.

Setting up the LVDT was the last step before testing could begin. First, the LVDT was turned on. The LVDT was fixed in front of knee and the indenter was compressed halfway against the tibial baseplate as depicted in Figure 9.8. The LVDT program was opened in LABView. The LVDT program records the position of the plunger which can be used to determine displacement.

Now that the Instron is setup to apply body weight the A/P drawer setup needs to be prepared. There are two pulleys on the xy-table, one on the front and one on the back. In order to apply an anterior force a hook was attached to an anterior notch in the center of the xy-plate. A rope that was tied to a 25 lb weight was attached to the other side of the hook. The rope is fed over the pulley located on the front of the xy-table. In order to apply a posterior force, a hook was attached to a posterior notch in the center of the xy-plate. A rope that was tied to a 15 lb weight was attached to the other side of the hook. This rope was looped around the pulley located on the back of the xy-table and fed back under the xy-plate and looped over the pulley in the front. Once the weight was ready to

be applied in either direction, it was lowered down the front pulley, pulling the xy-plate across the xy-table. This was performed in the next in the next step.
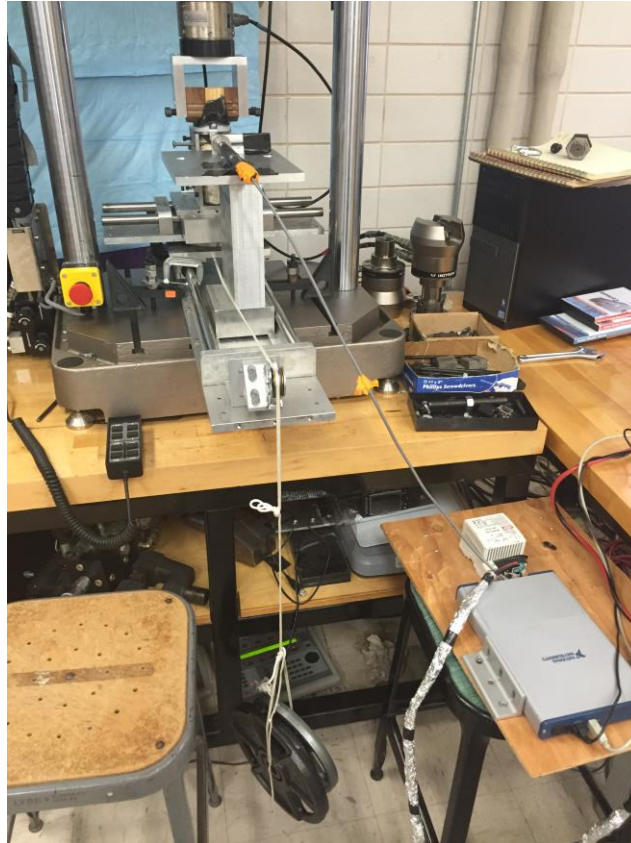
Figure 9.8: A/P drawer setup with weight lowered

Body load was applied with the Instron by opening WaveMatrix. A method was created in load control where the load was increased 50 N per second until it reached 710 N. The 710 N load was set to hold for 30 seconds. The test was started by clicking run. Instron began to increase the load on the implant to simulate body weight. Once it reached 710 N the LVDT program was started. The program ran for 5 seconds and then the weight was lowered slowly down the pulley system to simulate anterior or posterior

drawer. 25 lb and 15 lb were used for the anterior and posterior drawer test respectively. After the weight was lowered for 5 seconds, it was lifted and lowered again creating an oscillation. This was done three times total with 5 seconds between each oscillation. The LABView program was stopped 5 seconds after the third oscillation. Instron was switched to load control in order to raise the actuator and remove the load off of the implant. These steps were repeated 3 times for both the anterior and posterior direction at 0, 30, 60, 90, 120 degrees of flexion as depicted in Table 9.2. The flexion angle was changed by changing the location of the bolts that hold the femoral block to the femoral attachment. The side blocks were switched out, allowing for all angles to be tested.

Table 9.2: Tested 7 ligament combinations, 1 no ligament and 6 with ligaments containing specific ACL and PCL lengths. Tested at 0, 30, 60, 90, and 120 degrees of flexion. Anterior and posterior drawer tested applied three times each for each angle. The displacements were recorded.

Lig Combo	ACL Length [mm]	PCL Length [mm]	A/P Displacement									
			0 degree		30 degree		60 degree		90 degree		120 degree	
			Anterior	Posterior	Anterior	Posterior	Anterior	Posterior	Anterior	Posterior	Anterior	Posterior
			1-3	1-3	1-3	1-3	1-3	1-3	1-3	1-3	1-3	1-3
No ligaments	N/A	N/A										
1331	36.88	46.58										
1332	36.88	43.01										
2331	32.36	46.58										
2332	32.36	43.01										
3332	27.303	43.01										
1232	30.66	43.01										

Once the testing was finished the setup was broken down. First, the bolts were unscrewed from the femoral block. The implant system was moved out from underneath

the actuator. The console was switched to low and to off. The switch on the back of the

Instron computer was flipped to turn Instron off.
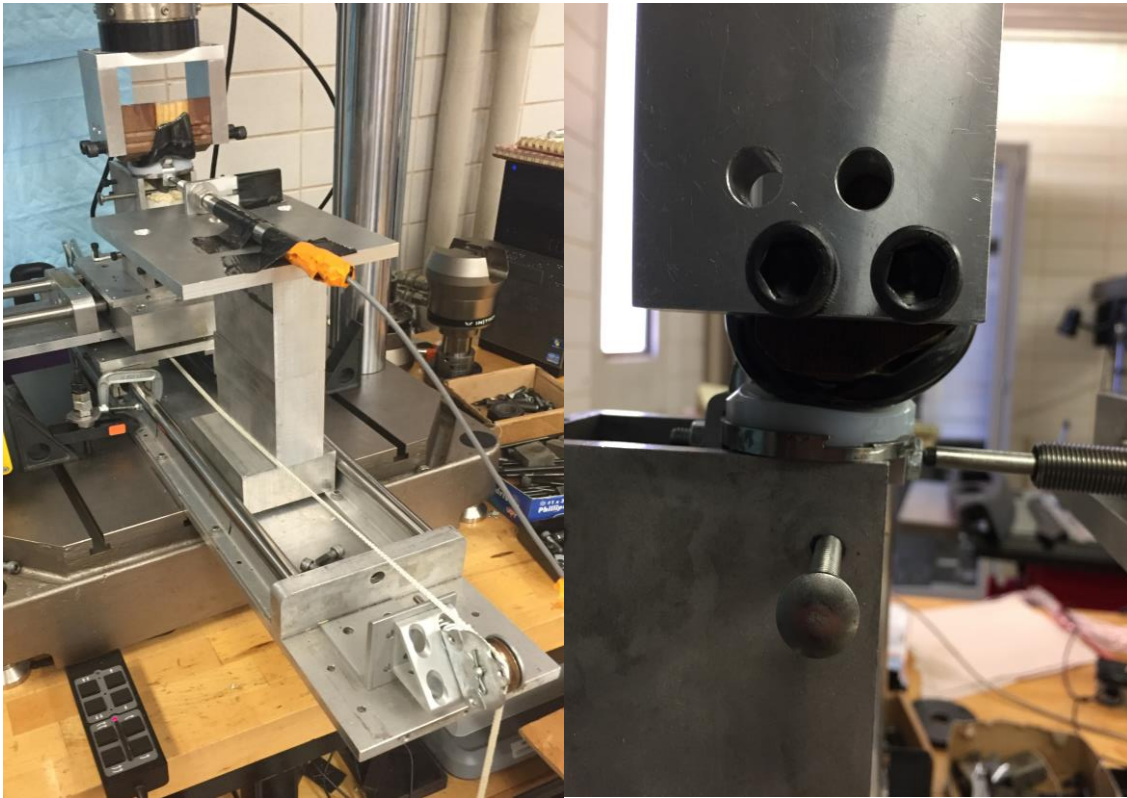
Figure 9.9 Complete Instron testing setup (left) and LVDT compressed against tibial

baseplate (right)

CHAPTER TEN

RESULTS

The results obtained during this study came from two different methods: computational modeling and mechanical testing. The first sets of results studied were from a tensile test in Instron that evaluated the attachment mechanism design. The second and third sets of results evaluated were computational data. The computational models yielded a large amount of data, so the results were presented in two ways: 1) ligament length and location combinations for trends between strain, length, and location, and 2) viable combinations. The final set of results evaluated was from AP drawer tests under compressive loading on the Instron system. The aims of the study were achieved with the data produced in the results.

10.1 LIGAMENT AND ATTACHMENT FAILURE ANALYSIS

The first aim of the study was to design an attachment mechanism that would incorporate synthetic ligaments into a knee replacement that was arthroscopically replaceable. The KoSa-hochfest ligament was tensile tested to failure twice to determine load at failure. It failed at 932.59 N and 1137.64 N. In both experiments the ligaments failed where the ligaments were sutured to form a loop. Figure 10.1 showed tensile load on the ligament where it ruptured at 1137.64 N.
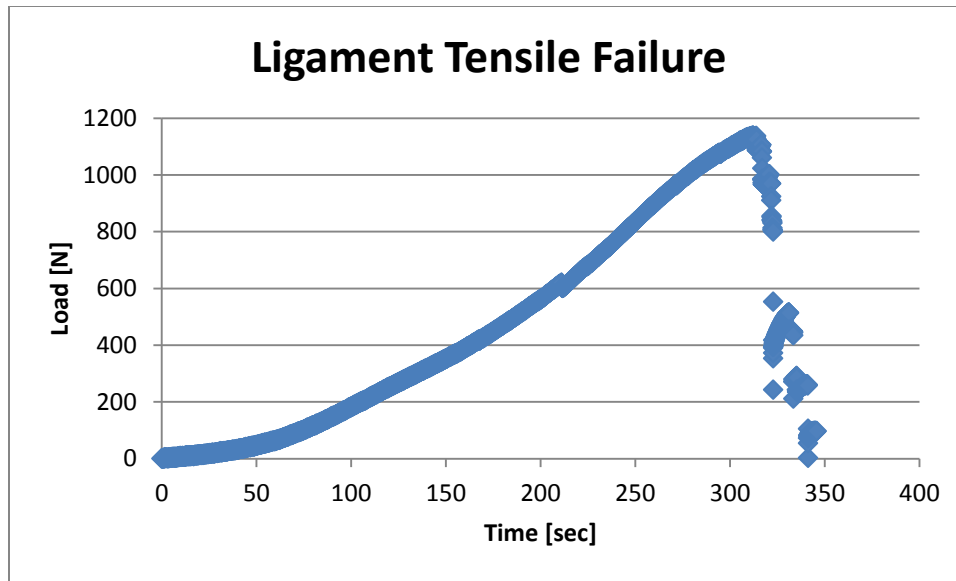
Figure 10.1: Failure load of KoSa-hochfest ligament

The second set of data from this experiment came from performing a tensile test with the attachment mechanism until failure. Failure was determined as not being able to pull the pin and ligament out using needle nose pliers within 30 seconds. Figure 10.2 showed the attachment system and pin at failure after 3800 N load. In Figure 10.2 the pin was clearly deformed at the 2" mark on the ruler.
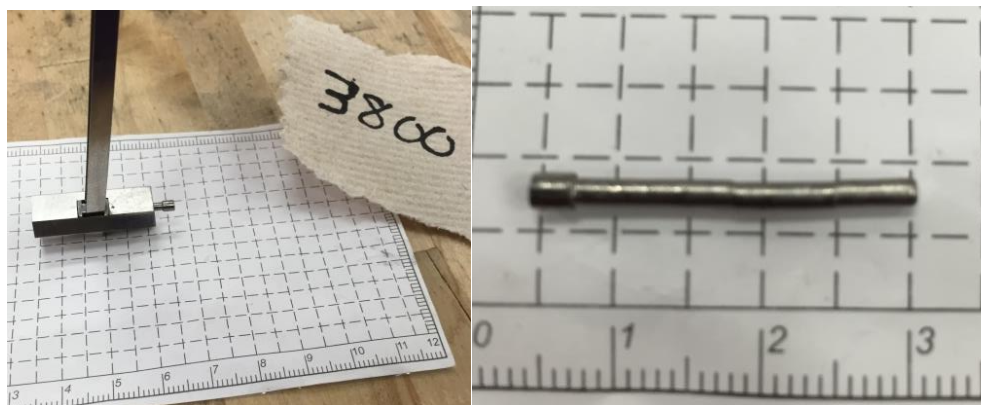
Figure 10.2 Attachment mechanism at failure (left) and pin deformation at failure (right)

10.2 COMPUTATIONAL: LIGAMENT STRAIN DURING KNEE FLEXION

The method of creating a 3D model with ligaments and knee flexion allowed for determining: flexion angles effect on ligament function, ligament locations effect on ligament strain, and ligament lengths effect on ligament strain.

Flexing the knee from 0 to 120 degrees allowed the ligament function to be evaluated by tracking ligament length. AnyBody outputted the data as ligament length during the time steps of flexion. Figure 10.3 shows an example of the length changes in the ACL (top two images) and PCL (bottom two images), before and after the insertion of the ACL is translated 15 mm posteriorly on the femur. The x-axis is the time steps during flexion, so the process of flexing the knee to 120 degrees is broken up into 100 times steps which are seen on the x-axis. The y-axis is the length of the ligaments in centimeters. The two graphs on the left are with no translation and the two on the right are after the ACL insertion is translated 15 mm posteriorly in the x-direction on the femur as depicted in the left image of Figure 10.4. The ACL constantly increased in length during flexion in the first graph. However, in the second graph the ACL decreased in length. The PCL constantly increased length during the first 80 time steps of flexion (equivalent to first 85 degrees of flexion) but became lax in the last 20 time steps (equivalent of flexion from 85-120 degrees) for both graphs.
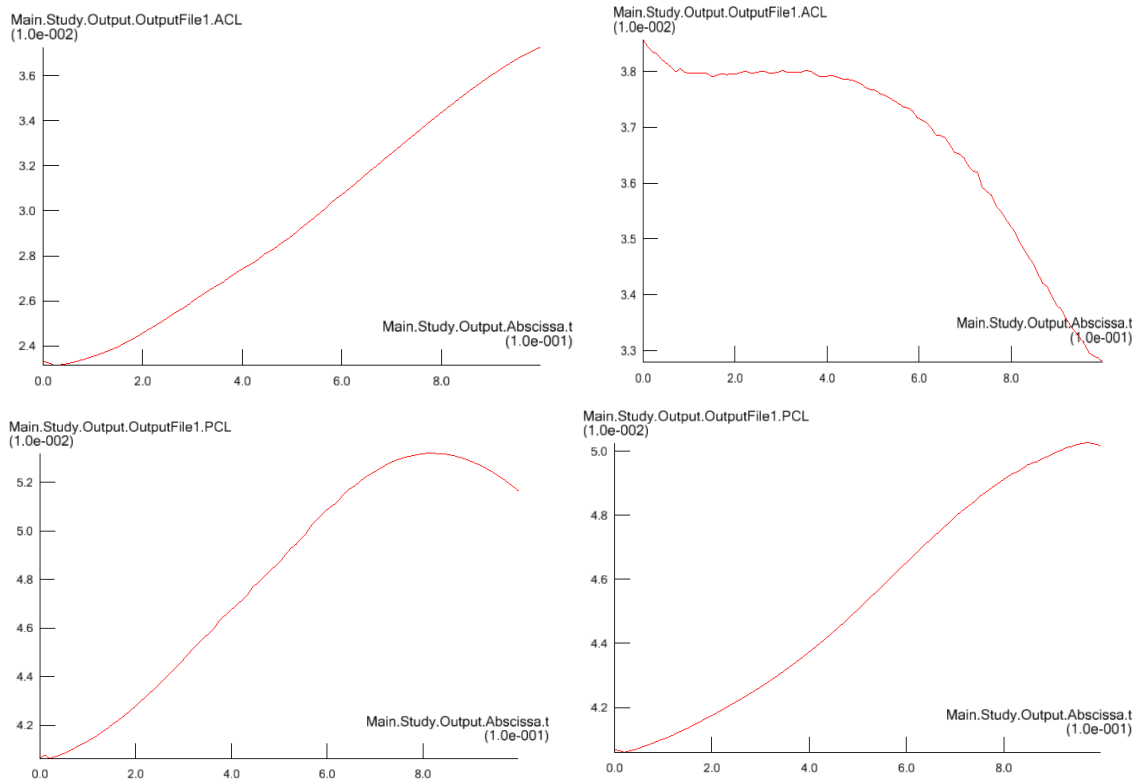
Figure 10.3: ACL (top) and PCL (bottom) change in function before (left) and after (right) ACL is moved 15 mm posteriorly on femur

ACL and PCL strain were determined at 81 different location combinations as seen in Table A.1. The 81 locations encompassed 3 insertion locations on the tibia and three origin locations on the femur for the ACL, and 3 insertion locations on the tibia and 3 origin locations on the femur for the PCL as seen in Figure 10.4. A completed list of these ligament configurations is shown in Table A.2.
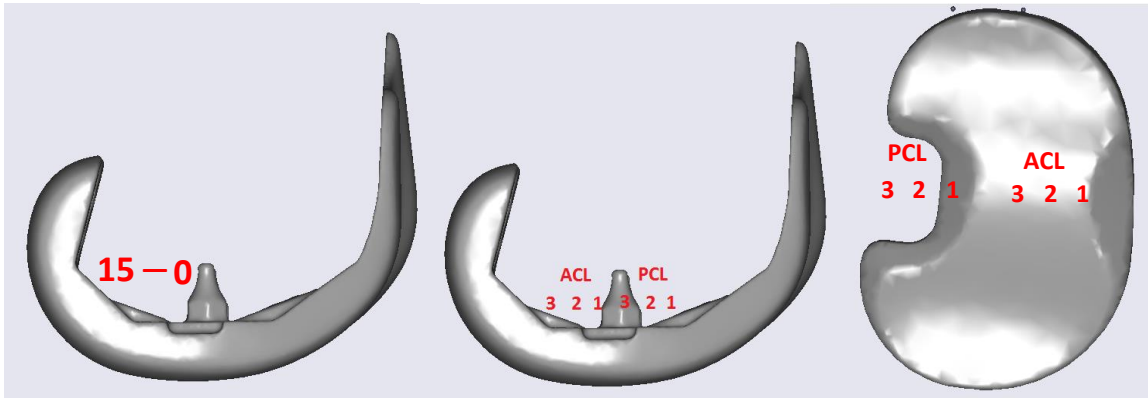
Figure 10.4: ACL is translated 15 mm posteriorly on femur (left), ACL and PCL insertion and origins on tibia (right) and femur (middle)

Strain was determined by subtracting the maximum length of the ligament during flexion from the slack length of the ligament, and the difference was divided by slack length. This data was used to determine the effect that ligament location has on ligament strain. Table A.1 in the appendix reported the slack length, elongation, and strain percent for both the ACL and PCL at each location combination. Figures 10.5 and 10.6 depicted the trend of strain percent changing with the change in location for the ACL and PCL. The first number for the location refers to the location on the tibia and the second number refers to the location on the femur. Figure 10.5 showed that ACL strain percent decreased as the insertion on the tibia was moved anteriorly and the insertion on the femur was moved posteriorly. Figure 10.6 showed that PCL strain percent decreased as the insertion on the tibia was moved posteriorly and the insertion on the femur was moved anteriorly. ACL locations 11, 21, 31, 22, 32, and 33 and PCL locations 11, 12, 13, and 23 experienced strain greater than 40% indicating they were not viable locations.
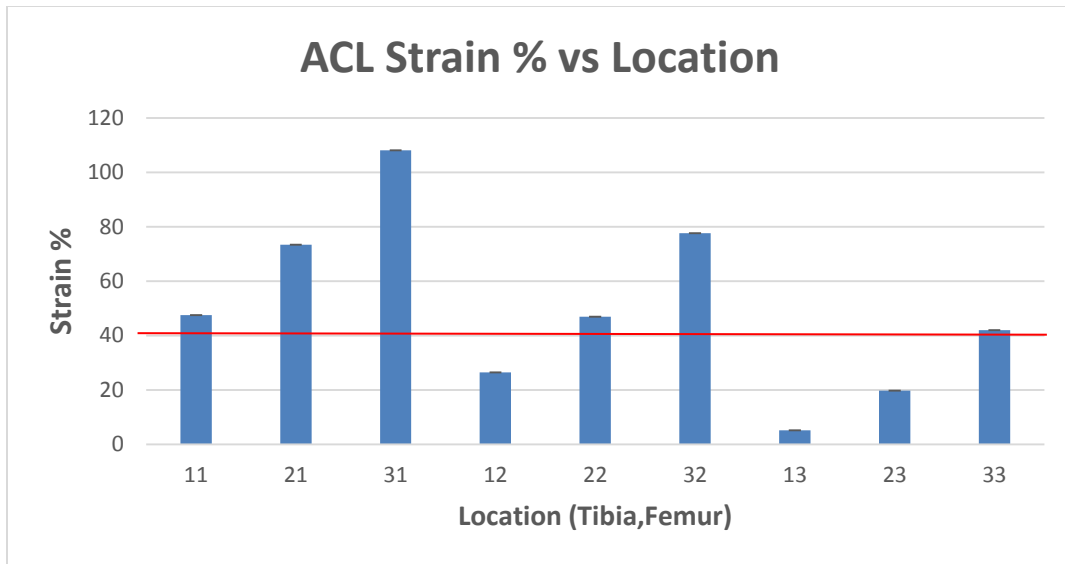
Figure 10.5: ACL strain percent at different PCL location combinations
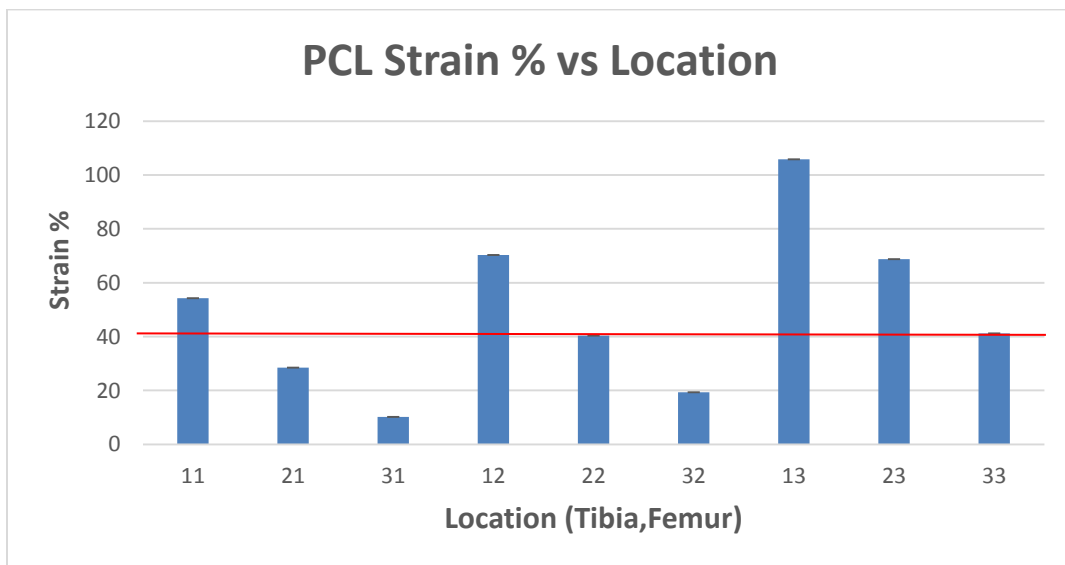
Figure 10.6: PCL strain percent at different PCL location combinations
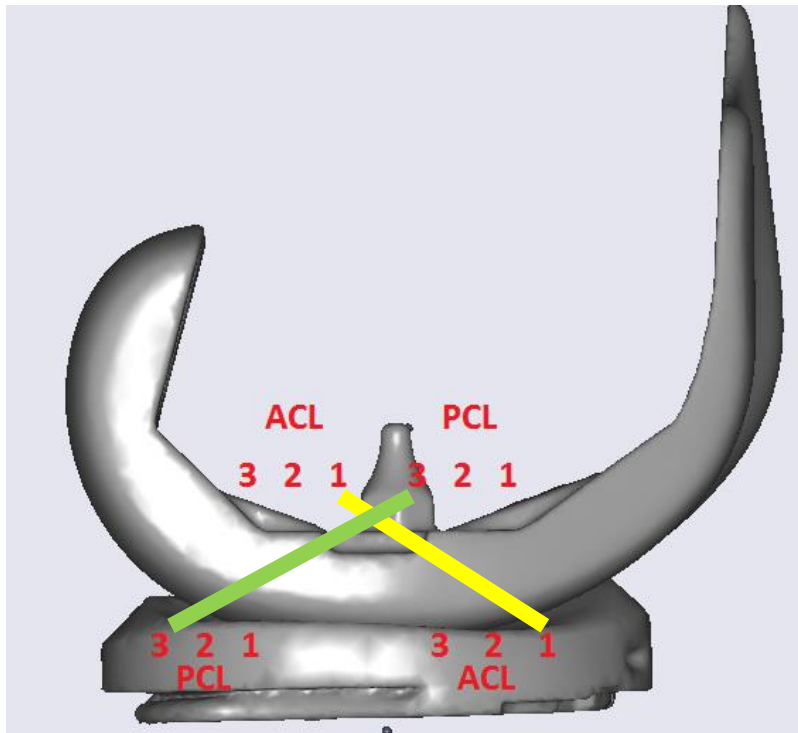
Figure 10.7: Example of an ACL 11 combination (yellow) and PCL 33 combination

(green)

Four additional locations were added for each insertion and origin group to have a total of 7 locations that covered a distance of 15±2 mm on the femur and tibia. Figures 10.8-10.11 demonstrated the trends experienced for ligament strain when moving the insertion location of one group while keeping the other 3 insertion groups constant. Figures 10.8 and 10.9 showed ACL strain percent decreased from 66.73% to 6.07% as the insertion on the femur was moved posteriorly and increased from 14.78% to 61.54% as the insertion on tibia was moved posteriorly. Note that the most anterior location of the ACL on the femur failed. Figures 10.9 and 10.10 showed PCL strain percent increased

from 23.46% to 37.33% as the insertion on the femur was moved posteriorly and decreased from 59.64% to 11.06% as the insertion on the tibia was moved posteriorly.
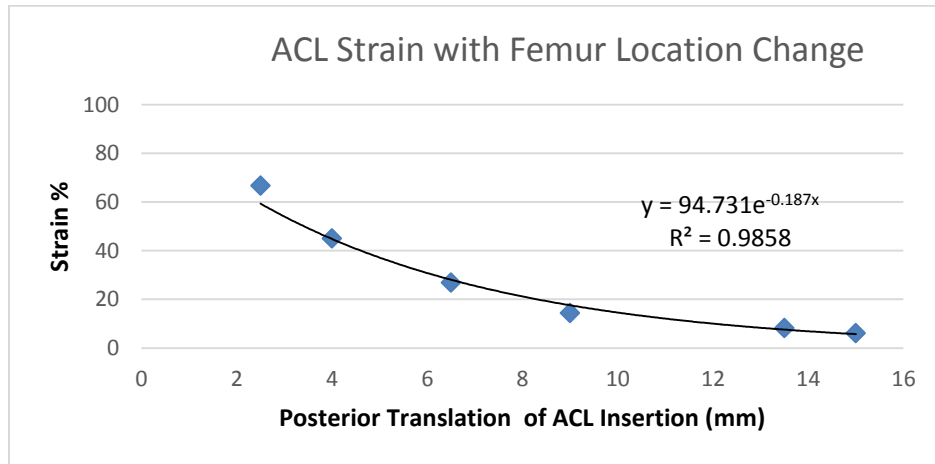
Figure 10.8: ACL strain with femur location change. Note: The initial location failed.
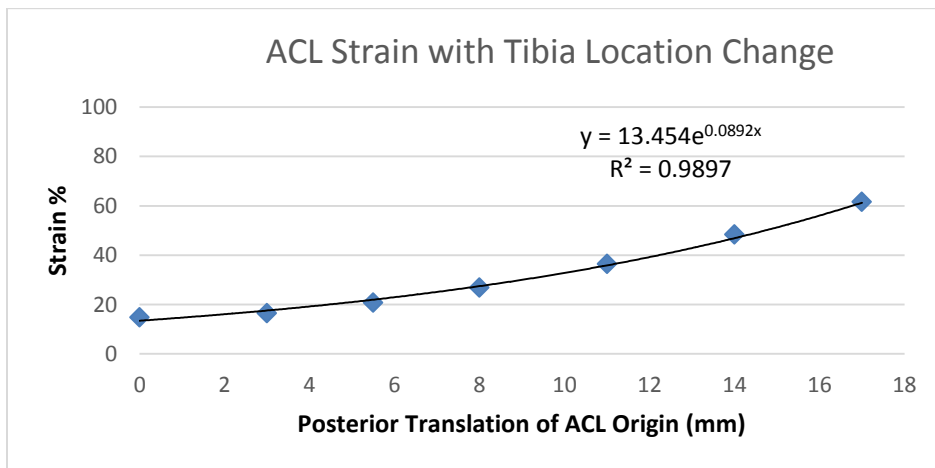
Figure 10.9: ACL strain with tibia location change
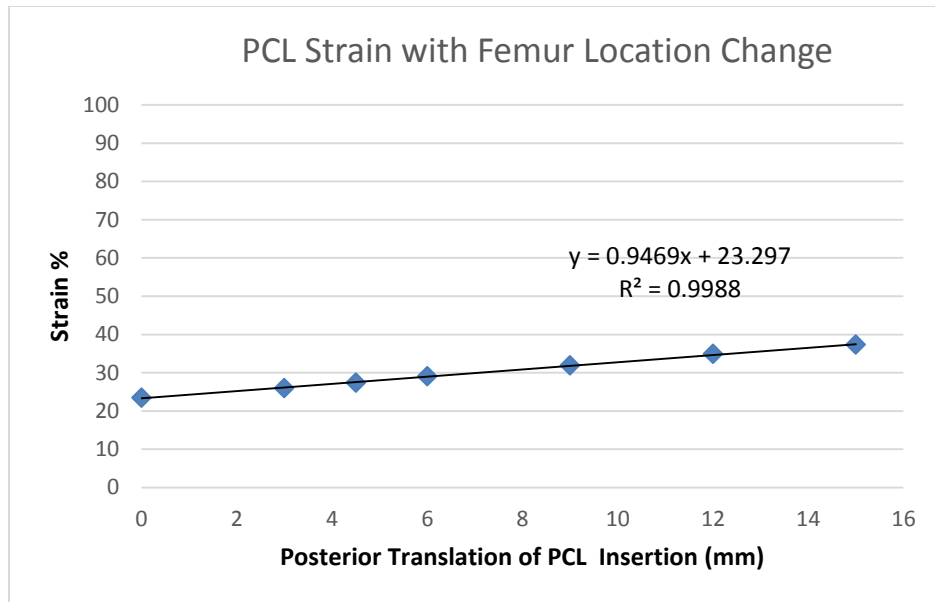
Figure 10.10: PCL strain with femur location change
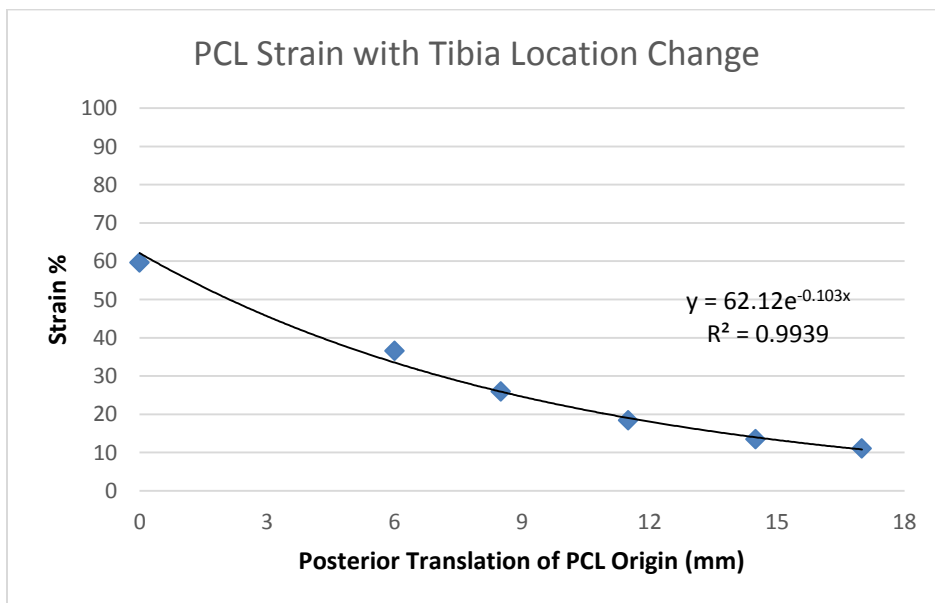
Figure 10.11: PCL strain with tibia location change

85

ACL and PCL lengths were increased by 5 mm in 1 mm intervals for 2321 location combination as depicted in Figure 10.12. Strain was recorded during flexion for each ligament length. Figures 10.13 and 10.14 demonstrate the effects ligament length has on ligament strain during flexion. Figure 10.13 showed, as the ACL length was increased, ACL strain percent decreased from 8.11% to 4.6%, and the PCL strain percent remained constant at 25.73%. Figure 10.14 indicated, as the PCL length was increased, ACL strain percent decreased from 8.11 % to 2.62%, and the PCL strain percent decreased from 25.93% to 13.92%. Note 4 and 5 mm additions to the ACL failed.
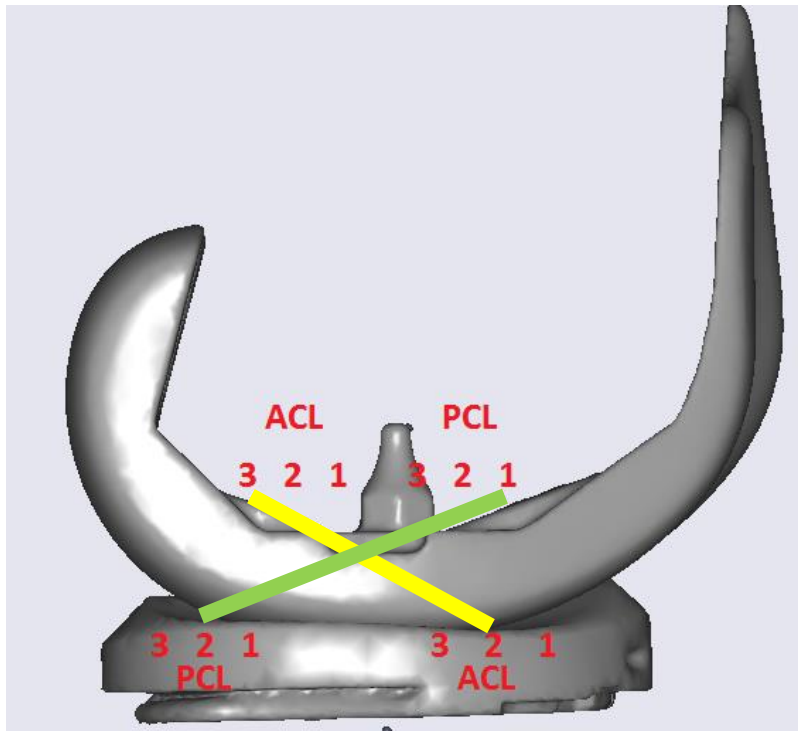
Figure 10.12: 2321 ligament combination: ACL (yellow) and PCL (green)
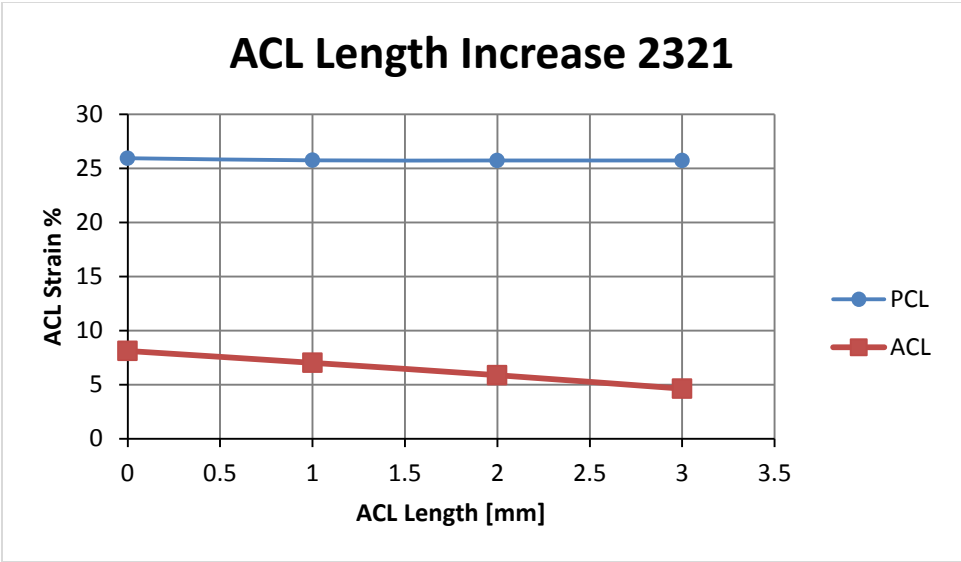
Figure 10.13: ACL and PCL strains as ACL length was increased. Note: 4 and 5 mm

length additions failed.
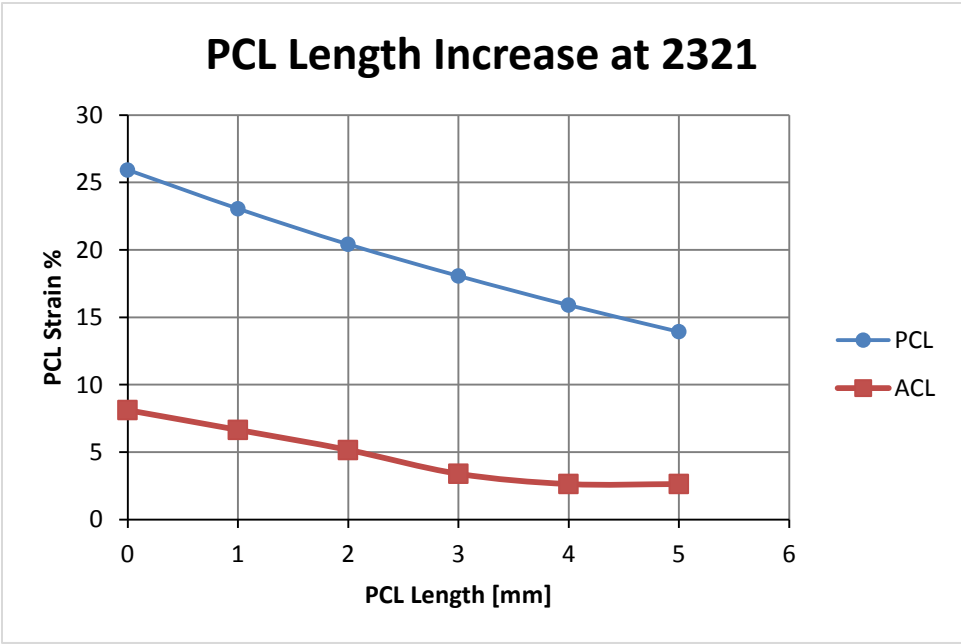
Figure 10.14: ACL and PCL strains as PCL length was increased

10.3 COMPUTATIONAL: A/P TRANSLATION AT VARYING

LOCATIONS AND LENGTHS

A/P translation was determined by creating a 3D model that simulated an anterior and posterior drawer test. Ligament location and length were varied to see their effect on the laxity of the knee. 2,916 iterations of different ligament location and lengths were evaluated.

A/P translation was evaluated at the viable ligament locations for 0 and 90 degrees. Figures 10.15-10.18 depict average anterior and posterior displacement of the knee at different ACL and PCL locations at 0 and 90 degrees without length change. The x-axis is the location combination of the specific ligament with the first number indicating its location on the tibia and the second number the location on the femur based off of Figure 10.4. Anterior posterior displacement at 0 degrees varied from 3.375 mm to 4.71 mm and 0.674 mm to 0.761 mm between location combinations respectively. Anterior and posterior displacement at 90 degrees varied from 1.042 mm to 1.679 mm and 0.663mm to 1.525mm respectively. There was not a lot of variability between locations.
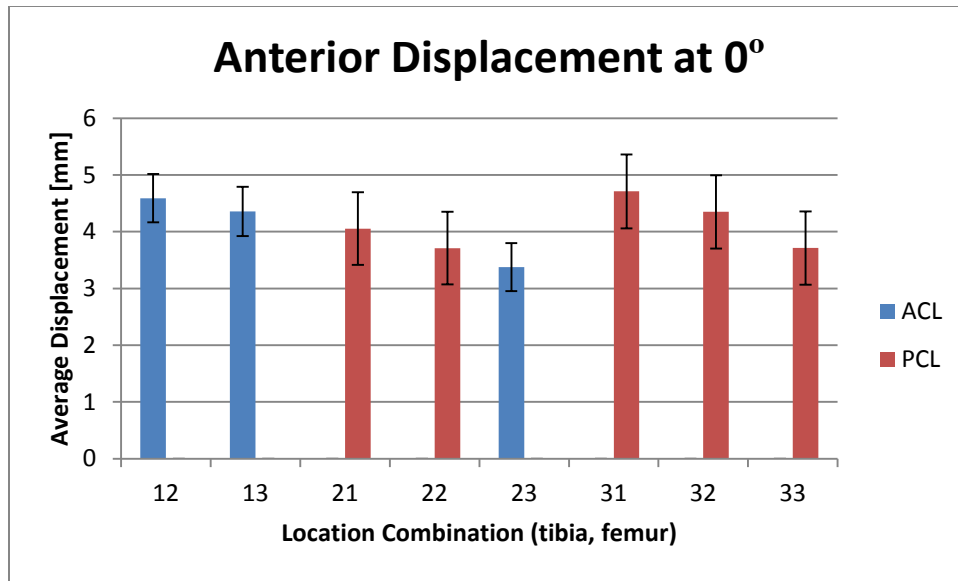
Figure 10.15: Anterior displacement for ACL and PCL location combinations at 0º
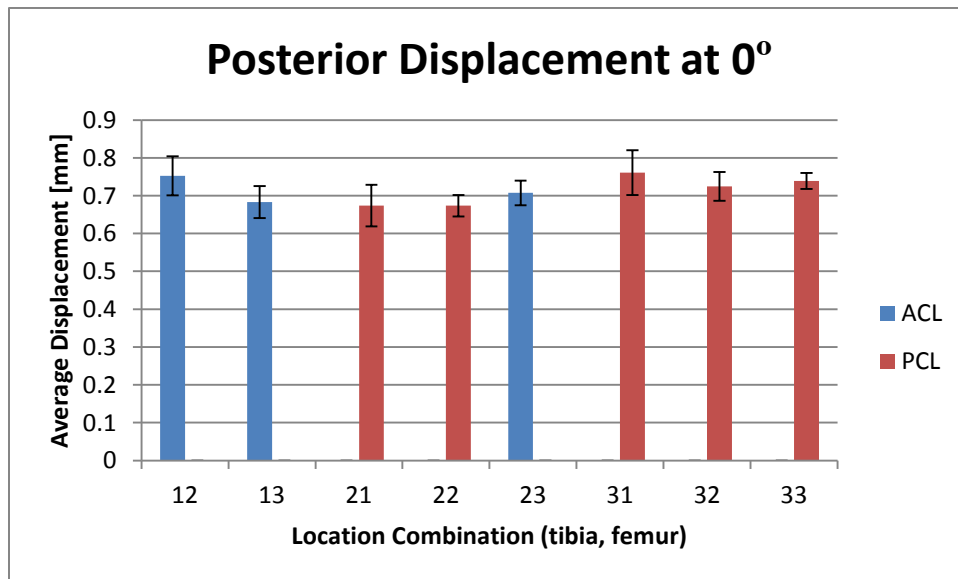
Figure 10.16: Posterior displacement for ACL and PCL location combinations at 0º
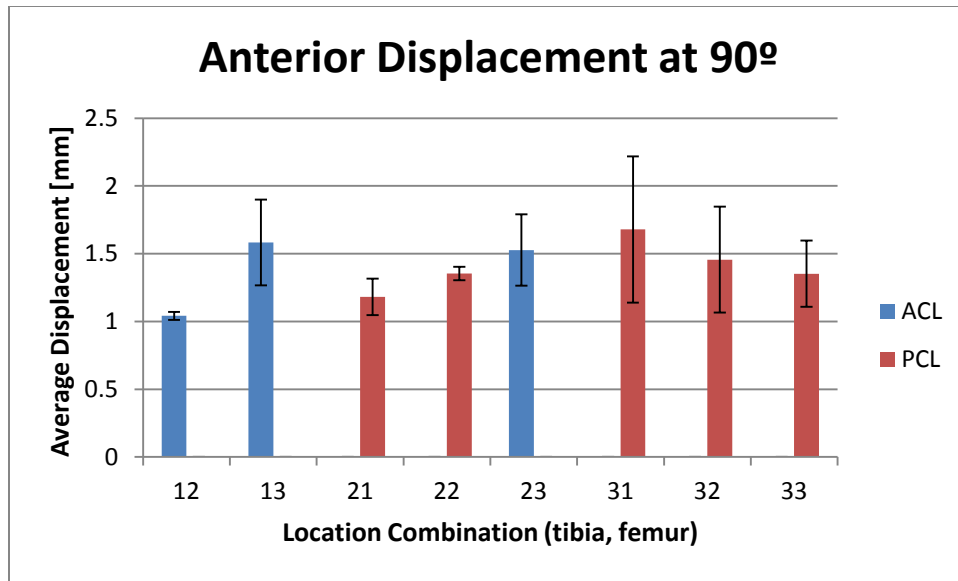
Figure 10.17: Anterior displacement for ACL and PCL location combinations at 90º
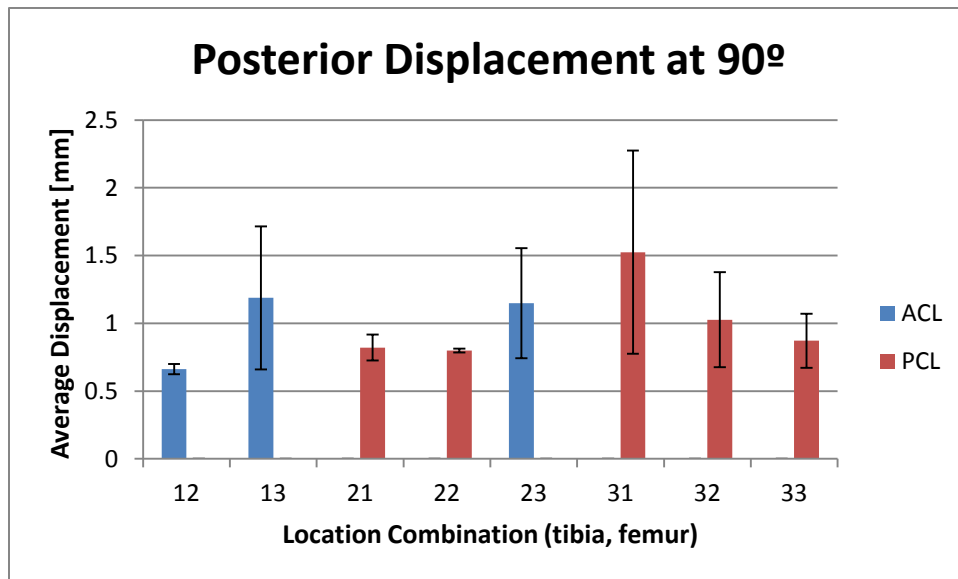
Figure 10.18: Posterior displacement for ACL and PCL location combinations at 90º

A/P translation was determined at different ligament lengths. Figures 10.19-10.22 demonstrate knee displacement as the ACL and PCL length were increased to 5 mm in increments of 1 mm at 0 and 90 degrees of flexion for location 2321. Anterior and posterior displacement increased from 3.33 mm to 6.56 mm and 0.69 mm to 4.06 mm respectively, as the length of the ACL was increased at 0 degrees of flexion. Anterior and posterior displacement increased from 3.33 mm to 4.77 mm and 0.69 mm to 4.85 mm respectively, as the length of the PCL was increased at 0 degrees of flexion. Anterior and posterior displacement increased from 1.266 mm to 1.96 mm and 0.877 to 1.156 mm respectively, as the length of the ACL was increased at 90 degrees of flexion. Anterior and posterior displacement increased from 1.266 mm to 3.459 mm and 0.877 to 1.998 mm respectively, as the length of the PCL was increased at 90 degrees of flexion. Note in Figure 10.21 the 4 mm and 5 mm additions to the ACL failed. Anterior displacement is affected more by ACL length increase and posterior displacement is affected more by PCL length increase. PCL length had a more significant impact than ACL length at 90 degrees.
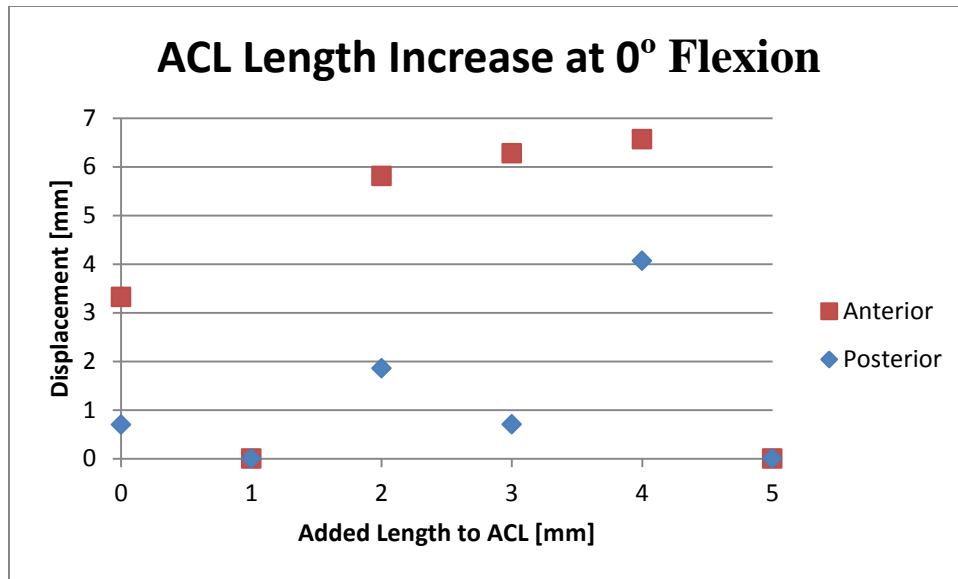
Figure 10.19: 2321 locations displacement as ACL length increased at 0 degrees
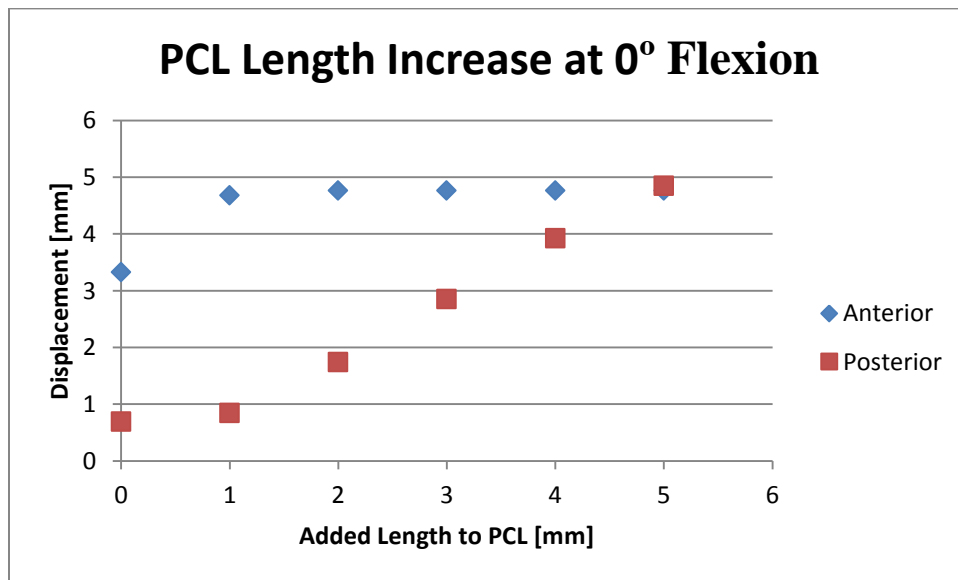
Figure 10.20: 2321 locations displacement as PCL length increased at 0 degrees
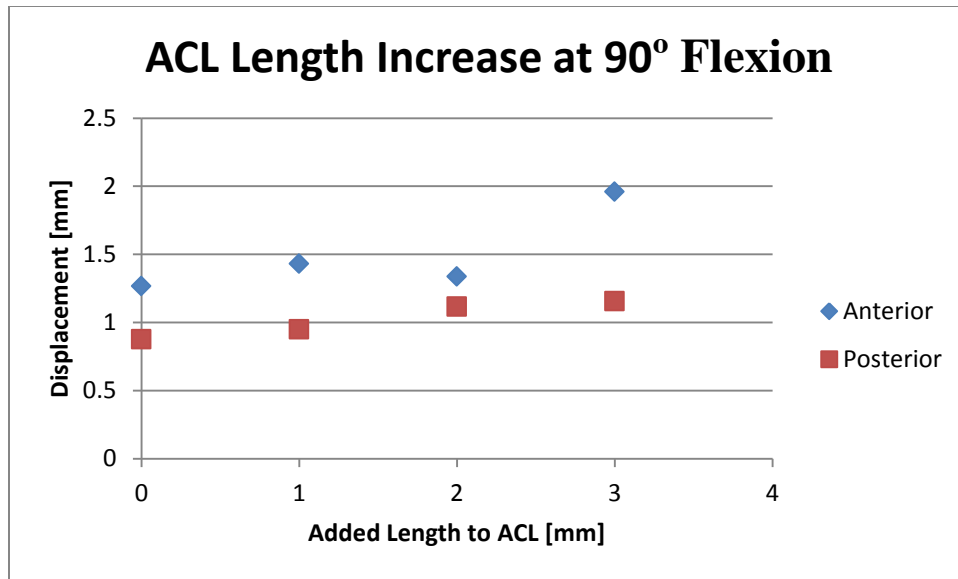
Figure 10.21: 2321 location displacement as ACL length increased at 90 degrees
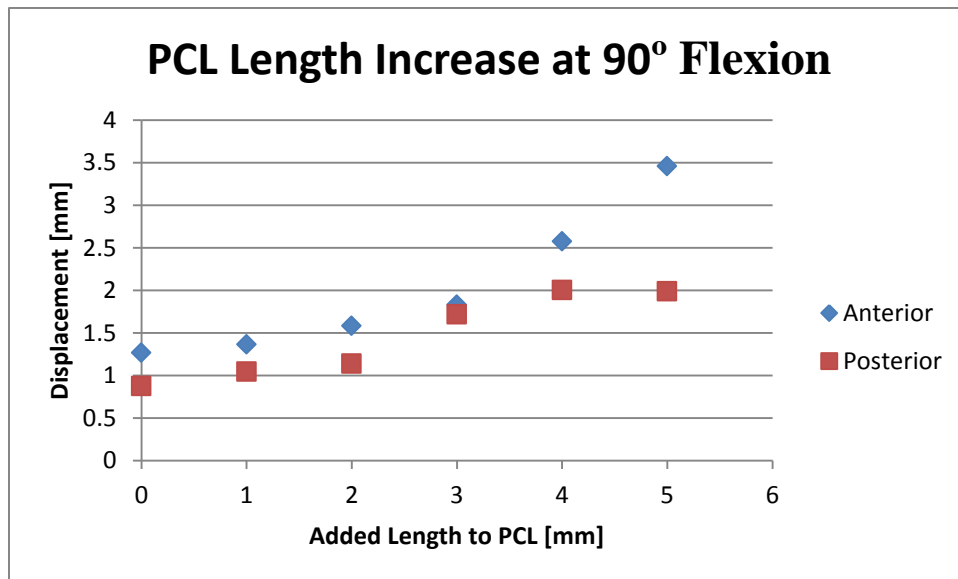
Figure 10.22: 2321 location displacement as PCL length increased at 90 degrees

Ligament length and locations were varied together to create over 2,916 iterations of possible combinations. Table 10.1 shows the 14 combinations that had 3-5 mm of displacement in both the anterior and posterior direction. Out of the viable combinations 12 of them included the "23" ACL combination and 10 of them were with 4 or 5 mm length additions to the PCL. Table 10.2 shows the 6 combinations of the 14 that also experienced less than 10% strain in both the ACL and PCL during 120 degrees of flexion. All of the viable locations have an ACL combination of "23" and 3 out of 6 of them have the PCL combination "31".

Table 10.1: Viable ligament location and length combinations between 3-5 mm of displacement both anteriorly and posteriorly

Location	ACL Length	PCL Length	Anterior Displacement [mm]	Posterior Displacement [mm]
2321	0	4	4.77	3.93
2321	0	5	4.77	4.85
2322	0	4	4.77	3.75
2322	0	5	4.77	4.75
2331	0	3	4.77	3.27
2331	0	4	4.77	4.26
2331	0	5	4.77	5.02
2332	0	3	4.77	3.01
2332	0	4	4.77	4.02
2332	0	5	4.77	4.97
2333	0	4	4.77	3.72
2333	0	5	4.77	4.72
1322	0	5	3.14	4.82
1331	3	1	3.13	4.83

Table 10.2: Viable ligament location and length combinations between 3-5 mm of

displacement and less than 10% strain

Location	ACL Length	PCL Length	Anterior Displacement [mm]	Posterior Displacement [mm]	ACL Strain %	PCL Strain %
2331	0	3	4.77	3.27	2.61	9.58
2331	0	4	4.77	4.26	2.61	8.61
2331	0	5	4.77	5.02	2.61	7.72
2332	0	4	4.77	4.02	2.61	9.30
2332	0	5	4.77	4.97	2.61	8.34
2333	0	5	4.77	4.72	2.61	9.37

10.4 LIGAMENT STABILITY

The ligaments' effect on knee stability was determined by creating a mechanical testing setup in Instron where a knee replacement with and without ligaments was evaluated with body weight. Figures 10.23 and 10.24 showed the anterior and posterior displacement values for a knee replacement with and without ligaments at flexion angles between 0 and 120 degrees in 30 degree intervals. One thing to note was the "No Ligament" displacement values for 90 and 120 degrees were the values right before dislocation because the external load caused complete dislocation. The "No Ligament" data shows the amount of translation the implant allows before it dislocates, which varied from 3.05 mm to 15.87 mm depending on flexion angle. The displacement values with ligaments were all below the no ligament data except 2331 at 0 degrees. Anterior displacement was much greater than posterior displacement.
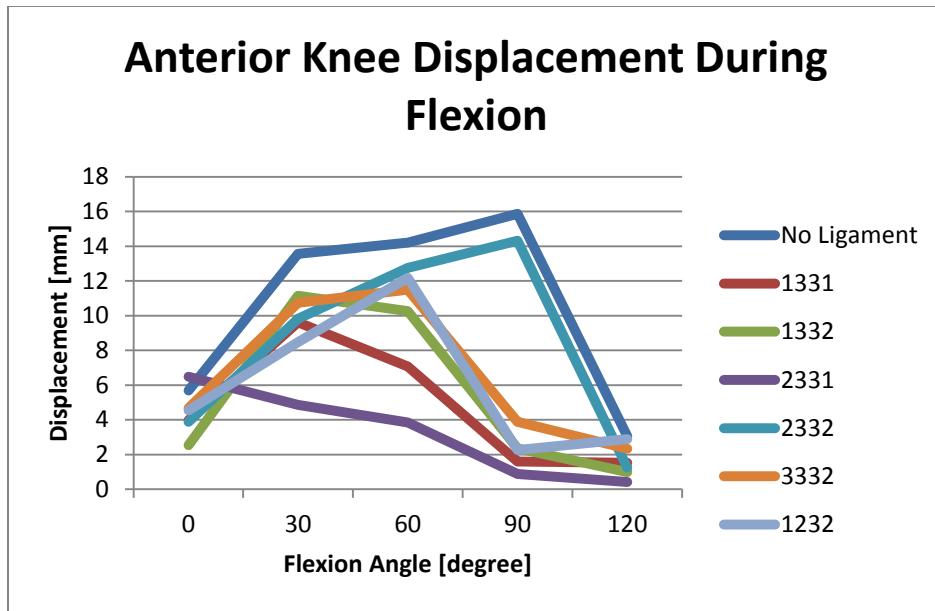
Figure 10.23: Anterior displacement at different flexion angles
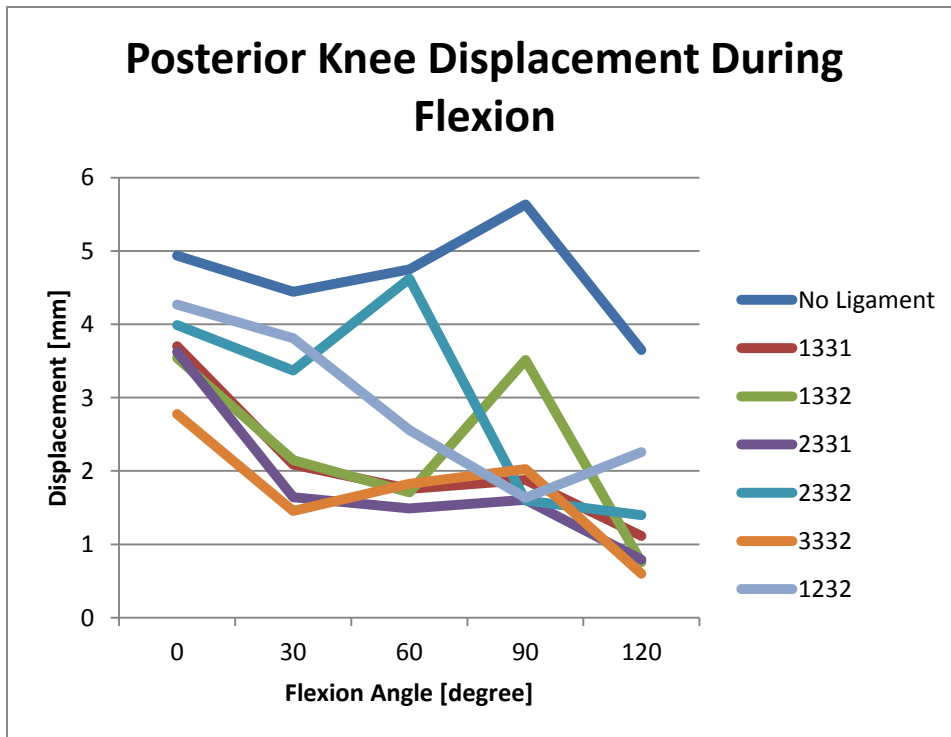
Figure 10.24: Posterior displacement at different flexion angles

Figures 10.25 and 10.26 showed the displacement reduction percentage for each ligament location compared to "No Ligament" at different flexion angles. Ligament location 2331 provided the most reduction for anterior displacement and ligament location 3332 provided the most reduction for posterior displacement for the majority of flexion angles. Displacement reduction increased with flexion angle for both anterior and posterior tests.
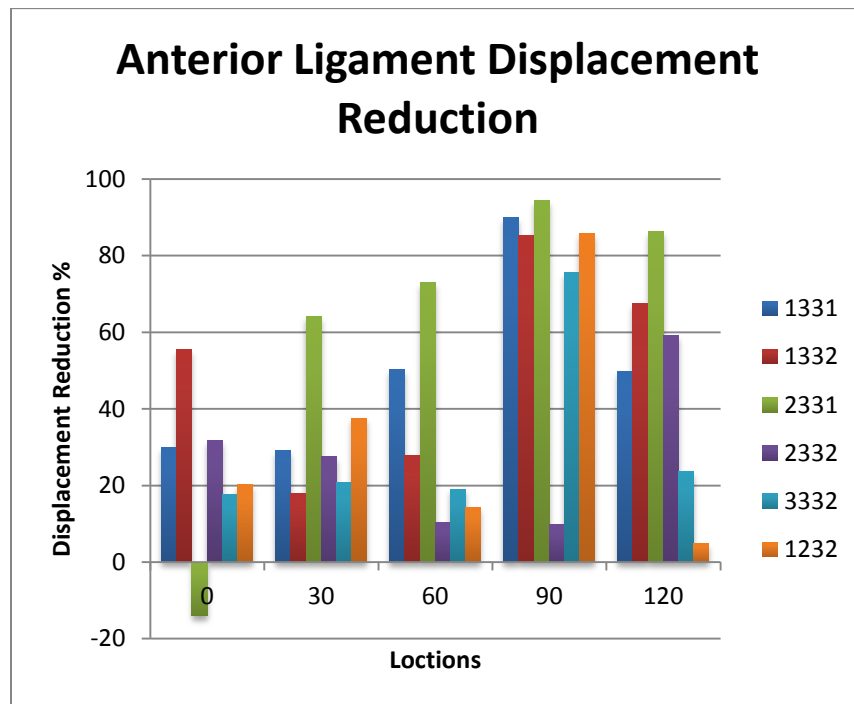
Figure 10.25: Anterior displacement reduction percentage with ligaments

97
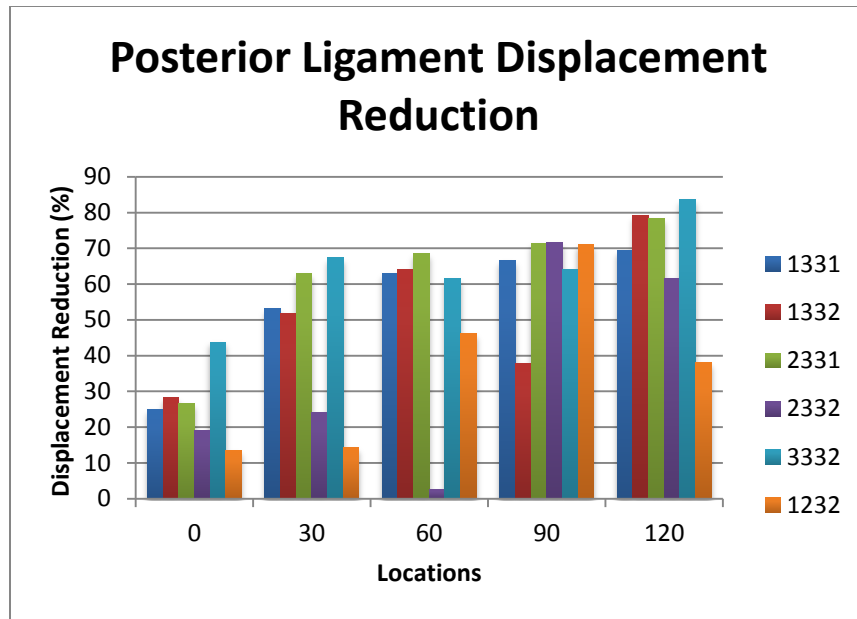
Figure 10.26: Posterior displacement reduction percentage with ligaments

CHAPTER ELEVEN

DISCUSSION

The results of this study were unique in that they defined possible ligament location and length combinations for a TKR implant that provided stability through the use of artificial ligaments. Literature focused on effects that ligament tension had on implant kinematics or ligament location for ligament reconstruction. No previous study had looked at the effects of synthetic ligaments on knee replacement kinematics. The design of the attachment mechanism was verified with the outputted data that compared relationships between ligament length, ligament location, and implant stability.

11.1 VERIFICATION OF ATTACHMENT DESIGN

The first aim of this study was to design a TKR that incorporated artificial ligaments. The attachment mechanism design requirements included the ability to withstand the forces of the knee, have a safety factor of three compared to synthetic ligaments, and arthroscopically replaceable. The attachment mechanism and synthetic ligaments were tensile tested with Instron to determine the failure loads for both. The ligament was tested to failure twice and failed at 932.59 N and 1137.64 N. Both times the ligament failed at the location of the suture. Anatomical ligaments do not experience more than 400 N of force during everyday activities, but can experience around 2000 N of force during strenuous activities. It was expected that the synthetic ligaments would have had a failure force closer to this 2000 N since they were designed to replace

ligaments. The addition of sutures may have weakened the ligament causing the lower failure force and rupture of the suture location. This suggested that, in the future, the ligaments should be attached to the knee in a manner other than suturing.

The attachment mechanism was tested similar to the synthetic ligament. Shim stock steel was used to replicate a stronger ligament. It was wrapped around the attachment mechanism like a ligament, and then tensile tested to failure. Failure was determined by inability to remove the pin using needle nose pliers. Failure occurred at 3800 N. This was over three times the failure value for the synthetic ligament, indicating the attachment mechanism had a safety factor of three. This was important because the attachment mechanism was not designed to be replaceable, but the ligaments were designed to be arthroscopically replaceable.

As mentioned earlier, the suture could have damaged the properties of the ligament causing it to fail prematurely. Even if the ligaments were damaged due to the suture, the attachment mechanism still withstood almost twice the force that a knee experiences during strenuous activities. The method of looping the ligament around the attachment mechanism will need to be evaluated further due to the possibility of sutures weakening the ligament, but overall the attachment mechanism design passed the design inputs.

11.2 IDEAL LIGAMENT LOCATIONS

The second aim of this study was to determine the optimal ligament location for the TKR design to provide normal stability using a computational model. A

computational model was designed in AnyBody that allowed for the ability to change the location of the ligaments. In ACL reconstruction surgery, the location of the ACL graft repair is debated between surgeons because the location of the ACL determines the success of the procedure. This indicated the importance of determining the ideal location.

Ideal ligament location is determined by ligament function, ligament strain, and ligament laxity. ACL and PCL function during flexion, determined by the change in length, for the viable ligament combinations, compared similarly to the data seen in the study performed by Li et al. The in vivo study published by Li concluded that the PL bundle of the ACL experienced maximum elongation at 0 degrees and the length continuously decreased to 90 degrees of flexion (Li et al., 2004). In a study by Levangie and Norkin, they concluded that the ACL experienced max elongation at 20 degrees of flexion and decreased in length as flexion continued (Levangie & Norkin, 2005). The in vivo study by Li observed this function in the AM bundle of the ACL. Both of these studies concluded that the PCL increased constantly through flexion. Furthermore, in the study by Levangie, they concluded that the PCL also decreases its length in flexion greater than 90 degrees (Levangie & Norkin, 2005). The data produced by the study in this thesis showed ligament function similar to both of these studies. However, ligament function was also observed in direct opposition to these two studies. The combinations where the ligaments function similar to the two previous studies produced strain percents and laxity values similar to anatomical values. The combinations that produced improper ligament function could be due to malpositioning of the ACL and PCL on the femur or excessive ligament tension at full extension. A study on the biomechanics of the ACL

and implications for surgical reconstruction by Dargel concluded that malposition of the ACL on the femur and excessive ligament tension are two of the most common causes or poor kinematics and function of the ACL after reconstruction (Dargel et al., 2007).

To determine the strain during knee flexion, ligament length was tracked and the maximum length was recorded. The maximum length was compared to the slack length of the ligament to determine the average strain percent for the ACL and PCL location combinations (Figure 10.5-10.6). Ligaments can strain 8-10 percent before rupture as seen in the study by Lenard, so the viable locations were based off of this value (Lenard, 2014). Any location combinations that experienced strain greater than 40 percent were not considered viable options. 40 percent was the cut off instead of 10 percent because ligament length could be added to lower the strain for possible location combinations to pass the 10 percent cut-off. By using the 40 percent cut off the number of possible combinations was cut from 2,916 to 540.

Strain percent was determined at different locations for the ACL and PCL, on both the femur and tibia, to evaluate trends in more detail (Figure 10.8-10.11). ACL strain percent decreased as the insertion on the tibia was moved anteriorly and the insertion on the femur was moved posteriorly. This related to knee function: as the femur rotates, the posterior end of the condyle moves closer to the anterior end of the tibia allowing the ACL to become lax. PCL strain percent decreased as the insertion on the tibia was moved posteriorly and the insertion on the femur was moved anteriorly. This related to knee function as well, because as the femur rotates, the anterior end of the condyle moves closer to the posterior end of the tibia, creating a shorter distance between

the insertion and origin. At the same time, these ligament locations were far enough apart to provide an adequate amount of stability.

The data of strain percent during flexion indicated that the femoral location of the ACL ligament had the most significant effect on the results compared to any other location change. An ACL reconstruction study by Dargel, mentions that anterior positioning of the femoral and tibial tunnel was the most common technical mistake during arthroscopic surgery. The study also stated that the location of the ACL on the femur has a much more significant impact on the length and function of the ACL then the tibia (Dargel et al., 2007).

The data for strain percent during flexion varied significantly as the values ranged from 5% to 105%. The viable combinations had strain percents under 10% but all the other combinations exceeded this. In the in vivo study by Li, they experienced strain percent that varied from 4.8% to 31% (Li et al., 2004). They concluded that the excessive elongation was due to the insertion and origin of ligaments being close together at full extension. A study by Dargel explained that anterior malposition of the ACL leads to strain in flexion and posterior malposition leads to strain in extension and impingement with the PCL. The Dargel study also suggested excessive pre-tensioning leads can lead to strain in the ligaments during flexion (Dargel et al., 2007). These two studies help to explain what caused the excessive strain values.

Average anterior and posterior displacement was determined at different viable ligament locations (Figures 10.15-10.18). The average anterior displacement was between 3-5 mm for all locations at 0 degrees. A healthy ACL allows 3-5 mm, so this

103

indicates that these locations are viable and should be further evaluated. The average posterior displacement was under 2 mm for all locations at 0 and 90 degrees. This could indicate that the PCL pre-tensioning was too tight or the lengths were too short. This was also seen with problems in ACL reconstructions and ligament balancing in TKR procedures. In the study by Dargel, they discussed excessive pre-tensioning of ligaments and the possible range of motion restriction as a results, which could explain the lack of displacement during the posterior drawer test. The lack of laxity leads to cartilage damage after an ACL reconstruction and polyethylene wear after a TKR. There was little variability between the ligament locations during the laxity test because the non-viable locations were removed with the 40 percent cut off of the knee flex test. Location also does not have as significant of an impact on laxity as it does on flexion.

11.3 IDEAL LIGAMENT LENGTHS

The second part of aim two was to determine the optimal ligament length for the knee replacement design using a computational model. A computational model was designed in AnyBody that allowed for the ability to change the length of the ligaments. Ligament tensioning was critical in outcomes for ACL reconstruction and PCL retaining knee replacements with ligament balancing. This indicated the importance of determining the ideal length.

To determine the effect of ligament length during knee flexion, ACL and PCL lengths were increased by 5 mm in 1 mm intervals and flexed to 120 degrees for the 2321 location combination (Figures 10.13 and 10.14). As ACL length was increased, ACL

strain percent decreased, and the PCL strain percent remained constant. As PCL length was increased, ACL and PCL strain percent decreased. ACL lengths were under 10 percent strain indicating that they were all viable options for 2321. PCL strain percent decreased from 25.93 to 13.92 percent as its length was increased. This indicates that length can continue to be added to the PCL in order to make 2321 a viable option. However, increasing length excessively caused the ACL to fail at 4 mm and 5 mm additions. The knee became unstable as the ACL became lax resulting in failure. This failure in AnyBody is equivalent to a knee dislocation. Excessive length increase was equivalent to insufficient pre-tension in a graft. The study by Dargel stated that if the surgeon does not tension the ligaments enough, it can lead to instability similar to what occurred with the 4 and 5 mm additions for the ACL.

To determine the effects of ligament length on knee laxity, ACL and PCL lengths were increased by 5 mm in 1 mm intervals, and evaluated using an anterior and posterior drawer test for all viable locations determined from the knee flexion study. Figures 10.19-10.22 depicted the length increase for 2321 location combination. As ACL and PCL length increased, anterior and posterior laxity increased. It became evident that increasing length resulted in increased knee laxity, as mentioned earlier, and is related to ligament tensioning in ACL reconstruction and ligament balancing in TKR surgeries. Clinically, a stable knee allows 3-5 mm of translation and around 9-13 mm of total A/P translation. As the ACL length was increased, the anterior laxity increased from 3.326 to 6.565 mm. However, it failed with the addition of 5 mm because it was approaching 7 mm of laxity, which, clinically, is considered a class II ACL sprain. As the PCL length

increased, its posterior laxity increased from 0.694 to 4.85 mm. This indicated that adjusting the length of a ligament could make a combination that was not viable become viable. This emphasizes the need to evaluate all the combinations of length and location.

11.4 VIABLE COMBINATIONS

To determine the combination of lengths and locations that were viable, the ligaments were increased together to evaluate over 2,916 possibilities. The number of possibilities was narrowed down to 540 after the knee flex test. The knee flex test was able to rule out the locations that were not viable. The 540 possibilities were examined with the knee laxity test. These possible combinations were considered to be viable if they experienced displacement between 3-5 mm for both the anterior and posterior test. Only 14 combinations remained viable after the knee flex test. It was evident that many of the combinations were either too stiff or too lax. The locations that were too lax failed, indicating they dislocated. The 14 viable combinations left were then tested in the knee flex test to determine if they experienced strain under 10%.

Out of the 2,916 possibilities only 6 were considered viable. Table 10.1 shows the 14 combinations that had 3-5 mm of displacement in both the anterior and posterior direction. Out of the viable combinations 12 of them included the "23" ACL combination and 10 of them were with 4 or 5 mm length additions to the PCL. Table 10.2 shows the 6 combinations that had both 3-5 mm of laxity and less than 10% strain. All 6 combinations were ACL "23" and 3 out of the 6 were PCL "31". This suggests that the "23" location of

106

the ACL is the most optimal combination for the ACL. "31" location of the PCL had the most viable locations suggesting it as the most optimal location for the PCL.

As mentioned in the ideal ligament length and ideal ligament location discussions, there are a variety of reasons why different combinations were eliminated. If a combination failed for exceeding 10% strain or not obtaining at least 3 mm of displacement, it could be due to excessive pre-tensioning, insufficient ligament length, or malposition of the ligaments, specifically the ACL excessively anterior on the femur and the PCL excessively posterior on the femur as discussed by Dargel. If a combination failed due to excessive laxity, it could be the result of inadequate pre-tensioning or the ligament being too long as discussed in the ligament balancing total knee replacement study by Babazadeh (Babazadeh, 2009).

11.5 VALIDATION OF COMPUTATIONAL MODEL AND DESIGN

The third aim of this study was to validate the computational model and the effectiveness of the attachment mechanism using Instron. To validate the computational model and device effectiveness, an anterior and posterior drawer test was designed with Instron. The top six ligament locations from the knee flexion study were evaluated in this study and compared to a knee with no ligaments. Anterior and posterior displacements were evaluated for all seven cases at 0-120 degrees at 30 degree increments (Figures 10.23-10.24). The ligament cases increased the stability compared to the no ligament case in every experiment except for one. The ligaments should have never allowed for more displacement than the no ligament case because the no ligament case is the max

displacement allowed before failure. This exception occurred because of the limitations of the study that will be discussed in the next section. The no ligament case allowed for translation that varied from 3.05 mm to 15.87 mm. It was observed that the polyethylene insert geometry provided enough force to prevent the knee from dislocating anteriorly. However, it was also observed that the polyethylene geometry did not provide enough force to prevent the knee from dislocating posteriorly. This could be due to the knee replacement designed around retaining the PCL ligament, which would provide the resistance to translation posteriorly. The smallest amount of translation was observed at 120 degrees for both the anterior and posterior test. This could be due to the lack of ligaments length causing the ligament to be taut. It was difficult to rotate the ligaments to 120 degrees for several of the ligament cases because the ligaments were so taut.

To validate the effectiveness of the design, the amount of stability the ligaments added was measured by the displacement reduction percentage (Figures 10.25-10.26). Ligament location 2331 provided the highest reduction percentage for anterior displacement, and ligament location 3332 provided the highest reduction percentage for posterior displacement for the majority of flexion angles. The 2331 and 3332 locations may have provided the most anterior and posterior stability respectively because the ligaments were too short or the ligament location provided extra stability in those directions. Displacement reduction increased with flexion angle for both anterior and posterior tests. This may have been caused by the tautness of the PCL in deep flexion for all the models as they were difficult to rotate to 120 degrees. The tautness could be due to

108

either the length of the PCL or a slight interference with the femoral block during deep flexion.

Laxity varied significantly from 0.006 mm to 17 mm. The viable combinations experienced laxity between 3-5 mm, as claimed to be normal laxity (Galbusera et al., 2014). However, other studies, like the study by Webright, measured anterior tibial translation in uninjured knees varying between 5.6 mm and 10.9 mm (Webright et al., 1998). In an in vivo study by Un, they measured anterior tibial translation between 6 mm and 8 mm and posterior tibial translation between 2 mm and 4 mm (Un et al., 2001). In a computational study by Amiri, they measured a total A/P laxity between 12.5 mm and 12.9 mm (Amiri & Wilson, 2012). A study by Angoules, comparing ACL deficient knees to healthy and reconstructed knees, determined anterior knee laxity of a healthy knee to be 2.0±1.21 mm and ACL deficient knees to be 6.7±1.95 mm (Angoules et al., 2013). There is a lot of variability between studies on the amount of laxity in a knee. This could be due to the patients measured, instruments used, flexion angle, and amount of force used in the drawer test. Due to all of the variability, it is hard to compare with one specific study, but throughout medical studies it is determined that 3-5 mm of A/P laxity is normal. The viable laxity in this study was based off the 3-5 mm found across literature. Combinations that had laxities less than 3 mm were most likely due to excessive pre-tensioning or ligament length being too short. Combinations that had laxities greater than 5 mm were most likely due to low initial ligament tensioning or ligament length being too long. In a study by Dargel and another study by Babazedeh, it is discussed that tension applied to a graft before fixation significantly influences the

ability of a graft to stabilize the knee joint. The study also discusses that low initial graft tension does not provide adequate joint stability, while excessive initial graft tension will restrain range of motion (Babazadeh, 2009; Dargel et al., 2007).

A/P drawer test with no ligaments in the Journey II knee produced displacement values that compared similarly to a study by Halewood. Anterior displacement values continuously increased from 5.5 mm to 16 mm during first 90 degrees of flexion in the study done by this thesis. In the study by Halewood, they measured 5 mm displacement at 0 degrees and continuously increased to 17 mm at 90 degrees (Halewood et al., 2014). From 90 to 120 degrees of flexion there is a significant difference between the two studies. This could be due to the difficulties of the femur slipping off of the tibia at 120 degrees of flexion when the force was applied in the drawer test.

As mentioned earlier there is a lot of variability in literature on the amount of laxity in a normal knee, but values most consistently found are between 3-5 mm in the anterior and posterior direction. Most A/P drawer tests in literature were performed at 30 degrees of flexion. Comparatively, the values obtained from the A/P drawer test in Instron, with ligaments at 30 degrees of flexion, varied between 5 to 11 mm anteriorly and 1.5 to 3.8 mm posteriorly. Even though this is wider range than the 3-5 mm, it is a similar range to the studies by Webright, Un, and Angoules.

Even though there was variability in the data, all ligament locations provided additional stability in the anterior and posterior directions. The ligaments added stability that varied from 0 to 94%. This increase in stability validated that the design functions as hypothesized.

110

11.7 LIMITATIONS OF STUDY

This study had several limitations that future research should seek to address. Additional samples of synthetic ligaments and attachment mechanisms need to be tensile tested to provide a larger sample size. A different method other than suturing the ligaments should be used to attach the ligaments to the attachment mechanism. This could provide more information on the tensile strength of the ligaments.

In order to obtain a more accurate in vivo model, a more complex knee joint should be created. The surrounding soft tissues and muscles could be modeled. This would take away the clear effect of the ligaments on stability, but it would provide more information on the stability of a normal knee including the effects of muscles and tissues.

The ligaments could be modeled as multiple bundles instead of a single bundle. This could provide a more accurate representation of a ligament. Ligaments do not attach to one single location and they consist of two bundles, so this would allow more anatomical function to be seen. Literature has shown that a double bundle ligament is more accurate than a single ligament. The ligaments in the computational model could also be modeled with the properties of the synthetic ligament instead of an anatomical ligament. This could eliminate some variability between the computational and mechanical results.

Another aspect that could be addressed is decreasing the variability between testers during the drawer tests on the Instron. A mechanism to lower the weight automatically needs to be designed because it was difficult to lower the weight consistently. This would eliminate the variability between each test. A more accurate

method of setting the ligament length needs to be designed. As depicted in the computational model, 1-2 mm in ligament length can significantly affect the results. This could increase consistency between the computational model and the mechanical testing.

CHAPTER TWELVE

CONCLUSION

Based on the results of this study, it can be concluded that the X-Fit knee can increase the stability of a TKR while maintaining motion by incorporating synthetic ligaments into its design. These results could then be further extrapolated to aid in the incorporation of synthetic ligaments into existing TKR to provide additional stability.

The X-Fit Knee's attachment mechanism produced a safety factor of 3 compared to the synthetic ligament. This indicates that the ligament will fail before the attachment mechanism, allowing the system to be repaired arthroscopically. This also suggest that the attachment mechanism is sturdy enough to anchor the ligaments that provide stability to the knee.

As evident in literature and the results of this study, TKRs lack stability. The results of this study showed stability of the TKR was increased with the incorporation of synthetic ligaments. The effectiveness of the ligaments was clearly dependent on two factors: length and location. Ligament length and location were found to significantly influence knee laxity and knee flexion. Knee flexion was determined to be more sensitive to the location of the ACL on the femur than on the tibia. ACL insertion location was found to decrease ligament strain indicating higher range of motion as it was moved posteriorly on the femur. Ligament length and laxity were found to have a linear relationship: as ligament length was increased, laxity increased concurrently. Interestingly, knee flexion was found to be dependent on ligament location compared to

knee laxity's dependence on ligament length. It is imperative to the success of the implant to obtain the correct lengths and location because improper placement or length, even by a couple of millimeters, can impact the outcome significantly. By narrowing down 2,916 combinations to 6 viable combinations, the proper placement and length can be used in the X-Fit knee to produce normal stability.

This study clearly showed that the incorporation of ligaments into the TKR design enhances stability compared to a normal TKR. These results emphasize the need for a knee replacement that incorporates synthetic ligaments, with calibrated location and lengths, to significantly influence stability and possible kinematic performance of the TKR system, and potentially influencing long-term functional outcomes.

Appendix A

Ligament Strain

Table A.1: ACL and PCL strain percent at different ligament location combinations

Location (AT,AF,PT,PF)	ACL Lo	PCL Lo	ACL Elongation	PCL Elongation	ACL Strain	PCL Strain
1111'	26.270	33.276	12.488	18.065	47.537	54.289
1121'	26.270	39.981	12.488	11.360	47.537	28.414
1131'	26.270	46.577	12.488	4.764	47.537	10.229
1112'	26.270	30.144	12.488	21.198	47.537	70.323
1122'	26.270	36.564	12.488	14.777	47.537	40.414
1132'	26.270	43.011	12.488	8.330	47.537	19.368
1113'	26.270	24.936	12.488	26.405	47.537	105.892
1123'	26.270	30.421	12.488	20.920	47.537	68.770
1133'	26.270	36.373	12.488	14.968	47.537	41.151
2111'	22.357	33.276	16.400	18.065	73.355	54.289
2121'	22.357	39.981	16.400	11.360	73.355	28.414
2131'	22.357	46.577	16.400	4.764	73.355	10.229
2112'	22.357	30.144	16.400	21.198	73.355	70.323
2122'	22.357	36.564	16.400	14.777	73.355	40.414
2132'	22.357	43.011	16.400	8.330	73.355	19.368
2113'	22.357	24.936	16.400	26.405	73.355	105.892
2123'	22.357	30.421	16.400	20.920	73.355	68.770
2133'	22.357	36.373	16.400	14.968	73.355	41.151
3111'	18.624	33.276	20.133	18.065	108.101	54.289
3121'	18.624	39.981	20.133	11.360	108.101	28.414
3131'	18.624	46.577	20.133	4.764	108.101	10.229
3112'	18.624	30.144	20.133	21.198	108.101	70.323
3122'	18.624	36.564	20.133	14.777	108.101	40.414
3132'	18.624	43.011	20.133	8.330	108.101	19.368
3113'	18.624	24.936	20.133	26.405	108.101	105.892
3123'	18.624	30.421	20.133	20.920	108.101	68.770
3133'	18.624	36.373	20.133	14.968	108.101	41.151
1211'	30.660	33.276	8.098	18.065	26.412	54.289
1221'	30.660	39.981	8.098	11.360	26.412	28.414
1231'	30.660	46.577	8.098	4.764	26.412	10.229
1212'	30.660	30.144	8.098	21.198	26.412	70.323
1222'	30.660	36.564	8.098	14.777	26.412	40.414
1232'	30.660	43.011	8.098	8.330	26.412	19.368
1213'	30.660	24.936	8.098	26.405	26.412	105.892

1223'	30.660	30.421	8.098	20.920	26.412	68.770
1233'	30.660	36.373	8.098	14.968	26.412	41.151
2211'	26.377	33.276	12.381	18.065	46.938	54.289
2221'	26.377	39.981	12.381	11.360	46.938	28.414
2231'	26.377	46.577	12.381	4.764	46.938	10.229
2212'	26.377	30.144	12.381	21.198	46.938	70.323
2222'	26.377	36.564	12.381	14.777	46.938	40.414
2232'	26.377	43.011	12.381	8.330	46.938	19.368
2213'	26.377	24.936	12.381	26.405	46.938	105.892
2223'	26.377	30.421	12.381	20.920	46.938	68.770
2233'	26.377	36.373	12.381	14.968	46.938	41.151
3211'	21.825	33.276	16.933	18.065	77.588	54.289
3221'	21.825	39.981	16.933	11.360	77.588	28.414
3231'	21.825	46.577	16.933	4.764	77.588	10.229
3212'	21.825	30.144	16.933	21.198	77.588	70.323
3222'	21.825	36.564	16.933	14.777	77.588	40.414
3232'	21.825	43.011	16.933	8.330	77.588	19.368
3213'	21.825	24.936	16.933	26.405	77.588	105.892
3223'	21.825	30.421	16.933	20.920	77.588	68.770
3233'	21.825	36.373	16.933	14.968	77.588	41.151
1311'	36.877	33.276	1.881	18.065	5.101	54.289
1321'	36.877	39.981	1.881	11.360	5.101	28.414
1331'	36.877	46.577	1.881	4.764	5.101	10.229
1312'	36.877	30.144	1.881	21.198	5.101	70.323
1322'	36.877	36.564	1.881	14.777	5.101	40.414
1332'	36.877	43.011	1.881	8.330	5.101	19.368
1313'	36.877	24.936	1.881	26.405	5.101	105.892
1323'	36.877	30.421	1.881	20.920	5.101	68.770
1333'	36.877	36.373	1.881	14.968	5.101	41.151
2311'	32.368	33.276	6.390	18.065	19.740	54.289
2321'	32.368	39.981	6.390	11.360	19.740	28.414
2331'	32.368	46.577	6.390	4.764	19.740	10.229
2312'	32.368	30.144	6.390	21.198	19.740	70.323
2322'	32.368	36.564	6.390	14.777	19.740	40.414
2332'	32.368	43.011	6.390	8.330	19.740	19.368
2313'	32.368	24.936	6.390	26.405	19.740	105.892
2323'	32.368	30.421	6.390	20.920	19.740	68.770
2333'	32.368	36.373	6.390	14.968	19.740	41.151
3311'	27.304	33.276	11.454	18.065	41.951	54.289
3321'	27.304	39.981	11.454	11.360	41.951	28.414
3331'	27.304	46.577	11.454	4.764	41.951	10.229
3312'	27.304	30.144	11.454	21.198	41.951	70.323

3322'	27.304	36.564	11.454	14.777	41.951	40.414
3332'	27.304	43.011	11.454	8.330	41.951	19.368
3313'	27.304	24.936	11.454	26.405	41.951	105.892
3323'	27.304	30.421	11.454	20.920	41.951	68.770
3333'	27.304	36.373	11.454	14.968	41.951	41.151

Table A.2: List of ligament configurations

Combination	ACL Insertion	ACL Origin	PCL Insertion	PCL Origin
1111	1	1	1	1
1121	1	1	2	1
1131	1	1	3	1
1112	1	1	1	2
1122	1	1	2	2
1132	1	1	3	2
1113	1	1	1	3
1123	1	1	2	3
1133	1	1	3	3
2111	2	1	1	1
2121	2	1	2	1
2131	2	1	3	1
2112	2	1	1	2
2122	2	1	2	2
2132	2	1	3	2
2113	2	1	1	3
2123	2	1	2	3
2133	2	1	3	3
3111	3	1	1	1
3121	3	1	2	1
3131	3	1	3	1
3112	3	1	1	2
3122	3	1	2	2
3132	3	1	3	2
3113	3	1	1	3
3123	3	1	2	3
3133	3	1	3	3

1211	1	2	1	1
1221	1	2	2	1
1231	1	2	3	1
1212	1	2	1	2
1222	1	2	2	2
1232	1	2	3	2
1213	1	2	1	3
1223	1	2	2	3
1233	1	2	3	3
2211	2	2	1	1
2221	2	2	2	1
2231	2	2	3	1
2212	2	2	1	2
2222	2	2	2	2
2232	2	2	3	2
2213	2	2	1	3
2223	2	2	2	3
2233	2	2	3	3
3211	3	2	1	1
3221	3	2	2	1
3231	3	2	3	1
3212	3	2	1	2
3222	3	2	2	2
3232	3	2	3	2
3213	3	2	1	3
3223	3	2	2	3
3233	3	2	3	3
1311	1	3	1	1
1321	1	3	2	1
1331	1	3	3	1
1312	1	3	1	2
1322	1	3	2	2
1332	1	3	3	2
1313	1	3	1	3
1323	1	3	2	3
1333	1	3	3	3
2311	2	3	1	1

2321	2	3	2	1
2331	2	3	3	1
2312	2	3	1	2
2322	2	3	2	2
2332	2	3	3	2
2313	2	3	1	3
2323	2	3	2	3
2333	2	3	3	3
3311	3	3	1	1
3321	3	3	2	1
3331	3	3	3	1
3312	3	3	1	2
3322	3	3	2	2
3332	3	3	3	2
3313	3	3	1	3
3323	3	3	2	3
3333	3	3	3	3

REFERENCES

Abdelgaied, A., Brockett, C. L., Liu, F., Jennings, L. M., Jin, Z., & Fisher, J. (2014). The effect of insert conformity and material on total knee replacement wear. *J Engineering in Medicine*, *228*(1), 98–106. http://doi.org/10.1177/0954411913513251

American Sensor Technologies. (2015). Spring Loaded LVDT. Retrieved from http://www.indiamart.com/american-sensor-technologies/lvdt.html

Amiri, S., & Wilson, D. R. (2012). A Computational Modeling Approach for Investigating Soft Tissue Balancing in Bicruciate Retaining Knee Arthroplasty. *Computational and Mathematical Methods in Medicine*, *11*. http://doi.org/10.1155/2012/652865

Angoules, A. G., Balakatounis, K., Boutsikari, E. C., Mastrokalos, D., & Papagelopoulos, P. J. (2013). Anterior-Posterior Instability of the Knee Following ACL Reconstruction with Bone-Patellar Tendon-Bone Ligament in Comparison with Four-Strand Hamstrings Autograft. *Rehabilitation Research and Practice*, *2013*, 1–6. http://doi.org/10.1155/2013/572083

ASTM Standard F1223. (2014). *Standard Test Method for Determination of Total Knee Replacement Constraint*. West Conshohocken. Retrieved from www.astm.org

Babazadeh, S. (2009). The relevance of ligament balancing in total knee arthroplasty: how important is it? A systematic review of the literature. *Orthopedic Reviews*, *1*(2), 26. http://doi.org/10.4081/or.2009.e26

Bach, B. R. (2009). ACL treatment current trends and future directions. *The Journal of Knee Surgery*, *22*(1), 5. Retrieved from http://www.ncbi.nlm.nih.gov/pubmed/19216344

Banks, S., Boniforti, F., Fregly, B., Rahman, H., Reinschmidt, C., & Romagnoli, S. (2003). The Kinematics of Deep Flexion in Bi-Cruciate Retaining Resurfacing Knee Arthroplasty. *ORS*.

Blackburn, T., & Craig, E. (1980). Knee Anatomy A Brief Review. *Phys Ther*, *60*, 1556–1560. Retrieved from http://ptjournal.apta.org/content/60/12/1556

Blankevoort, L., & Huiskes, R. (1991). Ligament-Bone Interaction in a Three-Dimensional Model of the Knee. *Journal of Biomechanical Engineering*, *113*.

Bloemker, K., Guess, T., Maletsky, L., & Dodd, K. (2012). Computational Knee Ligament Modeling Using Experimentally Determined Zero-Load Lengths. *The*

Open Biomedical Engineering Journal, *6*(1), 33–41.
http://doi.org/10.2174/1874230001206010033

Bollars, P., Luyckx, J.-P., Innocenti, B., Labey, L., Victor, J., Bellemans, J., & Victor,
J. (2011). Femoral component loosening in high-flexion total knee replacement AN
IN VITRO COMPARISON OF HIGH-FLEXION VERSUS CONVENTIONAL
DESIGNS. *J Bone Joint Surg Br*, *9393*(10), 1355–61. http://doi.org/10.1302/0301–
620X.93B10

Brindle, T., Nyland, J., & Johnson, D. L. (2001). The Meniscus: Review of Basic
Principles With Application to Surgery and Rehabilitation. *Journal of Athletic
Training*, *36*(2), 160–169. Retrieved from www.journalofathletictraining.org

Burgess, S. (1999). Critical Characteristics and the Irreducible Knee Joint. *Journal of
Creation*, *13*(2), 112–117. Retrieved from https://answersingenesis.org/human-
body/critical-characteristics-and-the-irreducible-knee-joint/

Byrd, C., Sanford, A., Earl, B., Claypool, J., Brown, J., & Pendleton, J. (2014). Total
Knee Implant. US Patent Office.

Castiello, E., & Affatato, S. (2015). *The first surgical approach for total knee
arthroplasty (TKA). Surgical Techniques in Total Knee Arthroplasty and Alternative
Procedures*. Woodhead Publishing Limited.
http://doi.org/10.1533/9781782420385.2.109

Chen, L., Kim, P. D., Ahmad, C. S., & Levine, W. N. (2008). Medial collateral ligament
injuries of the knee: current treatment concepts. *Current Reviews in Musculoskeletal
Medicine*, *1*(2), 108–113. http://doi.org/10.1007/s12178-007-9016-x

ChiroMatrix. (2016). The Knee Joint. Retrieved from http://drkhayami.com/treating-
conditions/lower-extremity/knee-pain.html

Conrad, D. N., & Dennis, D. A. (2014). Patellofemoral Crepitus after Total Knee
Arthroplasty: Etiology and Preventive Measures. *Clinics in Orthopedic Surgery*,
6(1), 9. http://doi.org/10.4055/cios.2014.6.1.9

Damsgaard, M., Rasmussen, J., Christensen, S. T., Surma, E., & de Zee, M. (2006).
Analysis of musculoskeletal systems in the AnyBody Modeling System. *Simulation
Modelling Practice and Theory*, *14*(8), 1100–1111.
http://doi.org/10.1016/j.simpat.2006.09.001

Dargel, J., Gotter, M., Mader, K., Pennig, D., Koebke, J., & Schmidt-Wiethoff, R.
(2007). Biomechanics of the anterior cruciate ligament and implications for surgical
reconstruction. *Strategies in Trauma and Limb Reconstruction*, *2*(1), 1–12.
http://doi.org/10.1007/s11751-007-0016-6

Dieppe, P. (2011). Developments in osteoarthritis. *Rheumatology (Oxford, England)*, *50*(2), 245–7. http://doi.org/10.1093/rheumatology/keq373

Donno, C., & Munchinger, M. (2012). Knee Prosthesis. US Patent Office.

Eguchi, A., Adachi, N., Nakamae, A., Usman, M. A., Deie, M., & Ochi, M. (2014). Proprioceptive function after isolated single-bundle posterior cruciate ligament reconstruction with remnant preservation for chronic posterior cruciate ligament injuries. *Orthopaedics & Traumatology, Surgery & Research : OTSR*, *100*(3), 303–8. http://doi.org/10.1016/j.otsr.2013.12.020

Fanelli, G. C., & Edson, C. J. (1995). Posterior cruciate ligament injuries in trauma patients: Part II. *Arthroscopy: The Journal of Arthroscopic & Related Surgery*, *11*(5), 526–529. http://doi.org/10.1016/0749-8063(95)90127-2

Ferretti, A., Monaco, E., & Vadalà, A. (2014). Rotatory instability of the knee after ACL tear and reconstruction. *Journal of Orthopaedics and Traumatology*, *15*(2), 75–79. http://doi.org/10.1007/s10195-013-0254-y

Galbusera, F., Freutel, M., Dürselen, L., D 'aiuto, M., Croce, D., Villa, T., … Pivonka, P. (2014). BIOENGINEERING AND BIOTECHNOLOGY Material models and properties in the finite element analysis of knee ligaments: a literature review. http://doi.org/10.3389/fbioe.2014.00054

Gianotti, S. M., Marshall, S. W., Hume, P. A., & Bunt, L. (2009). Incidence of anterior cruciate ligament injury and other knee ligament injuries: a national population-based study. *Journal of Science and Medicine in Sport / Sports Medicine Australia*, *12*(6), 622–7. http://doi.org/10.1016/j.jsams.2008.07.005

Halewood, C., Risebury, M., Thomas, N. P., & Amis, A. A. (2014). Kinematic behaviour and soft tissue management in guided motion total knee replacement. *Knee Surgery, Sports Traumatology, Arthroscopy*, *22*. http://doi.org/10.1007/s00167-014-2933-5

Harwin, S. F., & Kester, M. (2010). Single radius total knee arthroplasty: PCL sacrifice without substitution yields excellent outcomes minimum 8-year follow-up. *Surgical Technology International*, *19*, 191–8. Retrieved from http://www.ncbi.nlm.nih.gov/pubmed/20437364

Hosseini, A., Gill, T. J., & Li, G. (2009). In vivo anterior cruciate ligament elongation in response to axial tibial loads. *Journal of Orthopaedic Science*, *14*(3), 298–306. http://doi.org/10.1007/s00776-009-1325-z

Hosseini, A., Qi, W., Tsai, T.-Y., Liu, Y., Rubash, H., & Li, G. (2014). In vivo length change patterns of the medial and lateral collateral ligaments along the flexion path of the knee. *Knee Surgery, Sports Traumatology, Arthroscopy : Official Journal of*

the *ESSKA*, *23*(10), 3055–3061. http://doi.org/10.1007/s00167-014-3306-9

Huang, C.-H., Liau, J.-J., & Cheng, C.-K. (2007). Fixed or Mobile-Bearing Total Knee Arthroplasty. *Journal of Orthopaedic Surgery and Research*, *2*(1), 1. http://doi.org/10.1186/1749-799X-2-1

Instron. (n.d.). 8874 Axial-Torsion Fatigue Testing System. Retrieved from http://www.instron.us/en-us/products/testing-systems/dynamic-and-fatigue-systems/servohydraulic-fatigue/8874-axial-torsion

Julin, J., Jämsen, E., Puolakka, T., Konttinen, Y. T., & Moilanen, T. (2010). Younger age increases the risk of early prosthesis failure following primary total knee replacement for osteoarthritis. *Acta Orthopaedica*, *81*(4), 413–419. http://doi.org/10.3109/17453674.2010.501747

Kolisek, F. R., McGrath, M. S., Marker, D. R., Jessup, N., Seyler, T. M., Mont, M. A., & Lowry Barnes, C. (2009). Posterior-stabilized versus posterior cruciate ligament-retaining total knee arthroplasty. *The Iowa Orthopaedic Journal*, *29*, 23–27.

Komdeur, P., Pollo, F. E., & Jackson, R. W. (2002). Dynamic knee motion in anterior cruciate impairment: a report and case study. *Proceedings (Baylor University. Medical Center)*, *15*(3), 257–259.

Kuettner, K. (1992). Biochemistry of Articular Carilage in Health and Disease. *Clinical Biochemistry*, *25*(3), 155–163. http://doi.org/doi:10.1016/0009-9120(92)90224-G

Kurtz, S., Ong, K., Lau, E., Mowat, F., & Halpern, M. (2007). Projections of primary and revision hip and knee arthroplasty in the United States from 2005 to 2030. *The Journal of Bone and Joint Surgery. American Volume*, *89*(4), 780–5. http://doi.org/10.2106/JBJS.F.00222

Kweon, C., & Lederman, E. (2013). Anatomy and Biomechanics of the Cruciate Ligaments and Their Surgical Implications. *Spring Science*. http://doi.org/DOI 10.1007/978-0-387-49289-6_2

LaPrade, R., Engebretsen, A., Ly, T. V, Johansen, S., Wentorf, F. A., Robert LaPrade, B. F., … Engebretsen, L. (2007). The Anatomy of the Medial Part of the Knee. *J Bone Joint Surg Am. The Journal of Bone and Joint Surgery COPYRIGHT BY THE JOURNAL OF BONE AND JOINT SURGERY*. http://doi.org/10.2106/JBJS.F.01176

Legnani, C., Ventura, A., Terzaghi, C., Borgo, E., & Albisetti, W. (2010). Anterior cruciate ligament reconstruction with synthetic grafts. A review of literature. *International Orthopaedics*, *34*, 465–471. http://doi.org/10.1007/s00264-010-0963-2

Lenard, C. (2014). Basics of Biomechanics of Tendons and Ligaments. Retrieved from

http://www.pitchingnow.com/kinesiology/basic-biomechanics-of-tendons-and-ligaments/

Levangie, P. K., & Norkin, C. C. (2005). Joint Structure and Function: A Comprehensive Analysis. *F. A. Davis Company*, 393–436. http://doi.org/10.1002/art.1780240233

Li, G., DeFrate, L., Sun, H., & Gill, T. (2004). In Vivo Elongation of the Anterior Cruciate Ligament and Posterior Cruciate Ligament During Knee Flexion. *American Journal of Sports Medicine*, *32*(6), 1415–1420. http://doi.org/10.1177/0363546503262175

Losina, E., Thornhill, T. S., Rome, B. N., Wright, J., & Katz, J. N. (2012). The Dramatic Increase in Total Knee Replacement Utilization Rates in the United States Cannot Be Fully Explained by Growth in Population Size and the Obesity Epidemic. *The Journal of Bone & Joint Surgery*, *94*(3), 201–207. http://doi.org/10.2106/JBJS.J.01958

MACRO SENSORS. (n.d.). GHSE/ GHSER 750 Series. Retrieved from http://www.macrosensors.com/GHSE_GHSER_750.html

MATLAB. (n.d.). The Language of Technical Computing. Retrieved from http://www.mathworks.com/products/matlab/

Metzger, R., Uthgenannt, B., & Stone, K. (2013). Knee Prosthesis Assembly with Ligament Link. US Patent Office.

Nakagawa, S., Johal, P., Pinskerova, V., Komatsu, T., Sosna, A., Williams, A., & Freeman, M. A. R. (2004). The posterior cruciate ligament during flexion of the normal knee. *The Journal of Bone and Joint Surgery*, *86*(3), 450–456. http://doi.org/10.1302/0301-620X.86B3.14330

NextEngine 3D Laser Scanner. (n.d.). NextEngine Products. Retrieved from http://www.nextengine.com/products/scanner/features/accurate

Nissman D. (2008). Imaging the Knee: Ligaments. *Applied Radiology*, *37*(12), 25–32.

Owellen M. (1997). *The Effect of Lubricant and Load on Articular Cartilage Wear and Friction*. Virginia Polytechnic Institute and State University.

Papannagari, R., DeFrate, L. E., Nha, K. W., Moses, J. M., Moussa, M., Gill, T. J., & Li, G. (2007). Function of posterior cruciate ligament bundles during in vivo knee flexion. *The American Journal of Sports Medicine*, *35*(9), 1507–12. http://doi.org/10.1177/0363546507300061

Park, S., Defrate, L., Jf, S., Gill, T., Rubash, H., & Li. (2005). THE LENGTH CHANGE

OF THE MEDIAL AND LATERAL COLLATERAL LIGAMENTS DURING IN-
VIVO KNEE FLEXION. *ORS*.

Petersen, W., Ellermann, A., Gösele-Koppenburg, A., Best, R., Rembitzki, I. V.,
Brüggemann, G.-P., & Liebau, C. (2014). Patellofemoral pain syndrome. *Knee
Surgery, Sports Traumatology, Arthroscopy*, *22*(10), 2264–2274.
http://doi.org/10.1007/s00167-013-2759-6

Phisitkul, P., James, S. L., Wolf, B. R., & Amendola, A. (2006). MCL injuries of the
knee: current concepts review. *The Iowa Orthopaedic Journal*, *26*(Mcl), 77–90.
Retrieved from
http://www.pubmedcentral.nih.gov/articlerender.fcgi?artid=1888587&tool=pmcentr
ez&rendertype=abstract

Pritchett, J. W. (2015). Bicruciate-retaining Total Knee Replacement Provides
Satisfactory Function and Implant Survivorship at 23 Years. *Clinical Orthopaedics
and Related Research*, 2327–2333. http://doi.org/10.1007/s11999-015-4219-8

Rath, E., & Richmond, J. C. (2000). The menisci: basic science and advances in
treatment. *British Journal of Sports Medicine*, *34*, 252–257.
http://doi.org/10.1136/bjsm.34.4.252

Rodriguez-Merchan, E. C. (2011). Instability Following Total Knee Arthroplasty. *HSSJ*,
7, 273–278. http://doi.org/10.1007/s11420-011-9217-0

Shearer, R. (n.d.). 3D Scanning Using the NextEngine 3D Scanner HD. Retrieved from
http://www.instructables.com/id/3D-Scanning-using-the-NextEngine-3D-Scanner-
HD/

Smith & Nephew. (2015). OXINUM Oxidized Zirconium. Retrieved from
http://www.rediscoveryourgo.com/verilastkneeoxinium.aspx

Solidworks 3D CAD. (n.d.). Solidworks Standard. Retrieved from
http://www.solidworks.com/sw/products/3d-cad/solidworks-standard.htm

Stärke, C., Kopf, S., Petersen, W., & Becker, R. (2009). Meniscal repair. *Arthroscopy :
The Journal of Arthroscopic & Related Surgery : Official Publication of the
Arthroscopy Association of North America and the International Arthroscopy
Association*, *25*(9), 1033–44. http://doi.org/10.1016/j.arthro.2008.12.010

Taylor, D. (n.d.). 3Matic STL. Retrieved from http://software.materialise.com/3-
maticSTL

Telos. (n.d.). KoSa Synthetic Ligament. Retrieved from http://www.telos-
marburg.de/en/products/kosaproducts/kosaband

The AnyBody Modeling System. (n.d.). Retrieved from
    http://www.anybodytech.com/index.php?id=26

Un, B. S., Beynnon, B. D., Churchill, D. L., Haugh, L. D., Risberg, M. A., & Fleming, B.
    C. (2001). A new device to measure knee laxity during weightbearing and non-
    weightbearing conditions. *Journal of Orthopaedic Research*, *19*(6), 1185–1191.
    http://doi.org/10.1016/S0736-0266(01)00055-9

Waryasz, G. R., & Mcdermott, A. Y. (2008). Dynamic Medicine Patellofemoral pain
    syndrome (PFPS): a systematic review of anatomy and potential risk factors.
    Dynamic Medicine, *7*(79). http://doi.org/10.1186/1476-5918-7-9

Webright, W., Perrin, D., & Gansneder, B. (1998). Effect of Trunk Position on Anterior
    Tibia Displacement Measured by the KT-1000 in Uninjured Subjects. *Journal of
    Athletic Training*, *33*(3), 233–237.

Windsor, R., & Padgett, D. (2013). Understanding Implants in Knee and Hip
    Replacement. Retrieved from https://www.hss.edu/conditions_understanding-
    implants-in-knee-and-hip-replacement.asp

Withrow, T. J., Huston, L. J., Wojtys, E. M., & Ashton-Miller, J. A. (2006). The
    relationship between quadriceps muscle force, knee flexion, and anterior cruciate
    ligament strain in an in vitro simulated jump landing. *The American Journal of
    Sports Medicine*, *34*(2), 269–74. http://doi.org/10.1177/0363546505280906

Woo, S. L., Hollis, J. M., Adams, D. J., Lyon, R. M., & Takai, S. (1991). Tensile
    properties of the human femur-anterior cruciate ligament-tibia complex. The effects
    of specimen age and orientation. *The American Journal of Sports Medicine*, *19*(3),
    217–25. Retrieved from http://www.ncbi.nlm.nih.gov/pubmed/1867330